From Dark Matter to Leptoquarks: Phenomenology of Physics Beyond the Standard Model

by

Shayne K. Gryba

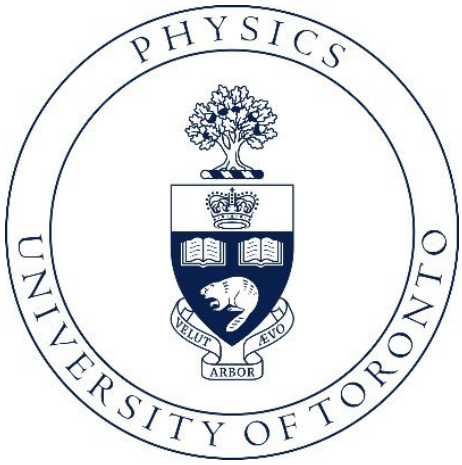

A thesis submitted in conformity with
the requirements for the degree of
Doctor of Philosophy
Graduate Department of Physics
University of Toronto

From Dark Matter to Leptoquarks: Phenomenology of Physics Beyond the Standard Model

Shayne K. Gryba, Doctor of Philosophy, Graduate Department of Physics, University of Toronto, 2022

The Standard Model of particle physics began as a simple "Model of Leptons" in 1967, but after more than five decades of theoretical development and experimental scrutiny it has grown to become the most successful scientific theory of all time. We begin with a short summary of the features of the Standard Model and a discussion of its explanatory power, taking the modern perspective. We then highlight three particular shortcomings of the SM in its current formulation: the electroweak hierarchy problem, the nature of dark matter, and the growing list of anomalies in the flavour sector, neutrino sector, and elsewhere. These shortcomings form the foundation of the work presented in this thesis.

We first show that the electroweak hierarchy problem and the nature of dark matter can be understood through the combination of a general Twin Higgs framework and an additional singlet scalar acting as dark matter. Then we turn our attention to minimal Twin Higgs models and reexamine the twin tau lepton as a dark matter candidate, in light of recent theoretical developments into the UV structure of these models. We find that the scenario is possible and may be discoverable in future direct detection experiments. Lastly, we search for a novel explanation to the MiniBooNE anomaly using scalar leptoquarks to induce lepton flavour violating pion decays, and consider $\mu - e$ conversion experiments as a future probe of important leptoquark couplings.

Acknowledgements

I remember clearly my first week of graduate school. I was gathered into a large auditorium with all the other new graduate students listening to a speaker explain the ways in which graduate school would be different from anything else we had likely done before. In particular, he reminded us to pace ourselves: "Grad school is a marathon, not a sprint."

I admit that I somewhat brushed this advice off. Undergraduate degrees are partitioned in a way I hadn't appreciated until it was no longer the case – no matter how ugly a semester looks, it will only ever be four months long. Graduate school has no such partitions. Months and months can drag on with startlingly little progress to show for it, and the days of red pen checkmarks are long behind you.

This is where people come in. The only way to get to the end of something like graduate school is to lean on all of the amazing people you are fortunate enough to have around you. These people show you new perspectives and remind you how far you've come. They provide comfort and relief when things get rough, and are enthusiastic accomplices in times of celebration.

Thank you to my family, Kevin, Carmon, and Kaylee, for your continual support and earnest attempt to read my first paper. Many thanks to Martin and Gil for your advice on the next stage of my career.

Thank you Jared and David for sharing all of your humour and wisdom in so many chalkboard conversations. I have learned so much from you two, and your presence is truly humbling. I am certain that you'll both end up wherever you're hoping to go. Thank you to Caleb, Aris, and Roy for keeping our group a vibrant and active space. Thank you to Jack and Rodolfo, who both went well out of their way to offer help whenever possible.

Thank you Dan and Jakub for working so hard to make our project together a success. Thank you to Pierre and Erich for keeping me honest, and to Mike, Bob, and A.W. for lending your expertise without hesitation.

Thank you to Krystyna, Helen, Liz, April, and all the rest of the administrative staff for your excellent organizational and interpersonal capacities. My experience with all of you has been nothing short of delightful.

Thank you David for taking such an active role in my education. Your enthusiasm and endless passion for physics is contagious. You have taught me so much, both within physics and well outside, too. Thanks for taking a chance on a prairie kid.

Lastly, thank you to my best friend and partner, Kelti. We have been through so much together – least of all a graduate degree each – and I'm certain I would have given up long ago without you by my side. Your support has been unwavering and irreplaceable. Thank you for always showing me the good side of things.

TABLE OF CONTENTS

LIST OF TABLES

LIST OF FIGURES

List of Appendices

PART 1:

THE STANDARD MODEL OF PARTICLE INTERACTIONS

1 The Standard Model of Particle Interactions

1.1 Formalism

The Standard Model (SM) is a gauge theory of quantum fields. Each field in the theory transforms under a particular representation of the underlying gauge group, and interactions between fields arise mathematically as products of fields in the Lagrangian. The set of possible interactions between fields is limited by the requirement that each product be invariant under the gauge transformations, as well as transformations under the Poincaré group, which includes translations, rotations, and boosts in Minkowski spacetime $SO(1,3)$ [15].

The particular gauge symmetry structure of the SM is $SU(3)_C \times SU(2)_L \times U(1)_Y$. Fields with nontrivial transformations under $SU(3)_C$ have interactions described by the theory of quantum chromodynamics (QCD), while fields transforming under $SU(2)_L \times U(1)_Y$ are described by electroweak interactions. The theory also admits two[1] global $U(1)$ symmetries, namely baryon and lepton number, denoted $U(1)_B$ and $U(1)_L$. Although each of these global symmetries is anomalous, the difference $U(1)_{B-L}$ is non-anomalous in the SM and so is often promoted to a gauge symmetry in models of physics Beyond the Standard Model (BSM) [16].

Fermionic degrees of freedom in the SM can be organized into particle multiplets based on their charges under the gauge group $SU(3)_C \times SU(2)_L \times U(1)_Y$. All known SM fermions that transform nontrivially under a SM gauge group do so in the fundamental representation. In order to have an invariant Lagrangian containing derivatives of fields, derivatives of a fermion multiplet $\partial_\mu \psi$ are promoted to *covariant* derivatives $D_\mu \psi \equiv (\partial_\mu - igA_a^\mu \tau^a)\psi$, where τ^a are the symmetry generators and g is a coupling constant. This requirement introduces corresponding spin-1 gauge bosons A_a^μ into the theory, one for each symmetry generator, with a ranging over the dimension of the gauge group representation. The Lagrangian is then manifestly gauge invariant, following the infinitesimal transformations

$$\psi(x) \to (1 + i\alpha^a(x)\tau^a)\,\psi(x) \tag{1.1}$$

$$A_\mu^a(x) \to A_\mu^a + (1/g)\partial_\mu \alpha^a(x) + f^{abc} A_\mu^b \alpha^c \tag{1.2}$$

where f^{abc} are the structure constants of the Lie algebra, defined by the commutator of the generators $[\tau^a, \tau^b] = if^{abc}\tau^c$ [17]. The SM also contains one scalar field, the Higgs field ϕ, which is a complex doublet charged under $SU(2)_L \times U(1)_Y$. Derivative couplings of the Higgs are also promoted to covariant derivatives containing the $SU(2)_L$ and $U(1)_Y$ gauge bosons. The full Lagrangian for the

[1] Actually four, if you count each generation of lepton number as a separate $U(1)$.

	$SU(3)_C$	$SU(2)_L$	$U(1)_Y$
Q	**3**	**2**	$1/6$
u_R	**3**	1	$2/3$
d_R	**3**	1	$-1/3$
L	1	**2**	$-1/2$
e_R	1	1	-1

Table 1. Gauge representations of the fermions in the Standard Model (SM).

SM can be written

$$\begin{aligned}\mathcal{L} = &-\frac{1}{4}\left(G^a_{\mu\nu}\right)^2 - \frac{1}{4}\left(W^b_{\mu\nu}\right)^2 - \frac{1}{4}\left(B_{\mu\nu}\right)^2 + \sum_k \bar{\psi}_k \left(i\not{D}_k\right)\psi_k \\ &- Y_l^{ij}\bar{L}_i\phi e_{R,j} - Y_d^{ij}\bar{Q}_i\phi d_{R,j} - Y_u^{ij}\bar{Q}_i\left(i\sigma_2\phi^*\right)u_{R,j} + \text{h.c.} \\ &+ \left(D_\mu\phi\right)^\dagger\left(D^\mu\phi\right) + \mu^2\left(\phi^\dagger\phi\right) - \lambda\left(\phi^\dagger\phi\right)^2\end{aligned} \tag{1.3}$$

where $\bar{\psi} = \psi^\dagger\gamma^0$ and $\not{D} = D_\mu\gamma^\mu$. The field strength tensors are generally defined $F^a_{\mu\nu} = \partial_\mu A^a_\nu - \partial_\nu A^a_\mu + g f^{abc} A^b_\mu A^c_\nu$, where g is a gauge coupling, f^{abc} are the structure constants of the Lie algebra, and the index a runs over the dimension of the representation. In the SM the gauge bosons are adjoints of their corresponding gauge groups; there are eight $SU(3)_C$ gauge fields A^a_μ, while the $SU(2)_L$ and $U(1)_Y$ gauge fields are comprised of W^b_μ ($b = 1, 2, 3$) and B_μ respectively. The fermion kinetic term indexed by k spans $\psi = Q, L, e_R, u_R, d_R$ for each of the three generations, and the covariant derivative $\not{D}_k$ is understood to include all of the symmetry generators and gauge bosons under which that fermion is charged. For example, since Q transforms as $(\mathbf{3}, \mathbf{2}, 1/6)$ under $SU(3)_C \times SU(2)_L \times U(1)_Y$, the covariant derivative is $\not{D} = \not{\partial} - ig_s\not{G}^a\lambda^a - ig\not{W}^b\tau^b - ig'Y_Q\not{B}$, where g_s, g, g' are gauge couplings of $SU(3)_C, SU(2)_L$, and $U(1)_Y$, and λ, τ, Y_Q are their respective symmetry generators.[2] The rest of the fermion gauge representations are listed in Table 1.1.

The Y^{ij} are the Yukawa couplings of the theory, which are grouped into couplings with the three generations of leptons (e, μ, τ), the up-type quarks (u, c, t) and the down-type quarks (d, s, b). Note that a Yukawa coupling $\bar{L}\left(i\sigma_2\phi^*\right)\nu_R$ can in principle be written down to give neutrinos a Dirac mass, but the mass generation mechanism and hence particle nature of the neutrinos is currently still unknown and so this term is typically not included in the SM. Majorana mass terms may also be written for right- and left-handed neutrinos, with the former trivially included since ν_R are gauge singlet states, and the latter being generated by the Weinberg operator $\frac{\mathcal{C}}{\Lambda}\left(\bar{L}\tilde{H}\right)^2$. Left-handed Majorana neutrino masses are considered to be BSM physics since they involve some new scale Λ. We also mention the omission of a CP-violating operator $\bar{\theta}\frac{g_s^2}{32\pi^2}\varepsilon^{\mu\nu\alpha\beta}G^a_{\mu\nu}G^a_{\alpha\beta}$ that can be generated by chiral

[2]The hypercharge generator is always proportional to the identity matrix, with the proportionality factor given by the hypercharge quantum number listed in Table 1.1. In the current example $Y_Q = (1/6)\mathbb{I}$.

rotations of $SU(3)_C$ fields. This term is expected to appear in the SM Lagrangian and yields observable consequences, for instance in the neutron electric dipole moment. However, experimental measurements have constrained $\bar{\theta} < 10^{-10}$ [16], suggesting that the operator is highly suppressed at low energy by some as-of-yet understood mechanism. This is called the strong CP problem and is the subject of a large body of literature (see e.g. [18] for a review). Finally, note the constant factors in the first line of Equation (1.3) are chosen such that the kinetic energies of the gauge fields are canonically normalized.

The last two terms of the Lagrangian comprise the scalar potential of the SM. The difference in sign between the two terms leads the Higgs field to acquire a nonzero vacuum expectation value (vev), $\langle|\phi|\rangle = \sqrt{\frac{\mu^2}{2\lambda}} \equiv \frac{v}{\sqrt{2}}$, which breaks the $SU(2)_L \times U(1)_Y$ symmetry down to $U(1)_{\text{EM}}$, resulting in 3 Nambu-Goldstone bosons and a radial mode. To study the effects of spontaneous symmetry breaking it is best to redefine the condensed field in order to parameterize fluctuations about the vacuum. We write

$$\phi = \frac{1}{\sqrt{2}} \begin{pmatrix} 0 \\ v + h \end{pmatrix} \exp\left(\frac{2i\eta^a \tau^a}{v}\right) \tag{1.4}$$

where τ^a are the $SU(2)_L$ generators[3], η^a the Nambu-Goldstone bosons, and the radial mode h is the Higgs boson particle. Moving to the unitary gauge and reinserting ϕ into the above Lagrangian, we find that three independent linear combinations of electroweak gauge bosons acquire a mass proportional to the Higgs vev, while the fourth linear combination remains exactly massless. The latter gauge boson is the familiar photon, which mediates the remaining $U(1)_{\text{EM}}$. The three massive eigenstates have integer couplings to the photon in units of the electric charge $e \equiv g \sin\theta_w$. Altogether we find:

$$W^+_\mu = \frac{1}{\sqrt{2}}\left(W^1_\mu - iW^2_\mu\right) \quad , \quad m_W = \frac{v}{2}g \tag{1.5}$$

$$W^-_\mu = \frac{1}{\sqrt{2}}\left(W^1_\mu + iW^2_\mu\right) \quad , \quad m_W = \frac{v}{2}g \tag{1.6}$$

$$Z_\mu = \cos\theta_w W^3_\mu - \sin\theta_w B_\mu \quad , \quad m_Z = \frac{m_W}{\cos\theta_w} \tag{1.7}$$

$$A_\mu = \sin\theta_w W^3_\mu + \cos\theta_w B_\mu \quad , \quad m_A = 0 \tag{1.8}$$

where $W^\pm_\mu$ have electric charge ± 1, Z_μ and A_μ are electrically neutral, g is the gauge coupling of $SU(2)_L$, and θ_w is the Weinberg angle. This process is the familiar Higgs mechanism; the 3 Nambu-Goldstone bosons of electroweak symmetry breaking have been eaten by the $W^\pm$ and Z gauge bosons, imbuing them each with an extra degree of freedom.

The nonzero Higgs vev also leads to fermion masses through the Yukawa couplings in Equation (1.3). The situation is complicated by the fact that the off-diagonal elements of Y^{ij} need not be zero;

[3]Technically the exponential should contain all of the broken generators, which are τ^1, τ^2, and $\tau^3 - Y$, but since $Q = \tau^3 + Y$ remains unbroken, the effect of τ^3 on the vacuum is the same as $\tau^3 - Y$. [19]

in fact, they are not, which implies that propagating fermion mass eigenstates are generally not the same as the flavour eigenstates. Rotating to the quark mass bases via the unitary transformations $u_L \to U_u u_L$, $d_L \to U_d d_L$, $u_R \to K_u u_R$, and $d_R \to K_d d_R$ generates weak interactions between quarks of different generations, and the sizes of these couplings are parameterized by the Cabibbo-Kobayashi-Maskawa (CKM) matrix, $V = U_u^\dagger U_d$.[4] The leptons mix under an analogous matrix, the Pontecorvo-Maki-Nakagawa-Sakata (PMNS) matrix. The SM predicts that the CKM and PMNS matrices should be unitary; deviations from unitarity would be a potential signal of physics beyond the SM. The elements of these matrices have now been measured quite precisely and agree with unitarity to within experimental error [20], but increasingly precise experiments continue to look for deviations [20–22]. In the mass basis, fermion masses are then given by the simple relation

$$m_f = y_f \frac{v}{\sqrt{2}} \tag{1.9}$$

where y_f is read off from the diagonalized Yukawa matrix after the appropriate rotations have been made.

1.2 Shortcomings of the Standard Model

The Standard Model has been a great triumph of modern physics. It can account for three of the four fundamental gauge forces of nature (weak, strong, and electromagnetic), correctly predicted the existence of many particles and properties prior to their discovery – most notably the Higgs boson, which was postulated in 1964 and discovered 48 years later – and it correctly predicts the electron's magnetic dipole moment to within 1 part per billion [23, 24].

However, mounting empirical evidence in a variety of different subfields necessitate a fuller and more complete description of Nature than the SM can offer. In particular, the SM cannot explain gravity, the strong CP problem [18], the origin of the matter-antimatter asymmetry [25], neutrino masses [26], or the reason for the large hierarchy of masses in the fermion sector [27, 28]. It also fails to justify why the Higgs boson mass lies at the electroweak scale, offers no description of dark matter or dark energy, and a growing list of $2-4\sigma$ experimental anomalies, particularly in the flavour sector, may be indicating that the SM will soon face a major upheaval. The latter three issues are of particular significance to the work done in this thesis, and we review each of them below.

1.2.1 The Electroweak Hierarchy Problem, Large and Small

Yukawa couplings are a double-edged sword. As shown in Section 1.1, Yukawa couplings between the fermions and the Higgs field are responsible for the generation of fermion masses after electroweak symmetry breaking, and these same Yukawa couplings, as well as gauge couplings between the Higgs and gauge bosons, also generate quadratically divergent loop corrections to the Higgs

[4] The right-handed mass rotations K_u, K_d have no effect on the weak mixing of quarks since the right-handed fields are $SU(2)_L$ singlets.

mass parameter. As an explicit example, the correction to the Higgs mass from a top loop is given by

$$\delta m^2 = \frac{\Lambda^2}{32\pi^2}\left(6y_t^2\right) \tag{1.10}$$

where Λ is some artificial cutoff scale that can be loosely interpreted as the scale of new physics [29]. Thus at first loop order, the relation between the bare mass m_b and pole mass m_p is

$$m_p^2 = m_b^2 - \delta m^2. \tag{1.11}$$

Here the hierarchy problem is manifest: the pole mass m_p is fixed by external measurement to be ~ 125 GeV, but the larger δm^2 becomes, the larger the bare mass parameter must become in order to compensate. Since the Higgs in the SM is a scalar boson, its mass corrections are not protected by any symmetry, and we expect that δm^2 will be affected by any new physics at any scale up to $M_{\rm Pl}$. Despite the UV sensitivity of δm^2, the Higgs mass is observed to lie at the electroweak scale, which seems to suggest that either Nature is fine-tuned to extremely high precision or there is some as-of-yet undiscovered symmetry reason for the smallness of the observed Higgs mass. [5]

In the 1980s supersymmetric (SUSY) extensions of the SM were highly favoured as solutions to the hierarchy problem [30], since cancellations in loops between particles and their superpartners allowed the Higgs mass to remain natural [31]. The advent of the LHC was particularly exciting for SUSY model builders who were eagerly anticipating hints of supersymmetric partner particles in the first runs; however, at the time of writing no evidence has been found for SUSY up to experimental scales of $\mathcal{O}(\text{TeV})$ (see Ref. [32] for a recent example of a null result).

SUSY is an example of a UV complete model that solves the full hierarchy problem by cancelling all dangerous contributions to the Higgs mass, order by order in perturbation theory. However, our current experimental reach for new physics at the LHC is still below the scale where two- and higher-loop corrections become important. Recent approaches to the hierarchy problem have therefore been less focused on UV complete models, and more focused on effective theories that can protect the Higgs mass only to first loop order. The assumption is that above the scale of the effective theory, any number of UV complete models could kick in and solve the full hierarchy problem, potentially with fantastic and unambiguous signatures that are simply not yet kinematically accessible to us. Given our experimental limitations, the prevailing wisdom is that it may be better to look for effective theories that protect the Higgs mass at first loop order and remain agnostic about eventual UV completions from which these effective theories arise.

[5] Another peculiar feature of the SM is the so-called flavour hierarchy, which is a statement about the fact that there are about six orders of magnitude separating the Yukawa couplings of the electron and the top quark. In the SM the Yukawa couplings are experimentally determined parameters that must be put in by hand, but SM extensions like the Froggatt-Neilsen model generate the hierarchy through the use of higher-dimensional operators [28]. This "hierarchy" is qualitatively different from the electroweak hierarchy because fermion masses are technically natural.

This pragmatic approach to model building reduces the immediate severity of the electroweak hierarchy problem, but it does not leave us fully satisfied. Our $\mathcal{O}(\text{TeV})$ experimental reach is already an order of magnitude above the electroweak scale, and yet we still have not seen any hint of the new physics that must ensure naturalness at first loop order. This lesser separation of scales is called the Little Hierarchy Problem.

The underlying assumption behind the Little Hierarchy Problem is that we have already excluded any new physics below $\sim$ TeV. While this may be true of particles with SM quantum numbers (which would be produced in large quantities at the Large Hadron Collider (LHC)), naturalness solutions with particles not charged under the SM gauge group are far less constrained and may well exist near the electroweak scale. These types of models are called Neutral Naturalness models [33–41]. The first and most widely studied of these models is the Twin Higgs framework [34–37, 39, 40], which forms the foundation of the work done in Chapters 2 and 3 and will be further discussed there.

1.2.2 Dark Matter

The presence of dark matter (DM) in our universe is all but undeniable, and must be included in eventual extensions of the Standard Model. The earliest evidence for dark matter comes from galactic rotation curves, whose velocity profiles depart from the predictions of the virial theorem, computed by estimating the mass of all the visible matter in a galaxy [42, 43]. The masses of galaxy clusters can be estimated in a similar way, and gravitational lensing measurements again suggest that a significant amount of the mass in these clusters must be non-luminous [42, 43]. In 2005, the Millennium collaboration produced simulations of large scale structure formation under the assumption that dark matter exists in the early universe [44], and found excellent agreement with experimental measurements [42]. Further evidence comes from Planck measurements of the matter power spectrum and CMB, with best fit parameters suggesting a dark matter relic density of $\Omega h^2 = 0.120 \pm 0.0001$ [11].

Precisely how dark matter came to exist in the cosmos at its present-day density is still an open question. There are two approaches commonly deployed, which are freeze in and freeze out scenarios [45]. In both cases we assume that there is some amount of coupling between the dark matter and visible matter that is capable of production and annihilation, for instance through $2 \to 2$ scattering. The difference between freeze in and freeze out scenarios then depends on the size of this coupling. In freeze in scenarios, the coupling is so small that dark matter is never in thermal equilibrium with the SM bath. There is, however, an assumed production channel (e.g. SM + SM $\to \chi + \chi$, where χ is the DM particle) that will slowly populate the dark sector, until such a time as the lightest SM particles participating in the production of DM become Boltzmann suppressed and decouple from the thermal bath. The comoving DM number density never reaches a level where annihilations occur, so the DM number density asymptotically approaches today's observed relic abundance [46, 47]. In freeze out scenarios, the coupling is large enough that DM is initially in thermal equilibrium with the SM bath. Roughly speaking, the DM remains in equilibrium with the bath until the Hubble expansion

rate outpaces the interaction rate ($\Gamma < H$). At this point the DM particles are too sparse to find each other and annihilate, and so the comoving number density freezes out to a constant value [45].

Dark matter can be detected in a number of different ways, depending on the type of interactions it may have with visible matter as well as their relative mass difference. Direct detection typically refers to elastic scattering between an incoming dark matter particle and a SM particle; the presence of DM is inferred by the change in momentum of the recoiling SM particle. This type of experiment is most effective if the recoiling particle and DM are near the same mass scale. Dark matter can also be detected indirectly, if it annihilates into visible sector particles (this is one explanation for the gamma-ray excess observed in the center of our galaxy, see e.g. [48]). Dark matter produced at colliders would look like missing energy in the final state, and some less minimal dark matter models invoke coannihilation partners to achieve the right relic abundance, which can lead to displaced signatures at colliders if the coannihilation partner is long lived [49].

One of the most daunting aspects of DM phenomenology is the broad range of possible DM masses. Particle explanations are of course limited to $m_{\text{DM}} < m_{\text{Pl}}$, and in fact any thermally produced particle DM candidate must satisfy $m_{\text{DM}} \lesssim 100$ TeV due to unitarity constraints [50, 51] (although models with cosmological dilution can relax this constraint slightly [52]). On the other side, bosonic dark matter can be as light as $\sim 10^{-22}$ eV, while fermionic dark matter is limited to $\mathcal{O}$(keV) since Fermi pressure would not allow a lighter DM species to have properties consistent with observations of galaxies [50]. Composite objects such as primordial black holes, quark nuggets, or axion stars are also possible candidates for some or all of DM, and their masses can be above Planck scale [50].

The work done in Chapters 2 and 3 focuses on the scenario where DM is a thermal relic weakly interacting massive particle (WIMP), meaning it has mass near the weak scale. The signatures studied in these sections are from direct detection experiments, as well as cosmological measurements in the form of ΔN_{eff}, the number of light, neutrino-like degrees of freedom present during big bang nucleosynthesis (BBN).

1.2.3 Experimental Hints of New Physics

We describe here five recent anomalies of particular relevance for the work done in Chapter 4:

- $R_{K^{(*)}}$: The most up-to-date measurements of the semi-leptonic rare decays $B^0 \to K^{(*0)} l^+ l^-$ and $B^+ \to K^+ l^+ l^-$ have been performed by the LHCb collaboration. The ratio

$$R_{K^{*0}} = \text{Br}(B^0 \to K^{*0} \mu^+ \mu^-)/\text{Br}(B^0 \to K^{*0} e^+ e^-)$$

  is reported to deviate from the SM prediction with a significance of $2.2 - 2.4\sigma$ in the $0.045 < q^2 < 1.1$ GeV^2 bin, and $2.4 - 2.5\sigma$ in the $1.1 < q^2 < 6.0$ GeV^2 bin [53]. Similarly, the ratio

$$R_{K^+} = \text{Br}(B^+ \to K^+ \mu^+ \mu^-)/\text{Br}(B^+ \to K^+ e^+ e^-)$$

differs from the SM at 3.1σ in the $1.1 < q^2 < 6.0$ GeV^2 bin [54]. Each of these ratios has an isospin partner (corresponding to a switch $u \leftrightarrow d$), denoted $R_{K^{*+}}$ and $R_{K_s^0}$ respectively, which have been recently measured as well and found to be consistent with the SM prediction [55]. However, the collaboration points out that due to the presence of long-lived mesons π^0 and K_s^0 in the final state, these ratios are significantly harder to measure than their isospin counterparts.

- $R_{D^{(*)}}$: Semileptonic rare decays $\bar{B} \to D l^- \bar{\nu}$ and $\bar{B} \to D^* l^- \bar{\nu}$ have also been measured to have anomalous ratios of branching ratios, R_D and R_{D^*}, defined as

$$R_{(D^*,D)} = \text{Br}(B \to (D^*, D)\tau\nu)/\text{Br}(B \to (D^*, D)l\nu)$$

  where l, ν can be either electrons or muons. Measurements by BaBar, LHCb, and Belle have been combined by the Heavy Flavour Averaging Group to yield anomalous results for R_D and R_{D*} of 1.4σ and 2.8σ respectively, for a combined significance of 3.3σ [56–58].

- Δa_μ: The muon anomalous magnetic moment has been recently measured by the Muon g-2 Collaboration operating out of Fermilab to be discrepant with the SM at a level of 4.2σ [59].

- m_ν: Nonzero neutrino masses have now been confirmed experimentally [20], but the origin of their mass is still unknown and constitutes physics beyond the SM.

- The MiniBooNE collaboration has detected a 4.8σ excess of ν_e events in their neutrino detector [60–62]. This result will be discussed further in Section 4.1.

Each of the above anomalies is interesting on its own, but they are particularly interesting when considered as a group, since many of them may have common explanations. One of the most promising classes of models used to explain recent anomalies are leptoquark models. There is already an extensive literature of leptoquark solutions to the first four anomalies listed above (see Chapter 4 for references), but at the time of writing nothing has been said about leptoquark solutions to the MiniBooNE anomaly. Scalar leptoquarks in the context of MiniBooNE will be a major focus of Chapter 4.

PART 2:

TWIN HIGGS THEORIES

2 Twin Higgs Portal Dark Matter

This Chapter has been previously published in the *Journal of High Energy Physics (JHEP)*.
Author list: David Curtin, SG
DOI:10.1007/JHEP08(2021)009 [63].

Statement of individual contributions
In this project I did essentially all of the calculations, made all of the Figures, and wrote about 90% of the text. David Curtin and I were equally responsible for the editing process and final organization of sections.

Many minimal models of dark matter (DM) or canonical solutions to the hierarchy problem are either excluded or severely constrained by LHC and direct detection null results. In particular, Higgs Portal Dark Matter (HPDM) features a scalar coupling to the Higgs via a quartic interaction, and obtaining the measured relic density via thermal freeze-out gives definite direct detection predictions which are now almost entirely excluded [10]. The Twin Higgs solves the little hierarchy problem without coloured top partners by introducing a twin sector related to the Standard Model (SM) by a discrete symmetry. We generalize HPDM to arbitrary Twin Higgs models and introduce *Twin Higgs Portal Dark Matter* (THPDM), which features a DM candidate with an $SU(4)$-invariant quartic coupling to the Twin Higgs scalar sector. Given the size of quadratic corrections to the DM mass, its most motivated scale is near the mass of the radial mode. In that case, DM annihilation proceeds with the full Twin Higgs portal coupling, while direct detection is suppressed by the pNGB nature of the 125 GeV Higgs. For a standard cosmological history, this results in a predicted direct detection signal for THPDM that is orders of magnitude below that of HPDM with very little dependence on the precise details of the twin sector, evading current bounds but predicting possible signals at next generation experiments. In many Twin Higgs models, twin radiation contributions to $\Delta N_{\rm eff}$ are suppressed by an asymmetric reheating mechanism. We study this by extending the νMTH and XMTH models to include THPDM and compute the viable parameter space according to the latest CMB bounds. The injected entropy dilutes the DM abundance as well, resulting in additional suppression of direct detection below the neutrino floor.

2.1 Introduction

The electroweak hierarchy problem was the subject of an intense research program long before the discovery of the Higgs boson at the Large Hadron Collider (LHC) in 2012 [64, 65], and to this day the

apparent instability of the Higgs mass to large radiative corrections continues to strongly motivate the existence of new physics near the TeV scale. Several theories could explain the observed Higgs mass without excessive fine-tuning, both in the form of UV-complete models that guarantee naturalness up to the Planck scale, such as Natural SUSY [66–70] or Composite Higgs [71], as well as proposals like the Little Higgs [72, 73] that seek only to stabilize the Higgs sector up to an experimental cutoff of 5 - 10 TeV, where additional physics can make the theory natural to higher scales. However, all of these solutions predict TeV-scale particles with SM quantum numbers, in particular QCD colour, which have not yet been observed at the Large Hadron Collider (LHC) contrary to earlier expectation [74–84]. Canonical solutions to the hierarchy problem with new states heavy enough to satisfy LHC bounds would therefore exhibit significant fine-tuning, giving rise to the so-called "little hierarchy problem."

The most important contributions to the Higgs potential come from top quark loops. These dangerous contributions can be canceled by introducing top partners related to the top by a symmetry, predicting top partners charged under SM colour that should be produced by the LHC at high rates. The growing tension with experimental null results has led to the creation of a new class of models, called neutral naturalness models [34–41], whose partner particles are SM singlets, or at least not charged under SM colour. This is possible if the symmetry which relates the top and the top partner does not commute with SM colour. These models solve the little hierarchy problem by providing an explanation for how TeV-scale top partners may have so far evaded our searches. Most notable among these models are the Twin Higgs (TH) models [34–37, 39, 40], which cancel quadratically divergent loop corrections to the Higgs potential through the introduction of a twin sector, related via a discrete $\mathbb{Z}_2$ symmetry to the SM. The Higgs sector of the theory transforms under an approximate global $SU(4)$ symmetry, which is broken by the gauge and Yukawa couplings of each sector, and the form of the potential induces spontaneous breaking from $SU(4)$ to $SU(3)$. After gauging an $SU(2)$ $\times$ $SU(2)$ subgroup of the $SU(4)$, under which H transforms as (H_A, H_B), only 1 of the 7 pseudo-Nambu Goldstone bosons (pNGBs) remains in the spectrum – this can be identified as the 125 GeV Higgs. The most dangerous quadratically divergent one-loop corrections are always found in $\mathbb{Z}_2$-symmetric pairs, so these corrections to the potential exhibit an accidental $SU(4)$ symmetry. Since the 125 GeV Higgs is a pNGB of $SU(4)$ breaking, its mass is necessarily protected until two-loop effects become important, typically up to scales of 5-10 TeV.

Phenomenological constraints force us to softly break the $\mathbb{Z}_2$ symmetry in the Higgs sector, analogous to soft SUSY breaking terms in e.g. the MSSM [85]. The completely $\mathbb{Z}_2$-symmetric TH model predicts large couplings between the Higgs and twin matter and a significant reduction in Higgs couplings to visible matter compared to the SM prediction. However, these couplings are tightly constrained by precision electroweak measurements [86, 87], and couplings to the mirror sector are constrained by invisible branching ratio measurements. The latest results from ATLAS and CMS indicate $\text{Br}(h \to \text{invisible}) \lesssim 0.13$ at 95% CL [88, 89], and the high-luminosity (HL) upgrade is expected to

tighten this to $\sim 4\%$ at 95% CL [90]. To satisfy these bounds, soft $\mathbb{Z}_2$-breaking terms are introduced to misalign the vevs of the two sectors such that $v/f \lesssim 1/3$, where v is the electroweak vev and f is the vev of the full Higgs sector. This necessity comes at the price of a very modest $2v^2/f^2 \lesssim 20\%$ tuning in minimal models [35, 91], with further relaxation possible in certain constructions [92–95].

If the $SU(4)$ symmetry is linearly realized, then the radial mode of the breaking is present in the spectrum, hereafter called the "heavy Higgs" or "twin Higgs." Current and future measurements are expected to be sensitive to this signature, in particular through di-boson production at the HL-LHC [87, 95–100]. The MTH also admits a number of ultra-violet (UV) completions, including supersymmetric models [95, 101–107], holographic models [108], composite Higgs scenarios [91, 108–110], and extra-dimensional orbifold gauge theories [36, 111]. Many of these models predict heavy, exotic states that carry both visible and twin sector quantum numbers that can be searched for at colliders [112–114].

It is interesting to ask whether Twin Higgs solutions to the little hierarchy problems are capable of providing plausible dark matter (DM) candidates as well. Indeed, the twin tau lepton and neutrino, twin neutralino, twin baryons, twin $W^{\pm}$, twin mesons, and the twin neutron have all been proposed as potential sources for DM in various TH constructions [115–123], but some are already significantly constrained by the latest direct detection experiments [1, 2, 5].

In this paper, we examine the simple possibility of Scalar Higgs Portal Dark Matter (HPDM) [10, 124–126], which is now essentially excluded [127–129], in a Twin Higgs context. We define the Twin Higgs Portal Dark Matter (THPDM) scenario by adding a stable scalar S coupled to the extended Twin Higgs sector through the $SU(4)$-symmetric quartic interaction $\lambda_{HS} S^2 (H_A^2 + H_B^2)$. This interaction provides a portal between the DM scalar and the visible and twin matter sectors, allowing for both thermal annihilation in the early universe and direct detection. Just as for HPDM, for a given cosmological history and DM mass, reproducing the measured DM relic abundance yields a definite prediction for the coupling constant λ_{HS}, and therefore for direct and indirect detection observables. However, unlike simple HPDM, the twin nature of the Higgs sector significantly changes the phenomenology and parameter space of the THPDM scenario. In this paper, we carefully explore the direct detection parameter space of THPDM, for both standard and motivated non-standard cosmological histories.

The crucial difference between the HPDM and THPDM models arises from the pNGB nature of the 125 GeV Higgs. At low energies far below the mass scale of the radial mode, its couplings are dominated by small $SU(4)$- and $\mathbb{Z}_2$ breaking interactions in the Twin Higgs potential, while at higher energies these couplings are highly momentum dependent and unsuppressed. Therefore, if the DM scalar in THPDM has mass near or below the 125 GeV Higgs mass, it reproduces the phenomenology of HPDM, predicting direct detection signals that are already excluded. On the other hand, if the DM mass is of a similar scale as the mass of the Twin Higgs radial mode, then it annihilates with the unsuppressed λ_{HS} coupling but scatters in direct detection experiments with the suppressions

arising from the pNGB nature of the 125 GeV Higgs. Compared to the HPDM scenario, this leads to a drastic reduction in the expected direct detection signal. Crucially, it is this latter scenario that is strongly favoured by naturalness considerations within the Twin Higgs setup, since loop corrections drive the DM scalar mass towards the mass scale of the radial mode. Within the THPDM scenario, we therefore do not expect direct detection signals in current experiments. On the other hand, a signal in next generation experiments such as LUX-Zeplin (LZ) [4], XENONnT [5], and DARWIN [6] is predicted across large regions of THPDM parameter space. This suppression of direct detection signals is also completely general for any DM candidate that couples to the Twin Higgs scalar sector in an $SU(4)$ invariant way, since it arises from the pNGB nature of the Higgs. [6]

The exact predictions for direct detection depend on the cosmological history of the Twin Higgs. The minimal Mirror Twin Higgs (MTH) predicts light degrees of freedom present during Big Bang Nucleosynthesis (BBN) [145] that are completely excluded by measurements of $\Delta N_{\text{eff}} \leq 0.23$ (at 2σ) [11]. A class of models that includes the Fraternal Twin Higgs [35, 37] solves this with hard $\mathbb{Z}_2$-breaking to remove light degrees of freedom while preserving a standard cosmological history, meaning direct detection signals of THPDM are uniquely determined by the DM mass. On the other hand, in the asymmetrically reheated Mirror Twin Higgs [12, 145, 146], the twin sector contribution to ΔN_{eff} is reduced by some massive, long-lived particle species that decays preferentially to the visible sector at late times, reducing the number density of twin radiation. In this departure from standard cosmology the DM relic abundance is diluted alongside the twin sector, implying that a smaller coupling during freeze out is required to match the observed density today.[7] This possibility further suppresses direct detection signatures of THPDM, anywhere from within the expected range of next generation direct detection experiments to below the neutrino floor. We review two explicit models of asymmetric reheating, the νMTH [145] and the XMTH [12], update bounds on their parameter space, and show how DM dilution is correlated with ΔN_{eff} signals. In such scenarios, direct detection of DM could be very challenging, but we would expect to detect the small but nonzero deviation in ΔN_{eff} at upcoming CMB-S4 experiments [14].

The paper is structured as follows. In Sections 2.2 and 2.3 we briefly review relevant details of Twin Higgs models and singlet Scalar Higgs Portal DM (HPDM). In Section 2 we define the THPDM scenario, analytically demonstrate the suppression mechanism for direct detection, and compare predictions for direct detection experiments to HPDM. Section 2.5 is devoted to THPDM models with asymmetric reheating. We conclude in Section 2.6.

[6] This suppression of direct detection signatures due to pNGB dynamics is reminiscent of pNGB-DM models, which typically feature either the Higgs and the DM both as pNGBs as in [130–136], or with only the DM as a pNGB as in [137–143]. To the best of our knowledge, our study is the first to encounter this phenomenon due to the Higgs but not the DM being a pNGB (although simply adding a Higgs-portal DM candidate to any composite Higgs model would achieve the same effect). Furthermore, the general idea of suppressing direct detection by enhancing the relative annihilation rate at early times has also been studied before, see e.g. [66, 73, 144].

[7] Alternatively, if dark matter is frozen in rather than a thermal relic, asymmetric reheating may help with achieving the correct abundance [147].

2.2 Twin Higgs Models

Twin Higgs models solve the little hierarchy problem through the introduction of a twin sector of new particles, whose structure is related by a discrete symmetry to the structure of the Standard Model. The original proposal for a Twin Higgs model was the Mirror Twin Higgs (MTH) [34], which features an extended gauge symmetry $SU(3)_A \otimes SU(2)_A \otimes U(1)_A \otimes SU(3)_B \otimes SU(2)_B \otimes U(1)_B$, where the SM fields are charged under SM_A gauge groups and an exact $\mathbb{Z}_2$-symmetric copy of the SM matter sector is charged under the SM_B gauge groups. Other varieties, mostly with varying degrees of hard $\mathbb{Z}_2$ breaking to modify the twin matter spectrum, have been proposed [35, 37, 148, 149] to solve the cosmological problems of the original setup. Here we review the basic Twin Higgs setup and the properties of the scalar sector that are common to most of these constructions and instrumental to the Twin Higgs Portal Dark Matter mechanism. We then comment on two benchmark scenarios for realistic Twin Higgs models, the Fraternal Twin Higgs [35] and the Asymmetrically Reheated Mirror Twin Higgs [12, 145], that we use to explore THPDM scenarios in this paper.

We follow mainly the exposition in Ref. [96], taking the extended Higgs sector to transform linearly as a global $SU(4)$ fundamental

$$H = \begin{pmatrix} H_A \\ H_B \end{pmatrix},$$

where A denotes the SM or visible sector and B denotes the twin sector. We denote the vacuum expectation values of these fields $\frac{1}{\sqrt{2}}v_A$, $\frac{1}{\sqrt{2}}v_B$. The full potential includes terms that both spontaneously and explicitly break the $SU(4)$, required to satisfy current bounds on Higgs phenomenology. It is given by

$$V = \lambda\left(H_A^\dagger H_A + H_B^\dagger H_B - \frac{f_0^2}{2}\right)^2 + \kappa\left(\left(H_A^\dagger H_A\right)^2 + \left(H_B^\dagger H_B\right)^2\right) + \sigma f_0^2 H_A^\dagger H_A. \tag{2.1}$$

Note the soft $\mathbb{Z}_2$ and $SU(4)$ breaking term σ, which we discuss further below. The λ term spontaneously breaks $SU(4)$ to $SU(3)$, generating 7 Nambu-Goldstone bosons (NGBs) in the process. Six of these are eaten by the electroweak bosons $W^\pm_{A,B}$, $Z_{A,B}$ of each sector, while the seventh remains uneaten and will eventually be identified as the observed 125 GeV Higgs. The spontaneous breaking of $SU(4)$ will also give rise to a massive radial mode with $m = \sqrt{2\lambda} f_0$ for $\sigma = \kappa = 0$, which can be integrated out in a non-linear sigma model (NLSM) effective description far below the symmetry breaking scale. We work in the linear sigma model (LSM) description where the radial mode is included in the spectrum, in order to understand its effect on THPDM freeze–out in a perturbative Twin Higgs construction. However, the NLSM picture will be helpful to understand key features of THPDM phenomenology, making manifest the pseudo-Goldstone nature of the Higgs (see Section 2.4.1).

If we are going to identify the NGB as the 125 GeV Higgs then the $SU(4)$ symmetry must be explicitly broken. This is done by introducing the κ and σ terms; the former induces a hard $SU(4)$ breaking, and the latter softly breaks both the $\mathbb{Z}_2$ and $SU(4)$ symmetries. In order to avoid unreasonable levels of fine-tuning, we demand that the symmetry-breaking coefficients always be smaller than the symmetry-preserving ones, $\kappa, \sigma \ll \lambda$. The κ term in the potential explicitly breaks $SU(4)$ but preserves the $\mathbb{Z}_2$ symmetry. This generates a small mass for the surviving NGB, rendering it instead a pseudo-Nambu Goldstone boson (pNGB) and allowing us to identify it as the 125 GeV Higgs. One-loop corrections to the Higgs potential must have the form

$$\Delta V_{\text{top}} = \frac{3\Lambda^2}{8\pi^2}\left(y_A^2 H_A^\dagger H_A + y_B^2 H_B^\dagger H_B\right) \tag{2.2}$$

where the $\mathbb{Z}_2$ symmetry enforces $y_A = y_B$, which is insensitive to soft $\mathbb{Z}_2$ breaking. These quadratic corrections therefore have an *accidental* $SU(4)$ symmetry and cannot affect the light Higgs degree of freedom, making it a pNGB of an accidental global symmetry. Note that this effect operates only at one-loop, so a UV completion to solve the big Hierarchy Problem is needed above scales of 5-10 TeV where two-loop effects become relevant; see e.g. [36, 91, 95, 101–108, 108–111].

The σ term breaks both $\mathbb{Z}_2$ and $SU(4)$, and its primary role is to misalign the vacuum. Without this term, the potential would be $\mathbb{Z}_2$ symmetric and the light pNGB would be shared equally between both sectors in field space, with $v_A = v_B$. In this case we would expect two related effects to occur: the couplings between the SM Higgs and the matter content of both sectors would become equal, and the size of the Higgs couplings to the SM would be reduced by a factor $1/\sqrt{2}$ relative to the SM prediction. However, the Higgs-SM couplings are already tightly constrained by precision electroweak measurements [86, 87], and current measurements find $\text{Br}(h \to \text{invisible}) \lesssim 0.13$ at 95% CL [88, 89], limiting the possible size of Higgs couplings to the mirror sector. It is therefore necessary to break the $\mathbb{Z}_2$ such that $\langle H \rangle$ lies mostly along the B direction, $v_B \gg v_A$. Dynamical methods of $\mathbb{Z}_2$ breaking are explored for example in [92, 93, 150–153], and these could easily be incorporated into our discussion, but we simply parameterize the soft $\mathbb{Z}_2$ breaking by adding the σ term. Regardless of the $\mathbb{Z}_2$-breaking origin, the result is that the couplings between the SM Higgs and the mirror sector are reduced, and the Higgs-SM couplings approach the SM prediction. Satisfying experimental constraints requires $v_A/v_B \lesssim 1/3$, while Refs. [35, 91] show that the tuning of the theory is roughly $2v^2/f^2$, where $f^2 = v_A^2 + v_B^2$ and $v \equiv v_A = 246$ GeV. With this in mind we consider a range of f/v from 3 to roughly 7 as being most motivated, which is within experimental limits and corresponds roughly to a tuning range of $4 - 20\%$.

We next examine the mass eigenstates of the theory. Minimizing the potential as in [96] leads to

nonzero vevs in both sectors:

$$v_A = \sqrt{2}\,\langle H_A \rangle = f_0 \sqrt{\frac{\kappa\lambda - (\kappa+\lambda)\sigma}{\kappa\,(\kappa+2\lambda)}} \tag{2.3}$$

$$v_B = \sqrt{2}\,\langle H_B \rangle = f_0 \sqrt{\frac{\lambda(\kappa+\sigma)}{\kappa\,(\kappa+2\lambda)}} \tag{2.4}$$

and the fluctuations about the vacuum can be parameterized in the unitary gauge by

$$H_A = \frac{1}{\sqrt{2}} \begin{bmatrix} 0 \\ v_A + h_A \end{bmatrix} \quad , \quad H_B = \frac{1}{\sqrt{2}} \begin{bmatrix} 0 \\ v_B + h_B \end{bmatrix}. \tag{2.5}$$

To find the resulting mass eigenstates we diagonalize the potential through a rotation angle θ,

$$\begin{pmatrix} h_- \\ h_+ \end{pmatrix} = \begin{pmatrix} \cos\theta & -\sin\theta \\ \sin\theta & \cos\theta \end{pmatrix} \begin{pmatrix} h_A \\ h_B \end{pmatrix} \tag{2.6}$$

which yields two mass eigenstates with masses given by

$$m_\pm^2 = f^2\,(\kappa+\lambda) \pm \sqrt{\left(v_B^2 - v_A^2\right)^2 (\kappa+\lambda)^2 + 4\lambda^2 v_A^2 v_B^2}. \tag{2.7}$$

Note that in the $SU(4)$-symmetric limit with $\kappa = \sigma = 0$ we recover a massless mode $m_- = 0$ and a radial mode with $m_+ = 2\lambda f^2$. The mixing angle θ is conveniently written as

$$\tan(2\theta) = \frac{2 v_A v_B}{\left(v_B^2 - v_A^2\right)(1+\kappa/\lambda)} = \frac{(2v/f)\sqrt{1 - v^2/f^2}}{(1 - 2v^2/f^2)\,(1+\kappa/\lambda)}. \tag{2.8}$$

In the limit that $\kappa \ll \lambda$ and $v/f \ll 1$, the mixing angle becomes $\theta \approx v/f$ and the mass eigenstates of the theory take the simple form

$$h_- \equiv h = \cos(v/f) h_A - \sin(v/f) h_B \tag{2.9}$$

$$h_+ \equiv \hat{h} = \sin(v/f) h_A + \cos(v/f) h_B \tag{2.10}$$

From here it can be seen that couplings between h and the visible sector will be modified by a factor of $\cos(v/f)$. The implication is that in this model the 125 GeV Higgs is in fact *mostly* the SM Higgs, but with a small twin Higgs component. As mentioned above, this mixing leads to predictions for invisible Higgs branching ratios and precision electroweak measurements.

It is well known that the original Mirror Twin Higgs model is thoroughly excluded by cosmological measurements (see e.g. [12, 145, 146]), since light mirror neutrinos and mirror photons produce

very large contributions to $\Delta N_{\rm eff}$. In realistic Twin Higgs models, this is addressed in one of two ways: either by removing or lifting the light degrees of freedom in the mirror sector, or by invoking a non-standard cosmological history which reduces mirror sector contributions to $\Delta N_{\rm eff}$.

Hard $\mathbb{Z}_2$ breaking, mostly in the fermion sector, can lift or eliminate light degrees of freedom. Since cancellations of the gauge and top loops corrections to the Higgs potential are the most important for naturalness, the $\mathbb{Z}_2$ symmetry can be broken for any of the lighter degrees of freedom in the twin spectrum. They can be removed or made heavier, which eliminates the problematic cosmology of the Mirror Twin Higgs. The Fraternal Twin Higgs (FTH) model [35] is in a sense the most minimal or extreme example of such an approach, eliminating the mirror photon and the first two mirror matter generations, but less extreme solutions with many mirror states at collider scales have also been considered [37, 117, 154]. Amongst the remaining states, only the mirror top mass has to be in agreement with the $\mathbb{Z}_2$ symmetry – the mirror bottom, mirror tau and mirror tau neutrino masses are left as free parameters. Thus there may be no sources of twin radiation during BBN, and bounds on $\Delta N_{\rm eff}$ can be trivially satisfied. The collider phenomenology of TH models without cosmological problems can be radically different from the MTH. In particular, the absence of light twin degrees of freedom can lead to the presence of long-lived particles in the twin spectrum, such as twin glueballs or twin bottomonium in the FTH [35]. These states can only decay through the small Higgs portal coupling that is required by naturalness, making them meta-stable. It has been shown [112, 155] that displaced vertex searches in ATLAS, CMS, or LHCb [156–160], or in external transverse LLP detectors for the HL-LHC like MATHUSLA and CODEX-b [161–164], can discover these states for FTH-type models with top partner masses in excess of a TeV. Other TH constructions with hard $\mathbb{Z}_2$ breaking can also give rise to a variety of LLP signatures, including decays via the twin photon portal [112].

The cosmological history in Mirror Twin Higgs models can be easily modified by including a source of asymmetric reheating [12, 145] while maintaining a $\mathbb{Z}_2$ symmetric twin spectrum. As mentioned in the introduction, these models feature late-decaying particles that can preferentially reheat the visible sector relative to the twin sector after the Higgs portal freezes out, thereby reducing the twin sector's contribution to $\Delta N_{\rm eff}$. If there is a small twin baryon asymmetry (motivated by the $\mathbb{Z}_2$ symmetry), these twin baryons could constitute a fraction of dark matter [117, 119, 165–170], though self-interaction bounds usually preclude them from making up its entirety. This leads to a rich array of cosmological signatures like mirror baryonic oscillations and their imprints in Large Scale Structure and the CMB [146], as well as potentially spectacular astrophysical predictions like the existence and observability of mirror stars [171, 172]. The asymmetric reheating also has important direct implications for dark matter direct detection, since any existing dark matter population is diluted alongside the twin sector. This can have important implications for direct detection experiments, since in many prominent dark matter models the coupling that controls the freeze-out abundance is the same one that is probed in the laboratory. Dilution of dark matter is a major point of interest in our analysis.

The Twin Higgs Portal Dark Matter mechanism is a general consequence of the Twin Higgs

setup. After briefly reviewing scalar Higgs Portal Dark Matter in Section 2.3, we therefore study the phenomenology of THPDM first by assuming standard cosmological history in Section 2.4 for two extreme cases of twin sectors, FTH-like and MTH-like. The former is the most minimal twin sector that can solve the little hierarchy problem, while the latter is a stand-in for a TH construction with the smallest hard $\mathbb{Z}_2$-breaking necessary to solve the $\Delta N_{\rm eff}$ problem. The results will depend only very weakly on details of the twin spectrum. In Section 2.5 we study the asymmetrically reheated scenario in detail, reviewing and extending calculations in the literature for the νMTH [145] and XMTH [12] and demonstrating the additional effect of DM dilution on the THPDM scenario.

2.3 Scalar Higgs Portal Dark Matter

The singlet-scalar Higgs portal DM (HPDM) [10, 124–126] scenario is one of the simplest models of dark matter.[8] The only addition to the SM is a minimal coupling of a stable scalar particle S to the Higgs through the potential

$$V = \frac{1}{2}m_S^2 S^2 + \frac{1}{4!}\lambda_S S^4 + \frac{1}{2}\lambda_{HS} H^\dagger H S^2. \tag{2.11}$$

Electroweak symmetry breaking then induces a 3-point interaction term between the Higgs and the scalar, $\left(\frac{1}{2}\lambda_{HS} v\right) h S^2$, which enables it to freeze out in the early universe via Higgs-mediated annihilation into SM particles. This gives rise to a relic density today of

$$\Omega_0 = \frac{1}{3M_{Pl}^2 H_0^2} m Y_0 s_0 \tag{2.12}$$

where s_0 is the current entropy density, H_0 is the current value of the Hubble parameter, and Y_0 is the present number of dark matter particles per comoving volume, defined $Y_0 \equiv \frac{n_0}{s_0}$. When comoving entropy is conserved, Y remains constant as the universe evolves. If comoving entropy is conserved at all times between freeze out and today, then $Y_0 = Y_f$ (where f stands for freeze-out) and

$$\Omega_0 = \frac{1}{3M_{Pl}^2 H_0^2} m Y_f s_0. \tag{2.13}$$

In the freeze-out paradigm the relic density of dark matter is directly related to its annihilation cross section, $\Omega_0 \sim Y_f \sim 1/\langle\sigma v\rangle$. The thermally averaged cross section is [176]

$$\langle\sigma v\rangle = \frac{1}{8m_S^4 T K_2^2\left(m_S/T\right)} \int_{4m_S^2}^{\infty} \mathrm{d}s\, \sigma(s)\left(s - 4m_S^2\right)\sqrt{s} K_1\left(\sqrt{s}/T\right) \tag{2.14}$$

[8] Note that we do not study fermionic HPDM that couples to the Higgs via a non-renormalizable operator $\frac{1}{\Lambda}|H|^2\bar{\psi}\psi$ (see e.g. [173–175]), but we expect the THPDM mechanism to work similarly for this case as well.

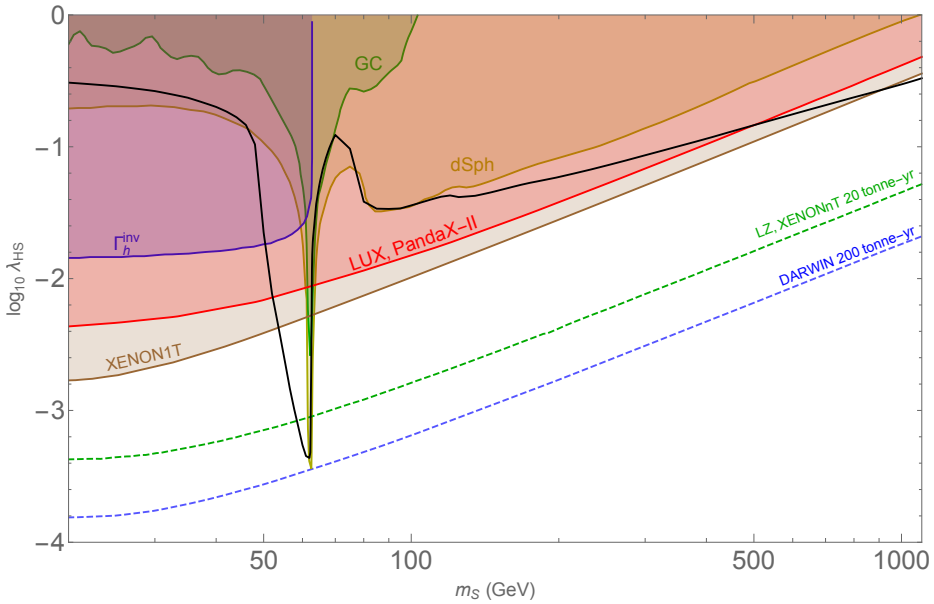

Figure 1. Direct and indirect detection constraints for singlet scalar Higgs portal dark matter (HPDM). Current direct detection constraints include LUX, PandaX-II [1, 2] (red) and XENON1T [3] (brown); projected direct detection constraints from LUX-Zeplin (LZ) [4] and XENONnT [5] after 20 tonne-years are shown in dashed green, while 200 tonne-year projections from DARWIN are shown in dashed blue [6]. Indirect detection constraints from the Galactic Center (GC) and spheroidal dwarf galaxies (dSph) come from Fermi-LAT data [7, 8] and are shown in dark green an orange respectively, while CMS constraints on the Higgs invisible decay width [9] are shown in blue. Constraints from GC, dSph, LUX, LZ and Γ_h^{inv} are derived in Ref. [10], while the XENON1T, XENONnT, and DARWIN bounds were added in the present work. The black curve indicates the expected coupling λ_{HS} for varying DM mass consistent with the observed DM relic density $\Omega h^2 = 0.120 \pm .001$ [11] (error bar on curve negligible), assuming that the scalar comprises all of DM.

where s is the squared center-of-mass energy, $\sigma(s)$ is the center-of-mass annihilation cross section, T is the temperature of the thermal bath, and the K_1, K_2 are modified Bessel functions of the second kind. Its exact relation to Y_f can then be found either by solving the Boltzmann equation numerically or through an analytical approximation, as done e.g. in [45]. In this work we follow the latter approach and find good agreement with known results.

At tree level, the total thermally averaged cross section $\langle \sigma v \rangle$ is simply proportional to λ_{HS}^2. Since larger annihilation cross sections lead to a smaller relic abundance today, the measured relic abundance of $\Omega h^2 = 0.120 \pm .001$ [11] leads to a prediction for the coupling λ_{HS} as a function of mass m_S, shown in Figure 1 as the black curve. This prediction reproduces known results from the literature, e.g. [10]. The curve was generated under the assumption that the scalar constitutes all of the dark matter; if the scalar dark matter fraction is $r < 1$, λ_{HS} is larger by a factor of $1/\sqrt{r}$. The cross section for scalar annihilation into visible matter was computed mainly following Ref. [128], and includes all 2-2 tree level processes as well as QCD one-loop corrections for all quark final states.

The coupling λ_{HS} can be probed by both direct and indirect detection experiments. Apart from the Higgs resonance, direct detection experiments constitute the dominant probe of the $\{\lambda_{HS}, m_S\}$ parameter space and there are many current and planned experiments aiming to constrain this space. The spin-independent direct detection cross section for scalar HPDM is [128]

$$\sigma = \frac{1}{4\pi} \frac{\lambda_{HS}^2 f_N^2}{m_h^4} \frac{\mu^2 m_N^2}{m_S^2} \tag{2.15}$$

where m_N is the nucleon mass, $\mu = \frac{m_N m_S}{m_N + m_S}$ is the reduced mass, and f_N encodes the individual quark contributions in the Higgs-nucleon coupling, $\frac{f_N m_N}{v}$. It is defined in [128] as

$$f_N = \sum_q \frac{m_q}{m_N} \langle N | \, \bar{q} q \, | N \rangle \, . \tag{2.16}$$

As shown in Figure 1, the parameter space of this model has been almost entirely excluded by Xenon1T, LUX, and PandaX-II [1, 2, 5], with DM masses above a TeV and the small window near the Higgs resonance expected to be covered by LZ, XENON and Darwin in the near future [4–6]. We now show in the next section how the HPDM idea, when applied to Twin Higgs models, automatically leads to suppressed direct detection signatures due to the pNGB nature of the Higgs. This evades current bounds but could be discoverable in future experiments.

2.4 Twin Higgs Portal Dark Matter

We now construct a Twin Higgs version of the scalar Higgs Portal DM model by simply adding a real singlet scalar particle that couples to the Twin Higgs scalar sector in an $SU(4)$-invariant way. The full potential is

$$V = V_{\rm TH} + V_{\rm S} \tag{2.17}$$

where $V_{\rm TH}$ is the Twin Higgs potential given by Equation (2.1), and

$$V_S = \frac{1}{2}\mu_S^2 S^2 + \frac{1}{2}\lambda_{HS} S^2 \left(H_A^\dagger H_A + H_B^\dagger H_B \right) . \tag{2.18}$$

We expect that a UV complete Twin Higgs model could be extended to give rise to this Lagrangian, but leave explicit construction of such a model to future investigations. To ensure S is stable we require it to be odd under an unbroken $\mathbb{Z}_2$ symmetry $S \to -S$. In UV completions this could arise as a subgroup of a larger symmetry (like $U(1)$ if S is complex), but this would not qualitatively change our analysis. We will consider this scalar potential for both an MTH-type model (where the mirror sector is a $\mathbb{Z}_2$ copy of the SM, except for the soft $\mathbb{Z}_2$ breaking term in $V_{\rm TH}$ necessary to ensure $v_B > v_A$) and an FTH-type model where the twin photon and first two twin matter generations have

been removed. The physical mass of the singlet is

$$m_S^2 = \mu_S^2 + \frac{1}{2}\lambda_{HS} f^2 \tag{2.19}$$

and we require this to be positive to ensure S does not acquire a vev and become unstable.

2.4.1 Pseudo-Goldstone Suppression of Direct Detection

The pseudo-Goldstone nature of the 125 GeV Higgs boson radically changes the phenomenology of Higgs portal dark matter in our scenario. This is most apparent in the non-linear sigma model picture. Since S couples in an $SU(4)$-invariant way, any non-derivative couplings to the light Higgs can only arise due to small explicit symmetry-breaking interactions. For $m_S \ll m_{\hat{h}}$, both SS annihilation in the early universe and scattering off nuclei via Higgs exchange in direct detection are dictated entirely by these small interactions, and the ratio between annihilation and direct detection cross sections is identical to HPDM. Therefore, the predictions of the direct detection signal for a given DM relic abundance are the same in THPDM as in HPDM for $m_S \ll m_{\hat{h}}$. On the other hand, for $m_S \gtrsim \frac{1}{2} m_{\hat{h}}$, annihilation of the singlets can now excite the radial mode, and the NLSM picture involving only exchange of the pNGB via small explicit symmetry-breaking interactions breaks down. SS annihilation is now dictated by the unsuppressed $SU(4)$-symmetric coupling λ_{HS}, while direct detection is still suppressed by the pseudo-Goldstone nature of the Higgs, since nuclear scattering is always a low-energy process. Relative to the scattering cross section, the annihilation cross section is now drastically enhanced. Therefore, to reproduce the correct relic abundance, λ_{HS} must be much smaller for $m_S \gtrsim \frac{1}{2} m_{\hat{h}}$ than for $m_S \ll m_{\hat{h}}$, which reduces direct detection signatures. For $m_S > m_h$, THPDM can evade current bounds on direct detection while being potentially detectable in future experiments.

We now demonstrate this mechanism analytically within the linear sigma model picture of the Twin Higgs scalar sector outlined in Section 2.2, and then present numerical predictions for direct detection of THPDM that confirm these arguments.

After electroweak symmetry breaking it is easy to show that the potential in Equation (2.18) takes the form

$$V_S = \frac{1}{2}\lambda_{HS} S^2 \left[h\left(v_A \cos\theta - v_B \sin\theta\right) + \hat{h}\left(v_A \sin\theta + v_B \cos\theta\right) + \frac{1}{2}h^2 + \frac{1}{2}\hat{h}^2 + \frac{1}{2}f^2 \right] \tag{2.20}$$

where we use the results of Section 2.2 and note that $f^2 = v_A^2 + v_B^2$. Defining

$$\lambda_{SSh} \equiv \lambda_{HS} \times \left(v_A \cos\theta - v_B \sin\theta\right) \tag{2.21}$$

$$\lambda_{SS\hat{h}} \equiv \lambda_{HS} \times \left(v_A \sin\theta + v_B \cos\theta\right) \tag{2.22}$$

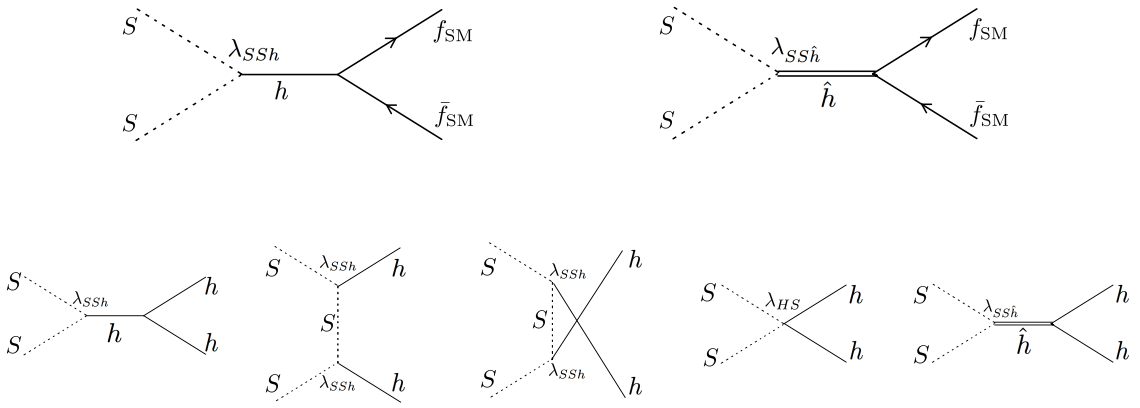

Figure 2. *Top*: contributions to $\mathcal{A}(SS \to \bar{f}_{\rm SM} f_{\rm SM})$. The first diagram dominates in the $v^2/f^2 \ll 1$ limit but vanishes in the $SU(4)$ and $\mathbb{Z}_2$ symmetric limit. *Bottom*: contributions to $\mathcal{A}(SS \to hh)$. In the $SU(4)$ and $\mathbb{Z}_2$ limit the first three diagrams are zero, while the last two cancel in the $SU(4)$ and $\mathbb{Z}_2$ limit with $s \to 0$.

we can show via Equation (2.8) that to first order in the $SU(4)$-violating coupling κ,

$$\lambda_{SSh} = \lambda_{HS} \left(\frac{\kappa}{\lambda}\right) v \left(1 - 2v^2/f^2\right) \left(1 - v^2/f^2\right)^{1/2} + \mathcal{O}\left(\frac{\kappa^2}{\lambda^2}\right) \tag{2.23}$$

$$\lambda_{SS\hat{h}} = \lambda_{HS} f + \mathcal{O}\left(\frac{\kappa^2}{\lambda^2}\right) \tag{2.24}$$

where we recall $v \equiv v_A$ in the LSM. Note that the $\lambda_{SS\hat{h}}$ coupling of the DM scalar to the heavy Higgs $\hat{h}$ is unsuppressed, while the same coupling to the light Higgs, λ_{SSh}, is only generated if there is both explicit $SU(4)$ breaking (i.e. $\kappa \neq 0$) and explicit $\mathbb{Z}_2$ breaking (i.e. $v \neq f/\sqrt{2}$). In particular, λ_{SSh} is suppressed by the small ratio κ/λ, and is simply $\lambda_{HS} v(\kappa/\lambda)$ to first order in v/f.

To elucidate the THPDM mechanism, let us first demonstrate how the HPDM phenomenology is recovered in the $m_S \ll m_{\hat{h}}$ limit. In that case, SS annihilation to the SM dominates, and the relevant diagrams are shown in Figure 2. The top two diagrams contribute to annihilation into SM fermions, and are (up to crossing symmetry) the same as the h- and $\hat{h}$-mediated diagrams that give the direct detection cross section. The h-mediated diagram is suppressed only by the small λ_{SSh} coupling, while the $\hat{h}$-mediated diagram is suppressed by the higher mass of the heavy Higgs, as well as its smaller coupling to SM fermions. In the low-momentum limit, the ratio of the second to the first diagram is

$$\frac{\lambda_{SS\hat{h}} \sin\theta / m_{\hat{h}}^2}{\lambda_{SSh} \cos\theta / m_h^2} \approx \lambda^2 \frac{v^2}{f^2} \ll 1 \tag{2.25}$$

if $v^2/f^2 \ll 1$, which is a reasonable approximation for our parametric arguments. We can therefore

assume that both annihilation into fermions and nuclear scattering in direct detection is dominated by h-exchange.

The bottom five diagrams in Figure 2 contribute to annihilation into two Higgs bosons $SS \to hh$, which is relevant if $m_S > m_h$. The first three diagrams have exact equivalents in the HPDM model. The last two are unique to the Twin Higgs setup, but together are equivalent to the quartic $SShh$ diagram in HPDM. The appearance of the fifth diagram in the THPDM calculation can be seen as an artifact of using the Linear Sigma Model picture,[9] since in the NLSM formulation the $SShh$ and $\hat{h}hh$ couplings are zero in the symmetric limit for a Goldstone h. In the LSM this requirement manifests instead as a cancellation between the last two diagrams. Explicitly, their combined amplitude is

$$\mathcal{A} = -i\lambda_{HS}\left[1 + \frac{2f}{s - m_{\hat{h}}^2}\left(v_A\left[\lambda\sin^3\theta + 3\kappa\sin\theta\cos^2\theta\right] + v_B\left[\lambda\cos^3\theta + 3\kappa\sin^2\theta\cos\theta\right]\right)\right], \tag{2.26}$$

which, to first order in κ/λ and $s \to 0$, reduces to

$$\mathcal{A} \approx -i\lambda_{HS}\frac{\kappa}{\lambda}\left(1 - \frac{8v^2}{f^2} + \frac{8v^4}{f^4}\right) \tag{2.27}$$

demonstrating that the 4-point interaction is generated by explicitly breaking the $SU(4)$.

The $s \to 0$ limit is relevant when $m_S \ll m_{\hat{h}}$. In this regime we can plainly see the connection between THPDM and HPDM: up to $\mathcal{O}\left(v^2/f^2\right)$ corrections, the SSh and $SShh$ couplings in THPDM are simply a factor of κ/λ smaller than the corresponding HPDM couplings, since the 125 GeV Higgs is a pNGB of the approximate $SU(4)$. However, the two couplings behave differently in the $\mathbb{Z}_2$ limit, since in this limit $h = \frac{1}{\sqrt{2}}\left(h_A - h_B\right)$ is odd, meaning SSh vanishes but $SShh$ does not.

It is now easy to understand what happens when m_S approaches or exceeds $\frac{1}{2}m_{\hat{h}}$. The Goldstone suppression demonstrated in Equation (2.27) breaks down, and annihilation to all kinematically accessible final state particles proceeds dominantly through the radial mode $\hat{h}$ via the unsuppressed coupling λ_{HS}.[10] Direct detection, by contrast, is still only determined by the suppressed λ_{SSh} coupling, and so to match the observed relic density λ_{HS} must be significantly smaller, leading to reduced direct detection signatures.

2.4.2 Direct Detection Predictions for THPDM

We now derive numerical predictions for direct detection of THPDM and compare to HPDM. SS annihilation is computed as outlined in Section 2.3, as a function of $\lambda_{HS}, m_S, f/v, m_{\hat{h}}$, which yields a prediction for the coupling λ_{HS} required to obtain the measured DM relic density. Making use of the fact that momentum exchange is negligible compared to the $h, \hat{h}$ masses, the direct detection cross

[9] We thank Jack Setford for bringing this to our attention.

[10] Annihilation is of course further enhanced at high masses since S can now annihilate to many more degrees of freedom in both the visible and twin sectors, but this effect is less important than the breakdown of the pNGB-suppression.

section in THPDM is

$$\sigma = \frac{1}{4\pi}\frac{f_N^2}{v^2}\left[\frac{\lambda_{SSh}\cos\theta}{m_h^2} + \frac{\lambda_{SS\hat{h}}\sin\theta}{m_{\hat{h}}^2}\right]^2 \frac{\mu^2 m_N^2}{m_S^2}. \tag{2.28}$$

In the language of effective field theory, both theories contain the same low energy operator, $S^2\bar{N}N$, whose coefficient is constrained by experiment regardless of what UV physics gives rise to that operator. Comparing Equations (2.28) and (2.15), we therefore see that THPDM predictions for direct detection can be shown in the same coupling-mass plane as for the HPDM if we parameterize the $S^2\bar{N}N$ operator via an an effective coupling to nucleons given by

$$\lambda_{\text{eff}}^2 \equiv \frac{m_h^4}{v^2}\left[\frac{\lambda_{SSh}\cos\theta}{m_h^2} + \frac{\lambda_{SS\hat{h}}\sin\theta}{m_{\hat{h}}^2}\right]^2. \tag{2.29}$$

For a given $m_S, f/v, m_{\hat{h}}$, this effective coupling is predicted by the observed DM relic density. This coupling reduces to $\lambda_{\text{HS}}\kappa/\lambda \approx \lambda_{SSh}/v$ in the $\theta \to 0$, or $f \gg v$, limit, consistent with the substitution required to recover the HPDM phenomenology for $m_S \ll m_{\hat{h}}$ explained above.

Our results are shown in Figure 3, for both MTH- and FTH-type mirror spectra. The breakdown of the NLSM picture in SS annihilation for m_S approaching or exceeding $\frac{1}{2}m_{\hat{h}}$ is clearly visible, resulting in a decrease in the effective predicted DM-nucleon coupling by one to two orders of magnitude compared to HPDM. This suppression is most pronounced near the $m_S \approx \frac{1}{2}m_{\hat{h}}$ resonance. It is interesting to note that THPDM becomes easier to discover in direct detection for larger f/v, providing an important complementarity to collider constraints on f/v from Higgs coupling measurements and invisible or exotic decay searches, which lose sensitivity for larger f/v. The difference between MTH- and FTH-type mirror sectors is minimal, since the FTH contains the states most important for solving the hierarchy problem and hence having the largest coupling to the scalar sector. This makes the direct detection predictions of THPDM robust with respect to the details of the twin spectrum. Future generations of experiments like LZ, XENONnT and DARWIN, together with collider searches, will be able to probe most of the THPDM parameter space in the coming years.

The calculations in this section assumed standard cosmology, as would be the case for Twin Higgs models with sufficient hard $\mathbb{Z}_2$ breaking to eliminate the problem of large ΔN_{eff} contributions from light twin degrees of freedom. In Section 2.5 we will examine Twin Higgs models that solve these cosmological issues with asymmetric reheating. We will see that this dilutes DM abundance and suppresses direct detection further – additionally, in the event of a positive signal the magnitude of dilution could actually be measured via the reduced direct detection cross section, in combination with cosmological and collider measurements. This would serve as a probe of the non-standard cosmological history in Twin Higgs models.

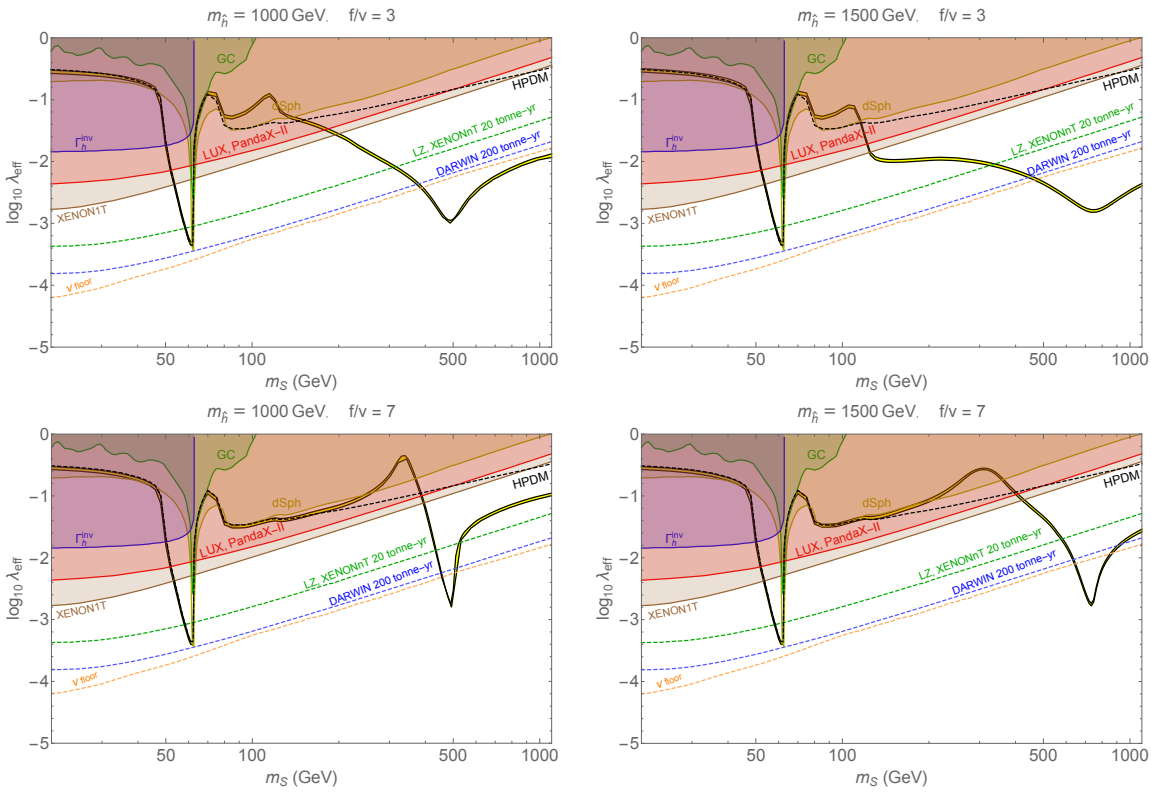

Figure 3. Parameter space for the Twin Higgs Portal Dark Matter (THPDM). The yellow band represents the effective coupling between the dark matter S and a nucleon that is consistent with the observed relic abundance of dark matter; the upper edge of the yellow band is for the reduced particle content of the Fraternal Twin Higgs (FTH) model, while the lower edge was computed for the full Mirror Twin Higgs (MTH). Experimental constraints are the same as those in Figure 1. For comparison, the singlet-scalar Higgs Portal DM (HPDM) curve is shown in dashed black.

2.4.3 Natural Mass of Twin Higgs Portal Scalar Dark Matter

Since the DM scalar S couples to the Twin Higgs scalar sector in an $SU(4)$-invariant way, it does not spoil the accidental symmetry protection of the light 125 GeV Higgs mass. This is also evident from the NLSM picture, where the pNGB only couples to SS via suppressed explicit symmetry-breaking interactions.[11] Direct detection relies on the same interactions, and Figure 3 shows that the effective size of this explicit symmetry-breaking coupling required for S to have the observed DM relic density is small, typically $\lesssim 10^{-2}$ over most of the parameter space of interest. Therefore, introducing S as a DM candidate does not spoil the Twin Higgs solution of the little hierarchy problem.

However, it is also evident that the scalar S itself enjoys no symmetry protection of its mass within the low-energy effective Twin Higgs model defined by Equations (2.17) and (2.18). In fact, it has an

[11] In the LSM picture, this is again manifest via a cancellation between quartic and $\hat{h}$-mediated contributions to 1-loop corrections of the light Higgs mass.

unsuppressed quartic coupling λ_{HS} to the heavy radial mode $\hat{h}$. The hierarchy $m_S \ll m_{\hat{h}}$, which requires sizeable λ_{HS} to overcome the pNGB suppression active during annihilation and achieve the observed relic abundance, is therefore unnatural for two reasons: first, 1-loop corrections to m_S from $\hat{h}$ loops would be large, and second, such a small but positive m_S^2 would require a tuning of the tree-level parameters in Equation (2.19). These problems disappear for $m_S \sim m_{\hat{h}}$, both because there is no mismatch of mass-scales and because the required λ_{HS} is smaller. Even within the realm of applicability of the low-energy effective Twin Higgs model, this suggests that the masses of $\hat{h}$ and S should not be too different from each other. From a UV perspective, it therefore seems that S with $m_S \sim m_{\hat{h}}$ should be interpreted as being part of the approximately $SU(4)$ invariant "UV structure" of the Twin Higgs scalar sector. The full hierarchy problem for S would then be solved by whatever UV completion makes the masses of $\hat{h}$ and h natural above 5-10 TeV.

All of these considerations strongly motivate the DM candidate S to have the same mass scale as the radial mode $\hat{h}$. This in turn pushes THPDM into the regime where the pNGB-suppression of direct detection compared to DM annihilation is most pronounced. Null results in direct detection experiments to date are therefore entirely natural in our model. By the same token, our predictions in Figure 3 show that future detectors will have a good chance of detecting THPDM in the most relevant regions of parameter space.

2.5 Asymmetrically Reheated Twin Higgs Portal Dark Matter

In the previous section, we showed how the Twin Higgs mechanism leads to significantly suppressed direct detection rates for THPDM assuming standard cosmology. This conclusion applies equally well to both MTH-type and FTH-type models, the latter being those that satisfy ΔN_{eff} constraints by modifying the twin spectrum to remove light degrees of freedom. An alternative solution to the cosmological problems of the MTH is asymmetric reheating following an early period of matter domination [12, 145]. Additional entropy is injected into the visible sector after it decouples from the twin sector, diluting the twin contribution to ΔN_{eff} during CMB times. This dilution also reduces the energy density of any DM candidate that froze out before asymmetric reheating by a *dilution factor* D: $\Omega \to \Omega/D$. In models with asymmetric reheating, the DM density at freeze-out must therefore be *larger* by a factor of D compared to the expectation from standard cosmology. If the same diagrams are responsible for both annihilation in the early universe and direct detection, this corresponds to a *decrease* in the direct detection rate by the same dilution factor D. This reduction in direct detection due to asymmetric reheating is universal and does not depend on the particular DM model. In this section we carefully examine the effect of asymmetric reheating on DM in general and THPDM in particular.

In order for our discussion to be self-contained, we first review basic MTH cosmology in Section 2.5.1 to establish notation and re-derive the well-known discrepancy between ΔN_{eff} in the $\mathbb{Z}_2$-symmetric MTH and measurements from the CMB. Then we review the asymmetric reheating mech-

anism in Section 2.5.2, largely following and updating the discussion in [145]. Readers familiar with Twin Higgs cosmology are invited to skip these sections.

In Section 2.5.3 we define the DM dilution factor D and discuss its relation to the $\Delta N_{\rm eff}$ prediction of asymmetrically reheated models. We will find that direct detection could potentially make the dilution a separate observable from $\Delta N_{\rm eff}$, allowing for an additional probe of Twin Higgs cosmology.

In Section 2.5.4 we compute the dilution factors that are generated by two representative Twin Higgs models of asymmetric reheating, the νMTH [145] in Section 2.5.4.1 featuring late-time decay of right-handed neutrinos, and the XMTH [12] in Section 2.5.4.2 where the reheating particle is a long-lived scalar X. We also re-examine the viability of these models in light of the updated $\Delta N_{\rm eff} < 0.23$ (at 2σ) constraints [11], and show how predictions for $\Delta N_{\rm eff}$ and the DM dilution factor D are correlated. Both models lead to a positive signal in future CMB-S4 measurements [14] for much of their respective parameter spaces.

Section 2.5.5 contains predictions for THPDM direct detection for the range of dilution factors $D \sim 100 - 1000$ motivated in realistic νMTH and XMTH models.

2.5.1 Review of Standard Mirror Twin Higgs Cosmological History

It is helpful to review basic Mirror Twin Higgs cosmology, explicitly demonstrating how the unmodified model predicts $\Delta N_{\rm eff} \sim 6$. We follow the discussion in [145]. The fact that the 125 GeV Higgs boson h is an admixture of h_A and h_B enables the visible and mirror sectors to maintain thermal equilibrium in the early universe down to $\sim \mathcal{O}(\text{ GeV})$ temperatures through Higgs-mediated fermion scattering. The thermally averaged interaction rate for these Higgs portal processes is of order

$$\langle \sigma v \rangle \approx \left(y_A^i y_B^j\right)^2 \left(\frac{v}{f}\right)^2 \frac{T^2}{m_h^4} \tag{2.30}$$

where y_A^i and y_B^j are the Yukawa couplings from the heaviest visible and mirror sector fermions still present in the thermal bath at temperature T. This crude approximation is sufficient to estimate the decoupling temperature of the Higgs portal. Freeze out occurs when $\Gamma = n \langle \sigma v \rangle \lesssim H$, where n is the fermion number density and H is the Hubble parameter. The approximate temperature T_D at which the two sectors thermally decouple can therefore be found by solving

$$\frac{3}{4}\left(\frac{\zeta(3)}{\pi^2}\right) g T_D^3 \left(y_A^i y_B^j\right)^2 \left(\frac{v}{f}\right)^2 \frac{T_D^2}{m_h^4} \simeq \sqrt{\frac{\pi^2}{90}} \frac{T_D^2}{M_{\rm Pl}} g_{*S}^{1/2} \,, \tag{2.31}$$

where g_{*S} is the total number of relativistic degrees of freedom in the bath at temperature T_D, and g is the number of degrees of freedom of the target fermion. To estimate T_D, we note that roughly 80% of the annihilations for a species leaving the bath happen in the interval $\frac{1}{6}m < T < m$ [177]. This means that to a good approximation we can construct continuous expressions for the effective Yukawa couplings y_A^i and y_B^j by linearly interpolating between the coupling of the lightest active particle at

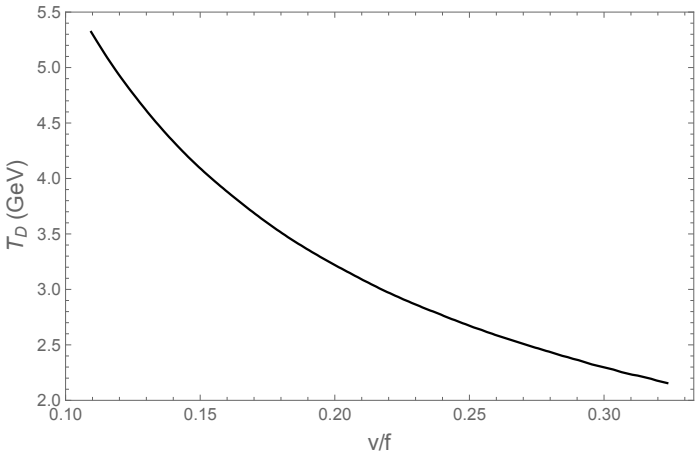

Figure 4. The temperature of decoupling between the visible and mirror sectors as a function of the ratio v/f. This plot was generated from the solution of Equation (2.31), where the Yukawa couplings y_A^i and y_B^j are those of the heaviest active fermions in the thermal bath of each sector. To reflect the continuous nature of particle freeze out, the Yukawas were linearly interpolated from the coupling of the lightest active particle at $T = m$ to the next lightest particle at $T = \frac{1}{6}m$, by which time approximately 80% of the particles of mass m have frozen out.

$T = m$ and the next lightest at $T = \frac{1}{6}m$, keeping the expression constant outside of these intermediary regions. The decoupling temperature is shown as a function of v/f in Figure 4, coinciding with the $\sim$ few GeV expectation found in e.g. [12, 37, 145]. Smaller v/f leads to earlier decoupling.

Once the two sectors are decoupled, each thermal bath evolves separately and the total entropy of each sector is independently conserved. During this radiation-dominated epoch we therefore have

$$g_{*A}T_A^3a^3 = \text{const} \quad , \quad g_{*B}T_B^3a^3 = \text{const} \tag{2.32}$$

where g_{*A} is the number of relativistic degrees of freedom in the visible sector, g_{*B} the mirror sector counterpart, and a is the scale factor. Note here that the constants for A and B are generally not equal to each other, and we assume that all relativistic degrees of freedom in a given sector have the same temperature so that $g_* = g_{*S}$. Where relevant, the difference between g_* and g_{*S} is accounted for.

Additionally, the energy density of a given sector during radiation domination is given by $\rho = \frac{\pi^2}{30}g_*T^4$. Therefore, as long as comoving entropy is conserved, the energy density of each sector evolves as

$$\rho_f = \left(\frac{g_{*i}}{g_{*f}}\right)^{1/3}\rho_i\left(\frac{a_i}{a_f}\right)^4 \tag{2.33}$$

where i and f denote some initial and final times. The decrease in energy density due the expansion of the universe is slowed by particles becoming non-relativistic and leaving the thermal bath.

We can now calculate the ratio of energy densities between the visible sector A and the mirror

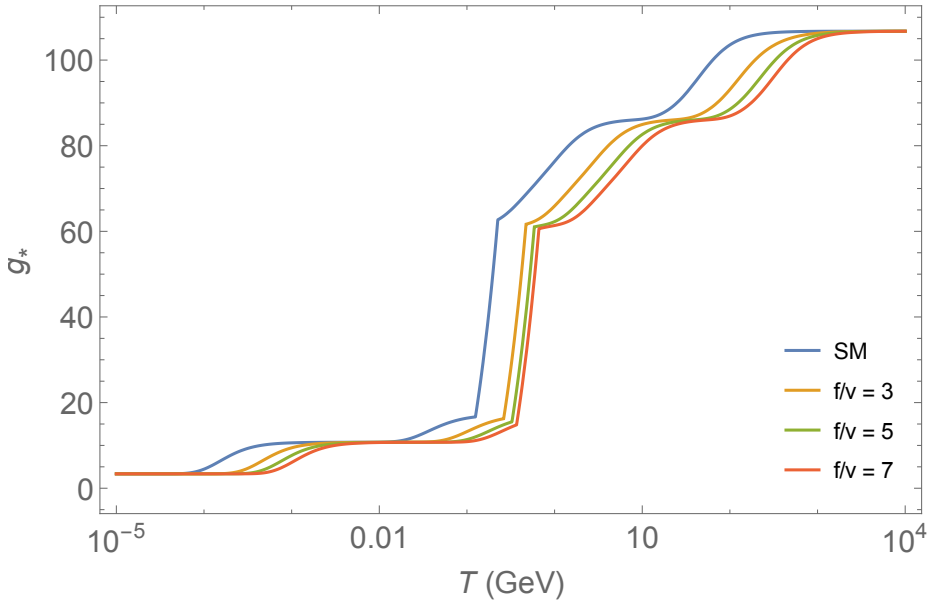

Figure 5. Values of the effective relativistic degrees of freedom g_* in the mirror sector for $f/v = 3, 5, 7$, shown in orange, green, and red respectively. The SM case is shown in blue for comparison (and corresponds to $f/v = 1$). In the region of the QCD phase transition we follow Ref. [12] and linearly interpolate between known values before and after the transition. For the SM case we interpolate from a temperature of 125 MeV to 225 MeV, while for the MTH case the central value and width of the interpolated region is scaled by $(1+\log(v/f))$. This reproduces and mildly extends the result in Ref. [12]. The contribution to g_* from neutrinos during their decoupling ($T \lesssim .01$ GeV) was calculated in this work following Ref. [13].

sector B at BBN. From Equation (2.33) we find that

$$\left.\frac{\rho_B}{\rho_A}\right|_{\text{BBN}} = \left(\frac{g_{*A,\text{BBN}}}{g_{*B,\text{BBN}}}\right)^{1/3} \left(\frac{g_{*B,D}}{g_{*A,D}}\right)^{1/3} \left.\frac{\rho_B}{\rho_A}\right|_{D} \tag{2.34}$$

where $g_{*A,\text{BBN}}$ and $g_{*A,D}$ denote the relativistic degrees of freedom in the visible sector at the time of BBN (in the visible sector) and mirror sector decoupling respectively, with analogous descriptions for $g_{*B,\text{BBN}}$ and $g_{*B,D}$ in the mirror sector. Further, since the temperatures of the two sectors are equal at decoupling and the two sectors have roughly the same number of active degrees of freedom at BBN in the symmetric MTH model, the above reduces to

$$\left.\frac{\rho_B}{\rho_A}\right|_{\text{BBN}} = \left(\frac{g_{*B,D}}{g_{*A,D}}\right)^{4/3}. \tag{2.35}$$

ΔN_{eff} can easily be written in terms of this ratio. Conventionally, ΔN_{eff} is defined as

$$\Delta N_{\text{eff}} \equiv \frac{\rho_B}{\rho_{\nu,i}} \approx 3\frac{\rho_B}{\rho_\nu} \tag{2.36}$$

where ρ_B represents the dark radiation density and $\rho_{\nu,i}$ is the energy density of a single SM neutrino species. To the extent that we can ignore mass differences in the neutrino species[12] , the total neutrino energy density ρ_ν is simply $\rho_\nu \approx 3\rho_{\nu,i}$. Since the neutrinos decouple from the bath prior to electron-positron annihilation, their temperature is reduced by a factor $(4/11)^{1/3}$ relative to the photons during BBN. As a result the SM neutrinos comprise roughly 40.5% of the total radiation in the SM bath. This implies

$$\Delta N_{\text{eff}} = 3\,\frac{\rho_B}{\rho_\nu}\bigg|_{BBN} \approx 7.4\,\frac{\rho_B}{\rho_A}\bigg|_{\text{BBN}}\,, \tag{2.37}$$

which for the completely mirror symmetric Twin Higgs is well approximated by

$$\Delta N_{\text{eff}} \approx 7.4\,\left(\frac{g_{*B,D}}{g_{*A,D}}\right)^{4/3}. \tag{2.38}$$

Because of the $\mathbb{Z}_2$ breaking, the mirror sector particles will be a factor of $\frac{v_B}{v_A} \approx \frac{f}{v}$ heavier than their SM counterparts, which will in turn affect the size of g_{*B} for a given temperature. This dependence is shown in Figure 5 for a variety of f/v. Regardless of the chosen f/v, the resulting number of effective neutrino species present during BBN is well outside the experimental bound of $\Delta N_{\text{eff}} \lesssim 0.23$ [11]. Concretely, the MTH predicts

$$\Delta N_{\text{eff}} \approx 6.3 \quad , \quad f/v = 3 \tag{2.39}$$

$$\Delta N_{\text{eff}} \approx 5.8 \quad , \quad f/v = 7 \tag{2.40}$$

indicating that without modification it is not a cosmologically viable model for any f/v.

2.5.2 Review of Asymmetric Reheating Mechanism

Asymmetric reheating occurs when massive, relatively long-lived particles, labeled Q, freeze out relativistically due to their weak couplings. This leads to an early period of matter domination before they decay out-of-equilibrium, preferentially reheating the visible sector compared to the hidden sector. If the decay products quickly thermalize with the respective baths, the visible sector temperature and hence energy density is raised relative to the hidden sector, and ΔN_{eff} is reduced – see Equation (2.37). Here we briefly review the model-independent description of the asymmetric reheating mechanism for Twin Higgs theories from [145]. We also take into account redshifting effects that are relevant when Q freezes out at $T \gg M_Q$, discussed in [12], and slightly update the discussion to include the latest bounds on ΔN_{eff} [11]. The properties of the decaying particles are left as general as

[12] Since we are concerned with temperature scales much larger than the neutrino masses this is an excellent approximation. However see Ref. [12] for a calculation of ΔN_{eff} with finite neutrino masses.

possible so that the results are easily applicable to the νMTH [145] and XMTH [12] models discussed in Section 2.5.4.

In general, the mirror sector's contribution to ΔN_{eff} depends on the ratio f/v, the heavy Higgs mass $m_{\hat{h}}$, and the properties of the Q. ΔN_{eff} is most sensitive to the decay width Γ_Q, the mass M_Q, the temperature at which it decouples from the thermal bath $T_{Q,0}$, and the mirror sector branching ratio ϵ, defined by

$$\epsilon \equiv \frac{\Gamma_{Q\to B}}{\Gamma_Q} \,, \tag{2.41}$$

where asymmetric reheating requires $\epsilon \ll 1$. In practice, ΔN_{eff} is relatively insensitive to $m_{\hat{h}}$, except insofar as it can determine whether Q ever thermalizes with the SM/mirror sector bath early in the universe in scenarios where Q is very weakly coupled.

There is a particular window of time during which the decay of the Q must take place in order for the dilution mechanism to be effective. If the decay happens before the visible and twin sector (denoted A and B respectively) are decoupled from each other, then the entropy dumped into A can easily leak back into B through the Higgs portal and the dilution will not be sufficient to satisfy ΔN_{eff} bounds. It can be seen from Equation (2.37) that satisfying $\Delta N_{\text{eff}} < 0.23$ requires the energy density in the visible sector to be at least a factor of 30 larger than the mirror sector after reheating. Since the mirror and visible sectors have similar numbers of degrees of freedom, it follows that no more than $\sim 1/15$ of the Q can have decayed before this time. This implies roughly that $\Gamma_Q \lesssim H/15$, where H is evaluated at T_D.[13]. For a radiation dominated universe, we then find

$$\Gamma_Q \lesssim \sqrt{\frac{\pi^2}{90}} \frac{1}{15 M_{\text{Pl}}} g_{*,D}^{1/2} T_D^2 \tag{2.42}$$

which leads to an upper bound of $\Gamma_Q \lesssim 5 \times 10^{-19}$ (2×10^{-18}) GeV for $f/v = 3$ (7), or a minimum lifetime of $\tau \gtrsim 1$ (0.3) μs.

On the other hand, the asymmetric reheating cannot be allowed to disrupt BBN. The temperature of the visible sector after reheating, $T_{A,R}$, must therefore be larger than $\mathcal{O}(1 - 10 \text{ MeV})$ [178]. A more precise constraint would require a dedicated analysis, but for the purposes of estimating the viable parameter space of asymmetrically reheated Twin Higgs models we will consider two lower bounds on $T_{A,R}$, 1 MeV and 10 MeV. This corresponds to $\Gamma_Q \gtrsim 4 \times 10^{-25}$ GeV, or $\tau \lesssim 1s$ for 1 MeV and $\Gamma_Q \gtrsim 4 \times 10^{-23}$ GeV, $\tau \lesssim 10^{-2} s$ for 10 MeV – see Equation (2.44) below. Respecting the BBN bound also ensures that reheating does not occur after the visible sector neutrinos decouple from the SM bath at $T^0_{\text{SM}} \sim 1$ MeV. This avoids dilution of the SM neutrino energy density due to entropy injection into the active SM bath, which could reduce ΔN_{eff} below the SM expectation. The situation is potentially a bit more complicated for twin neutrinos, which decouple from twin electrons when the mirror sector roughly has temperature $T^0_{\text{Twin}} = (f/v)^{4/3} T^0_{\text{SM}}$. Recall that both sectors

[13] Note that this is an updated prediction from [145] based on more recent ΔN_{eff} bounds.

have very similar temperature before asymmetric reheating. Requiring $T_{A,R} > 10$ MeV ensures that entropy injection takes place when twin neutrinos are still in thermal contact with the twin electron bath for most of our parameters of interest, and we can treat the surviving radiation components to be thermal, making estimation of $\Delta N_{\rm eff}$ straightforward. However, if the $T_{A,R}$ bound is relaxed to 1 MeV, then the twin neutrinos could receive a contribution to their number density from Q decays (depending on the precise branching ratios within each sector) that never thermalizes but instead has a distribution dictated by Q decays [12]. We leave a precise treatment of these non-thermal effects on $\Delta N_{\rm eff}$ for future investigation, and here simply present results for $T_{A,R} = 1$ MeV as if the twin neutrino radiation component is thermal as a first crude estimate.

When the Q become the dominant component of the universe's energy density, we find

$$\rho = 3H^2 M_{\rm Pl}^2 = M_Q n_Q \tag{2.43}$$

where H is the Hubble parameter, $M_{\rm Pl}$ is the reduced Planck mass, and n_Q is the number density of the Q. In the limit that all the decays happen at $H = \Gamma_Q$ we can then equate the energy density before and after to obtain

$$\rho_{A,R} = \frac{\pi^2}{30} g_{*A,R} T_{A,R}^4 = 3(1-\epsilon)\Gamma_Q^2 M_{\rm Pl}^2 \approx 3\Gamma_Q^2 M_{\rm Pl}^2 = M_Q n_{Q,R} \tag{2.44}$$

where $T_{A,R}$ is the temperature of the visible sector after reheating, $g_{*A,R}$ the associated degrees of freedom, $n_{Q,R}$ denotes the number density of the Q after reheating, and we are implicitly assuming that the original energy density in SM radiation is dominated by the radiation produced from the Q decay. Equation (2.42) then requires the reheat temperature of the visible sector to satisfy $T_{A,R} \lesssim 0.7\ (1.3)$ GeV for $f/v = 3\ (7)$.

The mirror sector receives a much smaller portion of the total energy density from the Q sector, so we have to take the pre-existing energy density into account. Within the instantaneous decay approximation, this gives

$$\rho_{B,R} = 3\epsilon\Gamma_Q^2 M_{\rm Pl}^2 + \left(\frac{g_{*B,D}}{g_{*B,R}}\right)^{1/3} \rho_{B,D} \left(\frac{a_D}{a_R}\right)^4 . \tag{2.45}$$

Dividing (2.45) by (2.44) then leads to

$$\left.\frac{\rho_B}{\rho_A}\right|_R \equiv \frac{\epsilon + R_Q}{1-\epsilon} \approx \epsilon + R_Q \tag{2.46}$$

where R_Q is the ratio of the hidden sector energy density before reheating compared to the total

entropy injected by Q decays, defined

$$R_Q = \frac{\left(\frac{g_{*B,D}}{g_{*B,R}}\right)^{1/3} \rho_{B,D} \left(\frac{a_D}{a_R}\right)^4}{M_Q n_{Q,R}}. \tag{2.47}$$

Thus from Equations (2.46) and (2.37) we find

$$\Delta N_{\text{eff}} \approx 7.4 \left.\frac{\rho_B}{\rho_A}\right|_{\text{BBN}} = 7.4 \left(\frac{g_{*B,R}}{g_{*A,R}}\right)^{1/3} (\epsilon + R_Q) \tag{2.48}$$

where the $(g_{*B,R}/g_{*A,R})^{1/3}$ factor accounts for the changing constituents of the thermal baths in both sectors between reheating and BBN. Intuitively, R_Q is a measure of how washed out the original energy density in the twin sector is after Q decays. At the same time, ϵ is a measure of how much energy density is sent back into the twin sector through the same process. In order for ΔN_{eff} to be brought to within experimental limits, both of these quantities are required to be small. Effective asymmetric reheating requires that a large amount of entropy be injected into the visible sector, with very little leaking back into the twin sector.

To compute ΔN_{eff} for a given Twin Higgs model of asymmetric reheating, our only remaining task is to compute R_Q. At the time of decoupling between visible and mirror sectors, the energy density of the bath is split according to the relativistic degrees of freedom in either sector,

$$\rho_{A,D} = \frac{\pi^2}{30} g_{*A,D} T_D^4 \quad , \quad \rho_{B,D} = \frac{\pi^2}{30} g_{*B,D} T_D^4 \, . \tag{2.49}$$

Q is assumed to be non-relativistic and long decoupled when the hidden and visible sectors decouple from each other:

$$n_{Q,R} \approx \left(\frac{a_D^3}{a_R^3}\right) n_{Q,D}. \tag{2.50}$$

Thus from Equations (2.44, 2.47-2.50) we find

$$R_Q = \frac{\pi^2}{30} \left(\frac{g_{*B,D}}{g_{*B,R}}\right)^{1/3} g_{*B,D} \left(\frac{3\Gamma_Q^2 M_{\text{Pl}}^2}{M_Q^4}\right)^{1/3} \left(\frac{T_D^4}{n_{Q,D}^{4/3}}\right) \, . \tag{2.51}$$

If Q freezes out at a temperature $T_{Q,0}$ not much higher than its mass, it becomes non-relativistic soon after and redshifting effects on its energy density can be neglected. In that case, we can write the number density as

$$n_{Q,D} \approx \tilde{g}_Q \frac{\zeta(3)}{\pi^2} T_{Q,0}^3 \left(a_0^3/a_D^3\right) \, , \tag{2.52}$$

where

$$\tilde{g} \equiv \sum_{\text{bosons}} g_i + \frac{3}{4} \sum_{\text{fermions}} g_i. \tag{2.53}$$

R_Q then takes the simplified form

$$R_Q = \frac{\pi^2}{90} \left(\frac{3\pi^2}{\zeta(3)} \right)^{4/3} \left(\frac{g_{*B,D}}{\tilde{g}_Q} \right)^{4/3} \left(\frac{g_{*0}}{g_{*D}} \right)^{4/3} \left(\frac{\Gamma_Q^2 M_{\text{Pl}}^2}{g_{*B,R} M_Q^4} \right)^{1/3}. \tag{2.54}$$

On the other hand, if Q is so weakly interacting that it freezes out at $T_{Q,0} \gg M_Q$, then it will redshift as decoupled radiation for a non-negligible period of time before becoming non-relativistic (which can be particularly important for the XMTH model). In that case, the number density must be calculated using a redshifted Fermi-Dirac or Bose-Einstein distribution [179]

$$n_{Q,D} = \frac{g}{2\pi^2} \int_0^\infty \mathrm{d}p\, p^2 \left(\exp \left[\frac{\sqrt{\left(\frac{T_{Q,0}}{T_{Q,D}} p \right)^2 + M_Q^2}}{T_{Q,0}} \right] \pm 1 \right)^{-1}, \tag{2.55}$$

where ± 1 is for Fermi-Dirac or Bose-Einstein statistics respectively and $T_{Q,D} = (g_{*D}/g_{*0})^{1/3} T_D$ is the temperature of the Q at the time of visible-twin sector decoupling.

2.5.3 Dark Matter Dilution

Any DM abundance that freezes out before asymmetric reheating will be diluted similar to the mirror sector (assuming no DM is produced in Q decays). The DM relic abundance in asymmetrically reheated Twin Higgs theories is therefore computed analogously to standard freeze-out – see Equation (2.13) – but with two important differences. First, when the Q decay they increase the total entropy of the universe by a factor Δ,

$$s_0 a_0^3 = \Delta s_f a_f^3. \tag{2.56}$$

This implies that

$$Y_0 = \frac{n_0}{s_0} = \Delta^{-1} \frac{n_f}{s_f} = \Delta^{-1} Y_f. \tag{2.57}$$

Second, the entropy density today is the sum of the entropy densities in the two sectors, $s_{0,\text{MTH}} = s_{0,A} + s_{0,B}$. Therefore the relic density is

$$\Omega_0 = \frac{1}{3 M_{Pl}^2 H_0^2} m Y_f s_{0,A} \left[\Delta^{-1} \left(1 + \frac{s_{0,B}}{s_{0,A}} \right) \right] \tag{2.58}$$

where we have factored out $s_{0,A}$ because this is the quantity we measure with CMB data. Comparing to Equation (2.13), we find that the observed relic abundance is given by

$$\Omega_0 = \frac{\Omega_{\Lambda\text{CDM}}}{D} \,, \tag{2.59}$$

where $\Omega_{\Lambda\text{CDM}}$ is the relic density formula in standard cosmology[14], and we have defined the *dilution factor*

$$D \equiv \Delta \left(1 + \frac{s_{0,B}}{s_{0,A}}\right)^{-1} \,, \tag{2.60}$$

which parameterizes the magnitude of dark matter dilution that arises from asymmetric reheating in Twin Higgs models.[15] To better understand this quantity, we now write it in terms of relevant cosmological parameters. First, notice that

$$\Delta = \frac{s_0 a_0^3}{s_f a_f^3} = \frac{s_R a_R^3}{s_D a_D^3} = \left(\frac{s_{A,R} + s_{B,R}}{s_D}\right)\left(\frac{a_R}{a_D}\right)^3 \tag{2.61}$$

since, by construction, all of the decays of the Q happen after the mirror and visible sector decouple. We then find

$$D = \frac{s_{A,R}}{s_D}\left(\frac{a_R}{a_D}\right)^3 \tag{2.62}$$

since comoving entropy is conserved after reheating. This expression can be written in terms of energy densities as

$$D = \frac{\rho_{A,R}^{3/4}\, g_{*A,R}^{1/4}}{\rho_D^{3/4}\, g_{*D}^{1/4}}\left(\frac{a_R}{a_D}\right)^3 \,, \tag{2.63}$$

and using Equations (2.44) and (2.47), as well as the fact that $\rho_D = \left(\frac{g_{*D}}{g_{*B,D}}\right)\rho_{B,D}$, we find the relatively simple form

$$D = \frac{1}{R_Q^{3/4}}\left(\frac{g_{*B,D}}{g_{*D}}\right)\left(\frac{g_{*A,R}}{g_{*B,R}}\right)^{1/4} . \tag{2.64}$$

Ignoring g_* factors, we see that D depends only on R_Q while ΔN_{eff} depends on both R_Q and ϵ (see Equation (2.48)). This arises because the amount by which DM is diluted depends only on the total amount of entropy injected by Q-decay, not on the asymmetry of the reheating. R_Q is defined as the twin sector energy before reheating compared to the total amount of energy injected, but since the

[14] Note that the value of Y_f is model-dependent and will vary depending on both the thermally averaged annihilation cross section of the DM candidate, as well as the constituents of the thermal bath as it freezes out. In this definition we take Y_f to be that of a Twin Higgs model in the absence of any asymmetric reheating. If one wishes to consider the dilution factor between an asymmetrically reheated Twin Higgs model and a more minimal model of dark matter (e.g. HPDM), then a factor $K = \frac{Y_{f,\text{CDM}}}{Y_{f,\text{MTH}}}$ should be included in the definition of D.

[15] This is a modified definition of the dilution factor compared to e.g. Ref. [180], specific to the Twin Higgs since the entropy of the twin sector plays a significant role.

former is straightforwardly related to the total energy density before reheating, the relative importance of the entropy injection is indeed specified by R_Q and not ϵ. The dilution factor can be related to the properties of Q using the simplified form of R_Q in Equation (2.54) which is valid if $T_{Q,0}$ is not much larger than M_Q. Ignoring constants, this gives

$$D \sim M_Q \left(\frac{g_{*A,R}^{1/4}}{\Gamma_Q^{1/2} M_{Pl}^{1/2}} \right) \left(\frac{\tilde{g}_Q}{g_{*0}} \right) \tag{2.65}$$

which shows that dilution increases if Q is heavier, decays later, or has more degrees of freedom.

Dilution affects direct detection of a thermal freeze-out DM candidate χ in a very simple way. If $\Omega_0 \sim 1/\langle \sigma v \rangle$ is reduced by a factor of D due to the reheating, and if the direct detection cross section $\sigma_{\chi N}$ is given by the same couplings that drive annihilation, $\sigma_{\chi N} \propto \langle \sigma v \rangle$, then both cross sections must decrease by a factor of D compared to standard cosmology to overproduce DM before reheating and therefore produce the correct DM relic abundance today. This effect of reheating and decreasing direct detection signatures compared to the predictions of standard cosmology applies generally to any DM candidate – see e.g. [181–185]. In THPDM, $\langle \sigma v \rangle \propto \sigma_{SN} \propto \lambda_{eff}^2$. Compared to the predictions of Section 2.4, direct detection in Twin Higgs models with asymmetric reheating will therefore be additionally suppressed, with $D > 1$ reducing the expected effective coupling by

$$\lambda_{\text{eff}} \to \frac{\lambda_{\text{eff}}}{\sqrt{D}}. \tag{2.66}$$

Further predictions require some information about the plausible size of the dilution factor D, and how D is correlated with ΔN_{eff}. We study this for two explicit Twin Higgs models with asymmetric reheating in Section 2.5.4 below, before showing predictions for direct detection in THPDM with asymmetric reheating in Section 2.5.5.

We point out that within a given DM framework, the dilution factor is observable in the event of a DM discovery by the lower direct detection rate compared to the standard cosmology expectation. D therefore provides a cosmological probe of the properties of Q that is complementary to ΔN_{eff}, allowing in principle independent probes of ϵ and R_Q. Together with other cosmological [146] and collider measurements [86, 87, 186], this can allow for detailed examination of the twin protection and asymmetric reheating mechanisms.

2.5.4 Asymmetrically Reheated Twin Higgs Portal Dark Matter

In this section we examine two asymmetrically reheated MTH models, the νMTH [145] and XMTH [12]. We review details of the models and their cosmological history, illustrate the viable parameter space in light of updated ΔN_{eff} bounds, and show the range of correlated predictions for ΔN_{eff} and DM dilution factor D, which allows us to make direct detection projections for THPDM with asymmetric reheating in Section 2.5.5.

2.5.4.1 νMTH

A simple way of incorporating the asymmetric reheating mechanism into the Twin Higgs framework is by adding right-handed neutrinos (RHN), proposed in Ref. [145]. This is particularly elegant since RHNs are highly motivated to exist for other reasons, most importantly to explain non-zero neutrino masses [187]. Ref. [145] examines the case of 3 generations of RHNs in both the visible and twin sectors that mix with each other as well as the active neutrinos of their respective sectors, generating small active masses through the familiar type-I seesaw mechanism. In specific scenarios the width of each RHN generation is proportional to one active neutrino mass, and the known differences in the neutrino masses can then be translated into differences in decay widths of the RHNs.[16]

Since the energy density of the RHNs continues to grow relative to the energy density of the thermal baths as the universe cools, later decays have a more significant effect on the subsequent asymmetric reheating and dilution. For this reason, many of the essential features of the more realistic 3 generation model can be captured with a 1 generation toy model, also covered in Ref. [145]. In what follows we review the details of this simpler model and address its implications for asymmetric reheating and dilution, pointing out expected behaviour for the full 3 generation model where appropriate.

Consider the extension of the Twin Higgs by a single generation of RHNs that respect the $\mathbb{Z}_2$ symmetry,

$$\mathcal{L} \supset -y\left(L_A H_A N_A + L_B H_B N_B\right) - \frac{1}{2} M_N \left(N_A^2 + N_B^2\right) - M_{AB} N_A N_B + \text{h.c.} \tag{2.67}$$

where for simplicity we invoke a hierarchy in the parameters $y\langle H\rangle \ll M_{AB} \ll M_N$ for both H_A and H_B. Prior to electroweak symmetry breaking, the RHNs combine to form $\mathbb{Z}_2$-symmetric mass eigenstates $N_\pm = \frac{1}{\sqrt{2}}\left(N_A \pm N_B\right)$ with nearly degenerate masses $M_N \pm M_{AB}$. After electroweak symmetry breaking these states mix with the active neutrinos, which generates masses for the active neutrinos

$$m_{\nu,A} = \frac{y^2 v_A^2}{2M_N}\left(1 + \mathcal{O}\left(\frac{M_{AB}}{M_N}\right)\right) \tag{2.68}$$

$$m_{\nu,B} = \frac{y^2 v_B^2}{2M_N}\left(1 + \mathcal{O}\left(\frac{M_{AB}}{M_N}\right)\right) \tag{2.69}$$

and allows the RHNs to decay to leptons through both neutral and charged currents. The decay width for the RHNs into the visible sector is proportional to

$$\Gamma_{N\to A} \propto \left(\frac{m_{\nu,A}}{M_N}\right) G_{F,A}^2 M_N^5 \tag{2.70}$$

[16] For concreteness, here and in Ref. [145] the normal ordering is assumed.

where $G_{F,A}$ is the Fermi constant with visible sector vector bosons, and we neglect final state masses as well as $\mathcal{O}(m_\nu/M_N)$ and $\mathcal{O}(M_{AB}/M_N)$ corrections to the sterile neutrino masses. For actual computations we again follow Ref. [145], which derives partial widths of the RHNs in Fermi theory, valid for $M_N \lesssim M_W$. The RHN decays into the mirror sector are similar,

$$\Gamma_{N\to B} \propto \left(\frac{m_{\nu,B}}{M_N}\right) G_{F,B}^2 M_N^5 \propto \left(\frac{v^2}{f^2}\right) \Gamma_{N\to A} \tag{2.71}$$

but the net result is an overall suppression of v^2/f^2 due to the heavier neutrino and vector bosons in the mirror sector. This leads to asymmetric reheating of the visible sector

$$\epsilon \approx \frac{v^2}{f^2}, \tag{2.72}$$

but note that this ratio can be adjusted through, for example, explicit $\mathbb{Z}_2$ breaking in the Lagrangian of Equation (2.67), as discussed in Ref. [145]. In what follows we pay particular attention to the case of $\epsilon = v^2/f^2$, but ultimately treat it as a free parameter of the model.

Lastly, asymmetric reheating is effective only if the RHNs are able to dominate the cosmology before decaying. It is therefore crucial that they reach equilibrium abundance within the bath before freezing out — otherwise they will not carry away enough energy to reheat the visible sector at late times. In a 3 generation model this is simple to achieve. Neutrino oscillation measurements indicate that at least one neutrino has mass $m_\nu \gtrsim 0.05$ eV [188], corresponding to a Yukawa coupling of $\mathcal{O}(10^{-7})$, sufficient to guarantee that the corresponding RHN is in thermal contact with the SM bath in the early universe. The observation of large mixing angles in the neutrino sector further suggests that all the RHN Yukawas are of comparable size, meaning all three RHN generations are in thermal equilibrium with the visible sector prior to freeze-out. In this work, we focus on the single-generation toy model to parametrically understand the correlation between ΔN_{eff} and dilution factor D, keeping in mind that a three-generation set up is likely more realistic. We therefore assume that regardless of the mass of our single RHN, it is thermalized at early times and freezes out with an equilibrium abundance at T_0, where

$$T_0 \approx \left(\frac{M_N}{m_\nu}\right)^{1/3} (1 \text{ MeV}) \tag{2.73}$$

since the interaction rate of the RHNs with the bath is a factor $\sim m_\nu/M_N$ weaker than the active neutrino interaction rate.

When the RHNs decay, they give rise to a suppressed ΔN_{eff} signature according to Equation (2.48) and a dark matter dilution factor given by Equation (2.64). Note that computations were done accounting for the redshift of the RHNs, using Equation (2.51) for R_N. The available parameter space for this toy model is shown in Figure 6, where we consider reheating temperatures $T_{A,R}$ ranging from 1 to 10 MeV. Results are shown both for $\epsilon = 0$ and for $\epsilon = v^2/f^2$ at $f/v = 5, 6, 7$.

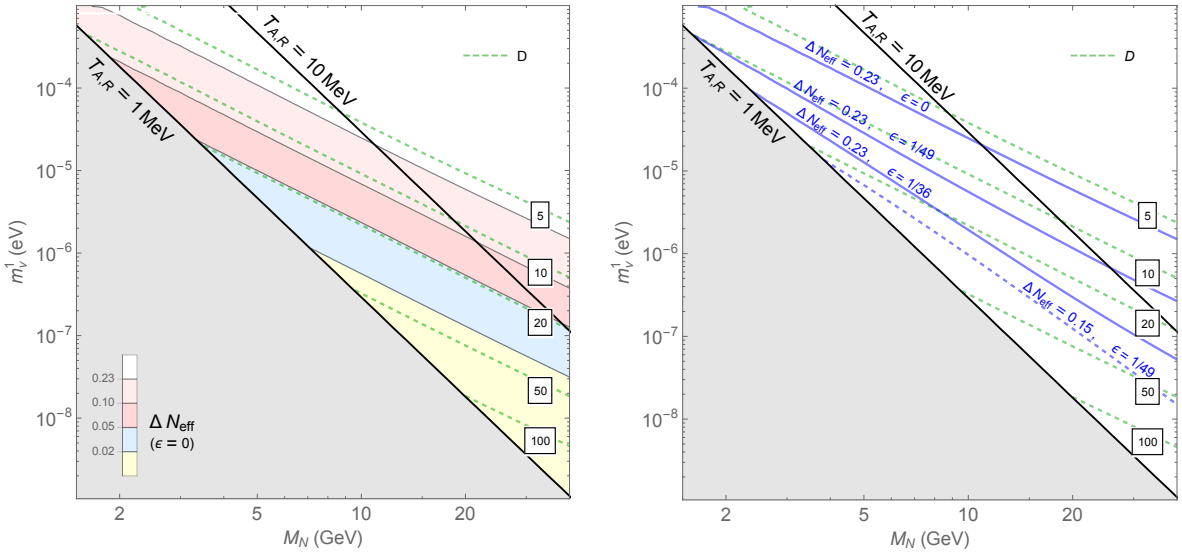

Figure 6. The parameter space for the universal 1 generation νMTH model, written in terms of the lightest active neutrino mass m_ν^1. Left: coloured contours show ΔN_{eff} for $\epsilon = 0$. Right: blue contours indicate $\Delta N_{eff} = 0.23$ or 0.15 for various choices of ϵ inspired by the minimal νMTH prediction $\epsilon = v^2/f^2$. In both plots, green dashed contours show the dilution factor D. The 1 MeV and 10 MeV lines are the optimistic and conservative estimates for bounds on $T_{A,R}$ respectively, due to BBN constraints.

The results of this one-generation toy model can generally be regarded as conservative estimates for results expected in a more realistic, 3 generation model. For example, consider the $\Delta N_{\rm eff}$ signature for the two models in terms of the branching ratio ϵ. If, in the 3 generation model, the branching ratio for the last decay is large enough that the injected energy density into the twin sector dominates over the preexisting energy density, then this new radiation is what sets the ratio T_B/T_A, and the cosmological history of the previous two decays is essentially irrelevant. In this case the $\Delta N_{\rm eff}$ signature for the 1 and 3 generation models should be similar. On the other hand, when $\epsilon = 0$ each successive decay will reheat the visible sector but not the twin sector, such that T_B/T_A is further reduced after each decay takes place. In this case we expect that $\Delta N_{\rm eff}$ will be smaller by a factor of a few in the 3 generation case.

Turning to the dilution factor, we note that the dark matter will be successively diluted relative to the visible sector for each RHN decay regardless of ϵ, since the branching ratio of the RHNs into dark matter is by definition zero. We therefore expect D to be a factor of a few larger for the 3 generation model in addition to a potential decrease in $\Delta N_{\rm eff}$. In either case, dilution factors up to $D \sim \mathcal{O}(100)$ are easily generated in the νMTH setup.

2.5.4.2 XMTH

The XMTH is another asymmetrically reheated Twin Higgs model. This model was first proposed in Ref. [12], and below we review the main features of the model and update some derivations and bounds.

The XMTH couples a scalar particle X to the Higgs sector in much the same way that the dark matter S is coupled. However, the X is made unstable by introducing x, which may be identified as the vev of X in some UV completion of the theory or a small linear coupling with the Twin Higgs multiplet:

$$V \supset \lambda_X X(X+x)(H_A^\dagger H_A + H_B^\dagger H_B) + \frac{1}{2} m_X^2 X^2 \tag{2.74}$$

Since our focus in this work is to solve the little hierarchy problem, we will simply treat this is as a low-energy effective theory and remain agnostic to the possible UV origins of this framework.[17] The small coupling $\lambda_X x$ allows X to decay to both visible and twin matter through mixing with the Higgs in each respective sector. As we will see, for $m_X \sim \mathcal{O}(10-1000)$ GeV the branching ratio into the visible sector will dominate over the mirror sector branching ratio, primarily due to the lower mass thresholds in the visible sector.

The form of the potential admits mass mixing between h_A, h_B, and X. After expanding H_A and H_B around their vevs the mass matrix can be read off directly via Equations (2.1) and (2.74):

$$M^2_{\text{gauge}} \equiv \begin{pmatrix} \lambda v_A^2 + \frac{1}{2}\lambda(f^2 - f_0^2) + \frac{3}{2}\kappa v_A^2 + \frac{1}{2}\sigma f_0^2 & \lambda v_A v_B & \frac{1}{2}\lambda_X x v_A \\ \lambda v_A v_B & \lambda v_B^2 + \frac{1}{2}\lambda(f^2 - f_0^2) + \frac{3}{2}\kappa v_B^2 & \frac{1}{2}\lambda_X x v_B \\ \frac{1}{2}\lambda_X x v_A & \frac{1}{2}\lambda_X x v_B & \frac{1}{2}m_X^2 + \frac{1}{2}\lambda_X f^2 \end{pmatrix} \tag{2.75}$$

To understand the mass eigenstates in the theory, it is instructive to diagonalize the mass matrix in two steps. First, we diagonalize the 2×2 (H_A, H_B) submatrix in exactly the same way as was done in Section 2.2. This is done by rotation through angle θ, and takes us to the $\{h, \hat{h}, X\}$ basis with mass matrix

$$M^2_{\text{partial}} \equiv \begin{pmatrix} \frac{1}{2}m_h^2 & 0 & \frac{1}{2}\lambda_X x\,(v_A\cos\theta - v_B\sin\theta) \\ 0 & \frac{1}{2}m_{\hat{h}}^2 & \frac{1}{2}\lambda_X x\,(v_A\sin\theta + v_B\cos\theta) \\ \frac{1}{2}\lambda_X x\,(v_A\cos\theta - v_B\sin\theta) & \frac{1}{2}\lambda_X x\,(v_A\sin\theta + v_B\cos\theta) & \frac{1}{2}m_X^2 + \frac{1}{2}\lambda_X f^2 \end{pmatrix}. \tag{2.76}$$

Since X has to be long-lived, we take $\lambda_X x \ll m_X, m_h, m_{\hat{h}}$. This means that M^2_{partial} is nearly diagonal, and so the states $\{h, \hat{h}, X\}$ are already approximate mass eigenstates. While the exact Higgs

[17] Both λ_X and x/m_X will be tiny in our regions of interest. Therefore, X itself does not inherit a hierarchy problem from its couplings to the Twin Higgs states within this effective IR description.

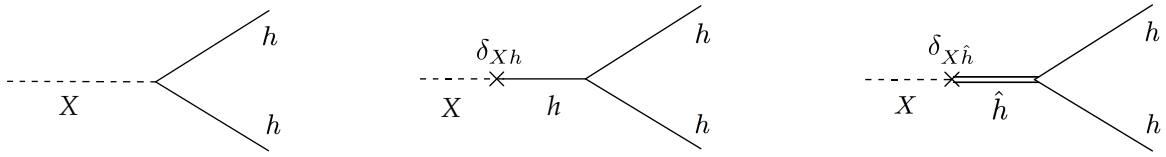

Figure 7. Contributions to $\Gamma(X \to hh)$.

mass eigenvalues will be shifted at $\mathcal{O}(\lambda_X x)$ from m_h and $m_{\hat{h}}$, and the X mass eigenvalue has already been shifted at $\mathcal{O}(\lambda_X)$, these corrections are small enough that throughout the rest of this paper we will refer to $\{h, \hat{h}, X\}$ as mass eigenstates, with the following mixing angles between X and $h, \hat{h}$:[18]

$$\delta_{X\hat{h}} \equiv \frac{\lambda_X x \left(v_A \sin\theta + v_B \cos\theta\right)}{m_X^2 - m_{\hat{h}}^2} + \mathcal{O}(\lambda_X^2) \tag{2.77}$$

$$\delta_{Xh} \equiv \frac{\lambda_X x \left(v_A \cos\theta - v_B \sin\theta\right)}{m_X^2 - m_h^2} + \mathcal{O}(\lambda_X^2) \tag{2.78}$$

Note that $\tan\theta = v_A/v_B$ in the $SU(4)$-symmetric limit with $\kappa, \sigma = 0$, and hence $\delta_{Xh} \to 0$, consistent with the pNGB nature of h.

It is also useful to translate Equations (2.77 - 2.78) into mixing angles between X and h_A, h_B, since these give decay rates into the visible and mirror sectors respectively via off-shell Higgs bosons:

$$\delta_{XA} = \delta_{Xh}\cos\theta + \delta_{X\hat{h}}\sin\theta \tag{2.79}$$

$$\delta_{XB} = \delta_{X\hat{h}}\cos\theta - \delta_{Xh}\sin\theta \tag{2.80}$$

To first order in v/f and $m_X \gtrsim m_{\hat{h}}$ these take the simple form

$$\delta_{XA} \approx \frac{\lambda_X x}{m_X^2 - m_{\hat{h}}^2}\, v \qquad (m_X \gtrsim m_{\hat{h}}) \tag{2.81}$$

$$\delta_{XB} \approx \frac{\lambda_X x}{m_X^2 - m_{\hat{h}}^2}\, f \qquad (m_X \gtrsim m_{\hat{h}}). \tag{2.82}$$

while for $m_X \ll m_h$ we expand to $\mathcal{O}\left(\kappa/\lambda\right)$:

$$\delta_{XA} \approx -\left(\frac{\kappa}{\lambda}\right) \times \frac{\lambda_X x}{4\kappa v} \qquad (m_X \ll m_h) \tag{2.83}$$

$$\delta_{XB} \approx -\left(\frac{\kappa}{\lambda}\right) \times \frac{\lambda_X x}{4\kappa v}\,\frac{v}{f} \qquad (m_X \ll m_h). \tag{2.84}$$

[18] This corrects a minor mistake in the derivation of these angles in [12].

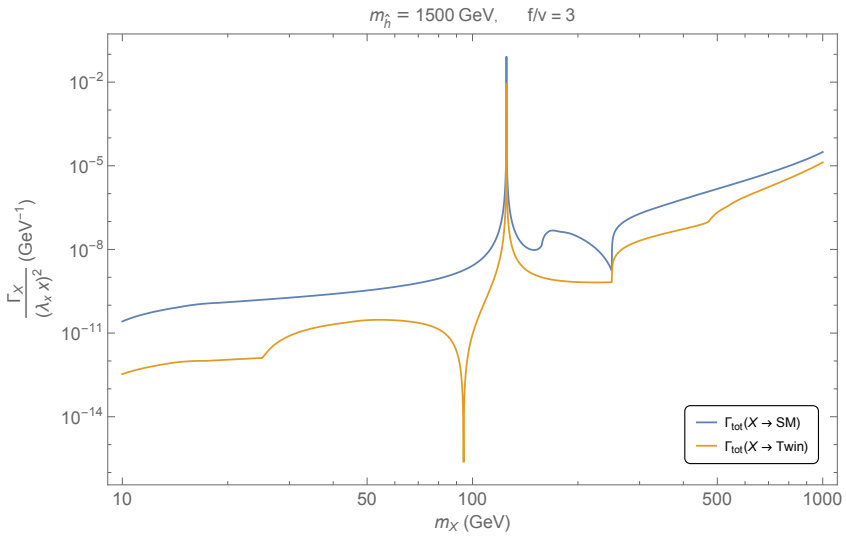

Figure 8. Complete decay width of X into visible (SM) and mirror (twin) sectors, normalized by $(\lambda_X x)^2$ which is common to all partial widths. In this figure we take $f/v = 3$ and $m_{\hat{h}} = 1500$ GeV.

Note however that both δ_{XA} and δ_{XB} generally have zeroes in the intermediate regime where m_X ranges from $\sim m_h$ to $\sim f$ due to cancellations between the two terms in Equations (2.79, 2.80) which are not captured by these simple approximations. Any numerical calculations should be performed using Equations (2.77 - 2.80).

X decays

Since the X only couples directly to the Higgs bosons of Twin Higgs theories, we divide discussion of the decay into two regimes, $m_X < 2m_h$, and $m_X \geq 2m_h$.

For $m_X < 2m_h$, all decays take place either through mixing with the Higgs bosons or to 3-body or higher final states via $X \to hh^*$. In all cases we find that hh^* final states are subdominant to other processes and are thus not included in what follows. As discussed in Ref. [12], the partial widths through mass mixing at tree level for all non-Higgs final states are simply

$$\Gamma_{\text{mix}}(X \to \text{SM}) = |\delta_{XA}|^2 \, \Gamma(h_A \to \text{SM})\Big|_{m_{h_A}=m_X} \tag{2.85}$$

$$\Gamma_{\text{mix}}(X \to \text{Twin}) = |\delta_{XB}|^2 \, \Gamma(h_B \to \text{Twin})\Big|_{m_{h_B}=m_X} \tag{2.86}$$

where we take m_{h_A} and m_{h_B} to mean the mass of a Higgs boson particle in either the visible or twin sector if we were to consider only that sector in isolation. That is, $\Gamma(h_B \to \text{Twin})|_{m_{h_B}=m_X}$ can be thought of as just the regular decay width of a Higgs of mass m_X to all non-Higgs matter with masses determined by f/v. While decays of the SM Higgs are well-documented across a wide range of masses (see e.g. Ref. [189]), for consistency we compute both $\Gamma(h_A \to \text{SM})$ and $\Gamma(h_B \to \text{Twin})$

by closely following the work of Ref. [190]. All processes relevant at the percent level or higher are included, and our results are in good agreement with Ref. [190].

For $m_X > 2m_h$, the X can decay directly into two light Higgs bosons h. Note that in addition to the direct Xhh vertex, this process will receive two extra contributions from mass mixing[19] that are shown in Figure 7. These contributions are important due to the pNGB nature of h, similar to the discussion in Section 2.4. The decay width of $X \to hh$ is suppressed by $\mathcal{O}(\kappa/\lambda)$ and $\mathcal{O}(\sigma/\lambda)$ factors, particularly for $m_X \gtrsim 2m_h$, which in our Linear Sigma Model picture is enforced by cancellations between these three diagrams. With this included, the decay $X \to hh$ vanishes in the $SU(4)$-symmetric limit. For $m_X \geq m_h + m_{\hat{h}}$, the X can decay into an $h\hat{h}$ pair. However, there is no direct coupling between these three states and so this process can only proceed through mass mixing interactions. Over all m_X of interest this decay channel is negligible compared to other processes and is not included in the remainder of the analysis. In principle we should also consider decays to $\hat{h}\hat{h}$ pairs, but we will find below that the signature space of this model is limited to regions where $m_X \lesssim 2m_{\hat{h}}$ and so we do not include this decay either (see [12] for a discussion of these processes). The decay rates to the twin and visible sectors are then given by

$$\Gamma_{\text{tot}}(X \to \text{SM}) \approx \Gamma_{\text{mix}}(X \to \text{SM}) + \Gamma(X \to hh)\text{Br}(h \to \text{SM})^2 \tag{2.87}$$

$$\Gamma_{\text{tot}}(X \to \text{Twin}) \approx \Gamma_{\text{mix}}(X \to \text{Twin}) + \Gamma(X \to hh)\text{Br}(h \to \text{Twin})^2, \tag{2.88}$$

and the rate for mixed decays (i.e. X decays to two SM states and two twin states) is found to be

$$\Gamma_{\text{tot}}(X \to \text{mixed}) \approx 2\Gamma(X \to hh)\text{Br}(h \to \text{SM})\text{Br}(h \to \text{Twin}). \tag{2.89}$$

The former two decay width estimates are illustrated in Figure 8 for $f/v = 3$ and $m_{\hat{h}} = 1500$ GeV, normalized by $(\lambda_X x)^2$ since this factor is common to all partial widths. We can see that across most of the range 10 GeV $\leq m_X \leq$ 1000 GeV, the branching ratio into the visible sector dominates over the mirror sector (with typically minor corrections owing to the mixed decays of Equation (2.89)). If λ_X is chosen such that X decays after the two sectors have thermally decoupled ($T \sim$ few GeV), then the visible sector will be preferentially reheated and ΔN_{eff} may be reduced to below experimental limits. The complete branching ratio into the twin sector is defined as

$$\epsilon \approx \frac{\Gamma_{\text{tot}}(X \to \text{Twin}) + \frac{1}{2}\Gamma_{\text{tot}}(X \to \text{mixed})}{\Gamma_{\text{tot}}(X \to \text{SM}) + \Gamma_{\text{tot}}(X \to \text{Twin}) + \Gamma_{\text{tot}}(X \to \text{mixed})} \tag{2.90}$$

which can easily be smaller than 10^{-2}, depending on f/v and the mass of X.

Thermalization and cosmological bounds

[19] These contributions were amongst those that were neglected in [12], which significantly modifies some numerical results but does not change the important qualitative behaviour of the model.

At temperatures $T \gg m_X, m_h, m_{\hat{h}}$, the X interactions with the bath scale as $\Gamma \sim T$ but the Hubble rate scales as $H \sim T^2$. Consequently, thermalization at high temperatures is not guaranteed. λ_X must be large enough for the X to make good thermal contact with the SM/twin bath in the early universe, ensuring their number density reaches its equilibrium value, but small enough that the X can freeze out with sufficient number density to eventually dominate the cosmology.[20]

For a given m_X, there is a minimum coupling such that the interaction rate can surpass the Hubble rate at some early temperature. Larger couplings increase the time interval during which the X are thermalized and lower the temperature at which the X freezes out. If the coupling is too large, the X particles stay in thermal equilibrium long enough to become Boltzmann-suppressed, reducing the amount of asymmetric reheating.

[20] If X is never in thermal contact until it decays, its initial abundance depends on the model of inflation, but to be conservative we do not consider this scenario here and instead require early thermalization.

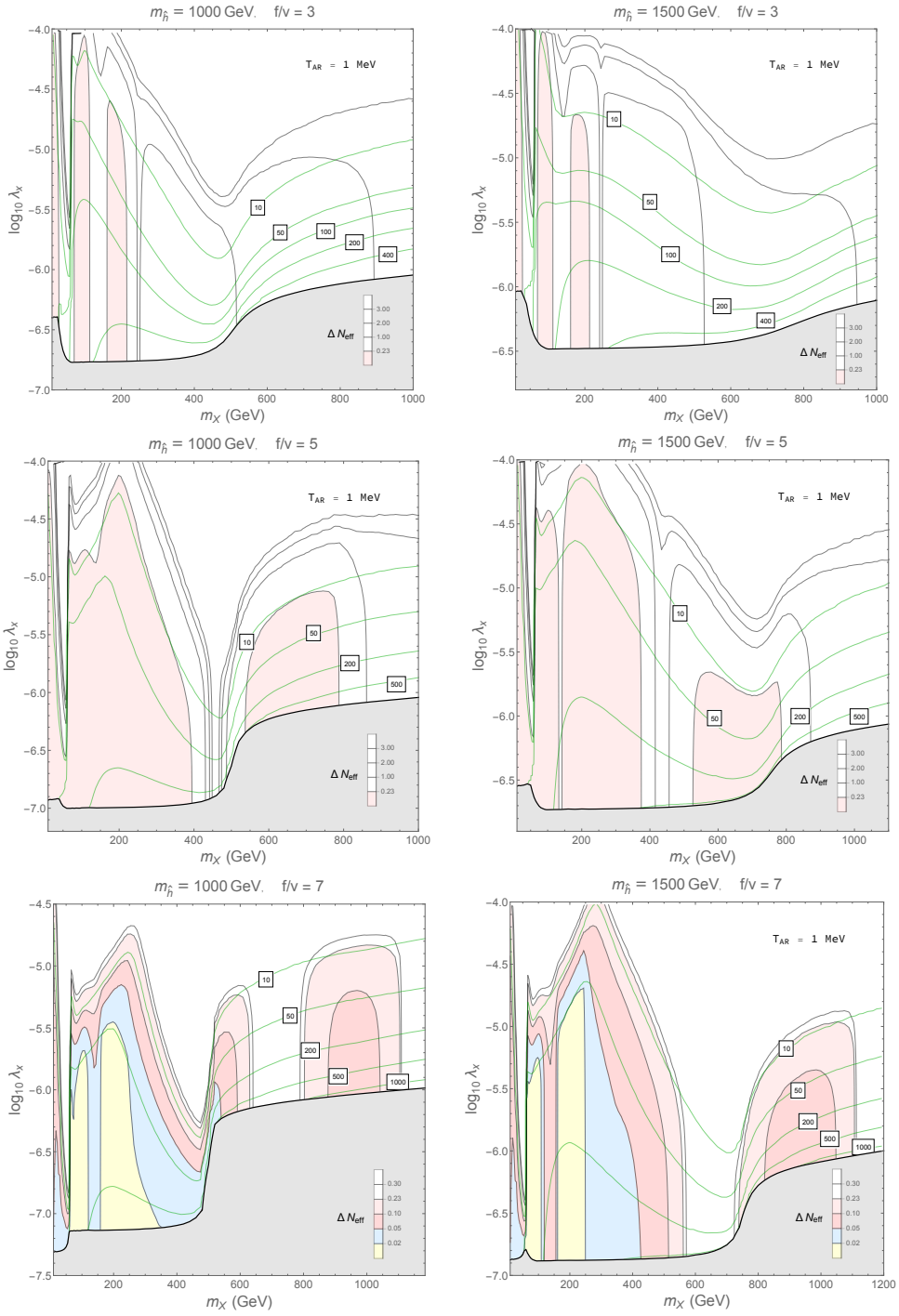

Figure 9. Contours of ΔN_{eff} (coloured regions) and DM dilution factor D (green contours) in the XMTH, where x is set such that X decays with a reheat temperature of $T_{A,R} = 1$ MeV, for different f/v and $m_{\hat{h}}$. X never thermalize in the gray region, and the blue, pink, and yellow shaded regions correspond to areas of parameter space where $\Delta N_{\rm eff}$ is within current experimental limits. All shaded regions except yellow are expected to be probed by CMB-S4 [14].

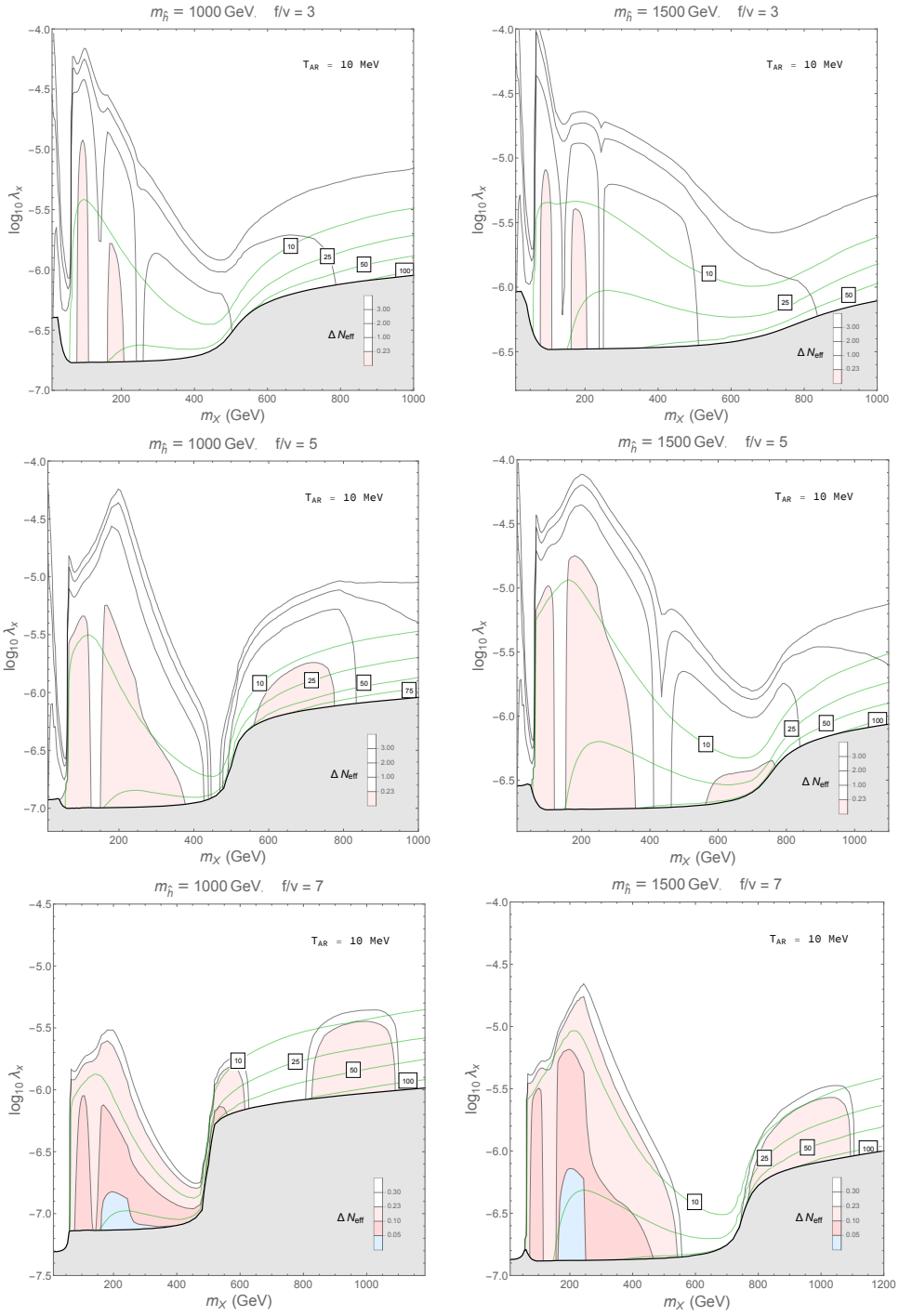

Figure 10. Contours of ΔN_{eff} (coloured regions) and DM dilution factor D (green contours) in the XMTH, where x is set such that X decays with a reheat temperature of $T_{A,R} = 10$ MeV, for different f/v and $m_{\hat{h}}$. X never thermalize in the gray region, and the blue and pink shaded regions correspond to areas of parameter space where $\Delta N_{\rm eff}$ is within current experimental limits. All shaded regions are expected to be probed by CMB-S4 [14].

Figures 9 and 10 show the values of $\Delta N_{\rm eff}$ and DM dilution factor D across the parameter

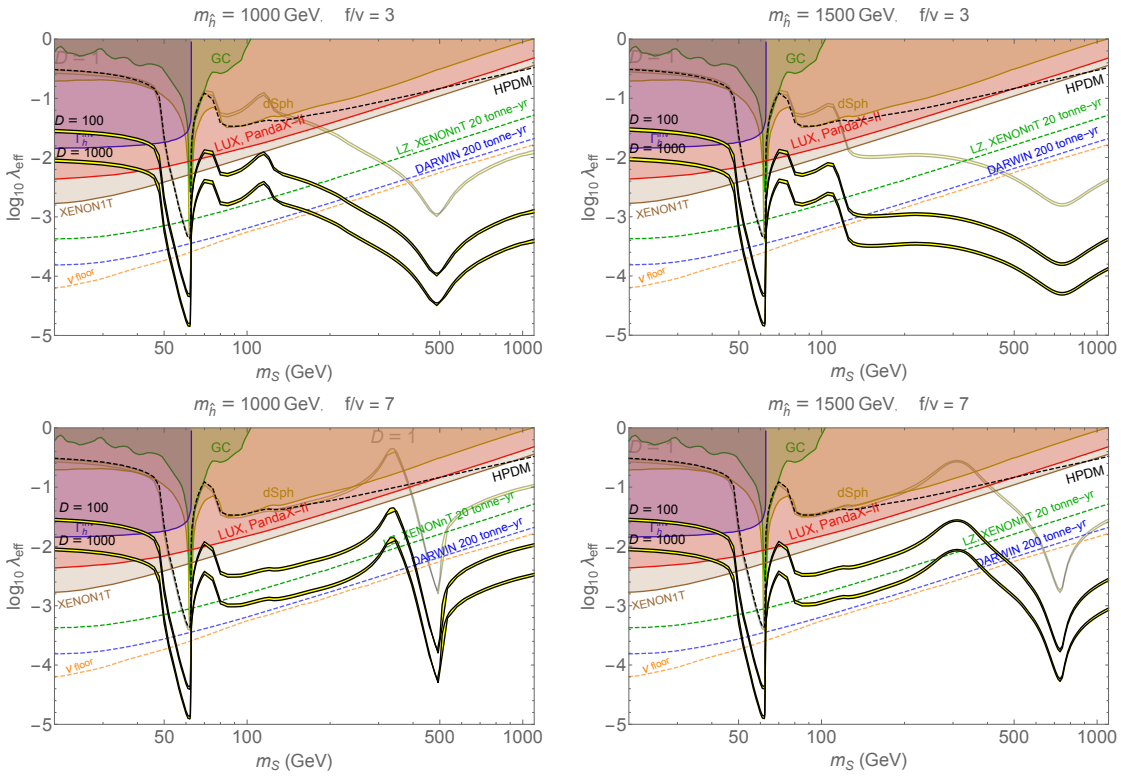

Figure 11. Direct detection parameter space of THPDM with asymmetric reheating. The opaque yellow band shows the effective THPDM coupling without dilution spanning FTH- and MTH-like mirror spectra, same as Figure 3. The lower two yellow bands correspond to dilution factors from asymmetric reheating of $D = 100$ and 1000, representing high dilution factors that can be produced in the νMTH and XMTH models.

range of interest, where x was chosen such that the decay width is fixed at the lower bounds of $\Gamma_X \approx 4.4 \times 10^{-25}$ GeV and $\Gamma_X \approx 4.5 \times 10^{-23}$ GeV, corresponding to reheat temperatures in the visible sector of $T_{A,R} = 1$ MeV and 10 MeV respectively. These plots therefore show the largest amount of dilution that is possible in this model. The black line depicts the limiting case where X thermalizes and promptly decouples. In the gray regions, X never thermalizes in the early universe. As expected, the largest dilution and smallest $\Delta N_{\rm eff}$ are found near the lower bound of λ_X, since a smaller coupling allows the X to freeze out earlier and carry away more energy from the thermal bath. There are large regions of parameter space that satisfy bounds on $\Delta N_{\rm eff}$, with dilution factors as large as $D \sim 1000$, which will significantly suppress direct detection signatures of THPDM.

2.5.5 THPDM Direct Detection with Asymmetric Reheating

In Section 2.5.4.1, we saw that the νMTH can generate dilution factors in excess of $D \gtrsim 100$ that are consistent with current bounds on $\Delta N_{\rm eff}$. For the XMTH, Figure 9 shows that dilution factors of $D \gtrsim 1000$ can be consistent with $\Delta N_{\rm eff}$ bounds for $m_X \gtrsim 800$ GeV, and generally $D \gtrsim 300$ is

possible. We therefore adopt dilution factors of $D = 100, 1000$ as reasonable benchmarks within the asymmetrically reheated MTH framework.

Figure 11 shows the predicted effective coupling for direct detection in THPDM with asymmetric reheating generating dilution factors of $D = 100, 1000$. Without asymmetric reheating, the DM mass is constrained to lie above $m_S \gtrsim 150, 400$ GeV for $f/v = 3, 7$, with a small unexplored region in the Higgs funnel that is present in the predictions of the HPDM as well. When asymmetric reheating is included, the DM mass is unconstrained above $m_X \gtrsim 50$ GeV.

As discussed in Section 2.5.3, the dilution factor is in principle a separate observable, since in the event of a discovery (and possibly corroboration of the Twin Higgs model in collider measurements), the observed DM direct detection rate can be compared to the prediction from standard cosmology. D can then be correlated with other cosmological measurements that may be sensitive to asymmetric reheating. For example, CMB-S4 measurements are expected to constrain $\Delta N_{\text{eff}} \lesssim 0.02$ [14]. In the event of a nonzero ΔN_{eff} measurement, any given asymmetrically reheated THPDM scenario will yield a range of expected dilution factors. Consistency between these two observations would constitute significant evidence in support of these models.

2.6 Conclusion

The Twin Higgs framework offers a compelling explanation for why new, coloured states have yet to appear in collider experiments. Its success as a theory of neutral naturalness is due to the pNGB nature of the 125 GeV Higgs, whose mass is protected from radiative corrections due to an accidental symmetry at one loop order.

In this work we define the Twin Higgs Portal DM (THPDM) framework by coupling a stable scalar particle S to the Higgs sector of a general Twin Higgs theory. The same accidental symmetry then suppresses interactions between the 125 GeV Higgs and the scalar DM at low energies. The scalar is a thermal WIMP, and the fact that freeze-out proceeds through the full Twin Higgs portal coupling, while direct detection is suppressed, leads to predictions for direct detection cross sections that can be several orders of magnitude smaller than is the case in regular scalar Higgs Portal DM (HPDM). As can be seen from Figure 3, HPDM is almost completely excluded, while THPDM is consistent with current constraints for $m_S \gtrsim \mathcal{O}(100 \text{ GeV})$. Indeed, this is the favoured parameter space of the model, based on naturalness considerations of the DM mass within the IR effective Twin Higgs theory. THPDM naturally predicts null results at current direct detection experiments but positive detections in next-generation experiments – a very compelling scenario. Furthermore, Twin Higgs models that predict dark radiation in excess of current experimental limits on ΔN_{eff} are consistent with CMB bounds if they include a source of asymmetric reheating, diluting the contribution of the twin sector. This dilution also affects any DM candidate, which further suppresses direct detection signatures for freeze-out DM since a smaller Twin Higgs portal coupling is needed to obtain the correct relic abundance after dilution.

We study two explicit models of asymmetric reheating, the νMTH [145] and XMTH [12], and find that in addition to alleviating the tension with cosmology, both lead to predicted DM dilution factors of $\mathcal{O}(100 - 1000)$. This further opens up the direct detection parameter space of the model, with THPDM masses as low as 50 GeV allowed by current constraints (see Figure 11). The dilution factor is also in principle observable by comparing the expected direct detection event rate for a given DM mass to observation, if the rest of the model is corroborated in collider experiments. The measured dilution therefore provides another probe of the cosmology of the asymmetrically reheated Twin Higgs.

THPDM is a simple and general extension of the Twin Higgs that naturally predicts DM heavier than $\sim \mathcal{O}(100\ \mathrm{GeV})$ and evades current direct detection experiments, but predicts a signal at next generation detectors such as LZ, XENONnT, and DARWIN in large regions of parameter space. Twin Higgs models will be additionally constrained by measurements of $\mathrm{Br}(h \to \mathrm{inv})$ and precision electroweak physics, searches for LLPs [112, 161–164], and searches for additional scalars [87, 95–100, 150]. New results from CMB-S4 will put stringent constraints on twin radiation and the dilution factor D. If naturalness and dark matter are explained by the Twin Higgs, it is therefore possible that a deluge of discoveries are on the horizon, which will not only provide compelling evidence of new physics but, taken together, tell a detailed story of how the Twin Higgs explains several fundamental mysteries of our universe.

3 Resurrecting the Fraternal Twin WIMP Miracle

This Chapter has been previously published in the *Physical Review D (PRD)*.
Author list: David Curtin, SG, Dan Hooper, Jakub Scholtz, Jack Setford
DOI:10.1103/PhysRevD.105.035033 [191].

Statement of individual contributions
In this project Jack Setford and I worked closely to compute the thermally averaged cross sections and resulting direct detection signatures, resulting in Figures 13 and 14. I personally produced Figures 13 and 14. Each author took a turn editing the paper into its final form, but I was not involved in the composition of the initial draft.

In Twin Higgs models which contain the minimal particle content required to address the little hierarchy problem (*i.e.* fraternal models), the twin tau has been identified as a promising candidate for dark matter. In this class of scenarios, however, the elastic scattering cross section of the twin tau with nuclei exceeds the bounds from XENON1T and other recent direct detection experiments [1, 3, 192]. In this paper, we propose a modification to the Fraternal Twin Higgs scenario that we call $\mathbb{Z}_2$FTH, incorporating visible and twin hypercharged scalars (with $Y = 2$) which break twin electromagnetism. This leads to new mass terms for the twin tau that are unrelated to its Yukawa coupling, as well as additional annihilation channels via the massive twin photon. We show that these features make it possible for the right-handed twin tau to freeze out with an acceptable thermal relic abundance while scattering with nuclei at a rate that is well below existing constraints. Nonetheless, large portions of the currently viable parameter space in this model are within the reach of planned direct detection experiments. The prospects for indirect detection using gamma rays and cosmic-ray antiprotons are also promising in this model. Furthermore, if the twin neutrino is light, the predicted deviation of $\Delta N_{\rm eff} \approx 0.1$ would be within reach of Stage 4 CMB experiments. Finally, the high luminosity LHC should be able to probe the entire parameter space of the $\mathbb{Z}_2$FTH model through charged scalar searches. We also discuss how searches for long-lived particles are starting to constrain Fraternal Twin Higgs models.

3.1 Introduction

The hierarchy problem and the unknown nature of dark matter have long motivated searches for new physics at colliders and direct detection experiments. Proposed solutions to the hierarchy problem

involve new states with masses near the weak scale which stabilize the mass of the Higgs boson. The problem of dark matter is also suggestive of new physics near the weak scale, motivated by the fact that a stable particle with a weak-scale mass and an annihilation cross section similar to that associated with the Standard Model (SM) weak interaction will freeze out of equilibrium in the early universe with a relic abundance similar to the measured density of dark matter. This so-called "WIMP miracle" has inspired an enormous range of dark matter models over the past several decades (for a historical review, see Ref. [193]). Naturally, any physics beyond the SM that is capable of solving both of these mysteries would be particularly well-motivated. This has long bolstered interest in supersymmetry [85], which requires each fermion to be accompanied by a bosonic partner (and vice versa) with identical gauge charges and couplings, thereby canceling quadratically divergent contributions to the Higgs mass. Some of these superpartner particles, in particular the neutralinos, are weakly interacting, and thus could serve as a dark matter candidate in the form of a weakly interacting massive particle (WIMP). Naturalness considerations, however, lead one to expect the superpartners of the top quark to be light enough to be produced at a high rate at the Large Hadron Collider (LHC), in tension with the null results presented by the ATLAS and CMS collaborations [78, 79, 194–197]. Similarly, across most of the supersymmetric parameter space, the lightest neutralino is predicted to scatter with nuclei at a rate that is excluded by direct detection experiments [1, 3, 192]. In light of these considerations, it is well motivated to consider alternatives to supersymmetry that can address the hierarchy problem and provide a dark matter candidate without conflicting with the constraints produced by the LHC and direct detection experiments.

Several scenarios have been proposed in which the quadratic contributions to the Higgs boson mass are cancelled by particles without SM gauge charges, constituting a paradigm known as "Neutral Naturalness" [34, 35, 41, 154, 198–202]. The most well-known and perhaps most promising of these models are those which fall within the Twin Higgs framework [34, 35, 38, 103, 154, 198, 203]. In Twin Higgs models, a discrete $\mathbb{Z}_2$ symmetry stabilizes the Higgs mass at one-loop to solve the little hierarchy problem, with supersymmetry or compositeness solving the full hierarchy problem in the UV completion [91, 95, 101–106, 108, 110, 149]. This symmetry does not commute with SM gauge charges, giving rise to a twin sector of particles that have the same spin as their SM counterparts, but that are charged under twin versions of the SM forces. Since the twin tops are singlets under the SM strong force, this mechanism naturally evades standard LHC searches for top partners.

Just as supersymmetry must be broken in the infrared, the discrete symmetry of Twin Higgs models must be softly broken in order to make this framework a realistic theory of nature. In the perfect $\mathbb{Z}_2$-symmetric limit, the lightest Higgs mass eigenstate is an equal admixture of the visible and twin sector Higgs bosons, in significant conflict with measurements of the Higgs couplings [86, 204, 205]. Some source of $\mathbb{Z}_2$-breaking must therefore lift the twin Higgs vacuum expectation value (VEV), f, to a value that is a few times larger than that of the visible Higgs, typically $f/v \sim 3-5$. As a result, the 125 GeV Higgs boson contains a $\sim v^2/f^2 \sim \mathcal{O}(10\%)$ admixture of the twin sector

Higgs, similar to the degree of tuning that the $\mathbb{Z}_2$ breaking must satisfy (though that tuning can be reduced in non-minimal constructions [92, 93, 206]). This Higgs portal, which is essential for the solution to the little hierarchy problem, provides a means by which this class of models can be probed at the LHC and future colliders. In particular, the mixing predicts universal deviations among the Higgs couplings [86], which could be detected at the high-luminosity LHC and would be exhaustively probed at future lepton colliders [207, 208]. The Higgs portal also allows for exotic Higgs decays into the twin sector, which may result in the production of long-lived particles [35, 155].

In the unbroken $\mathbb{Z}_2$-limit, Twin Higgs models include a massless twin photon and three light twin neutrinos, all of which are problematic for cosmology. In particular, these particles are collectively predicted to contribute to the energy density of radiation at a level corresponding to $\Delta N_{\text{eff}} \sim 5$, while CMB measurements have produced an upper limit of $\Delta N_{\text{eff}} < 0.23$ (2σ) [11]. Realistic Twin Higgs models must therefore either eliminate these light degrees of freedom by introducing a hard breaking of the $\mathbb{Z}_2$ symmetry (while retaining the cancellation between the top and twin top contributions to the Higgs mass) [35, 118], or by introducing an asymmetric reheating mechanism that increases the temperature of the visible sector relative to the twin sector, thereby lowering ΔN_{eff} [12, 145].

The Fraternal Twin Higgs (FTH) model [35] is a particularly simple and appealing representation of the first possibility. The twin sector in the most minimal version of this model consists of t', b', τ', and ν'_τ, which are charged under twin QCD and twin weak interactions in analogy to the SM. Twin electromagnetism is either not gauged in the most minimal version of this model, or is broken at a high scale. For the most $\mathbb{Z}_2$-preserving version of this particle content, the masses of the twin fermions are set by SM-like Yukawa couplings to the twin Higgs, making them heavier than SM fermions by a factor of f/v. Alternatively, one could break the $\mathbb{Z}_2$ symmetry further, allowing for us to treat $m_{b'}, m_{\tau'}$, and $m_{\nu'_\tau}$ as free parameters (although the twin top mass must remain fixed to $(f/v) \times m_t$ in order to stabilize the mass of the light Higgs).

By virtue of an accidental global $U(1)$ symmetry, the twin tau is stable in the FTH model, making it a potential candidate for dark matter [116, 118]. (See [63, 117, 119–121, 123, 135, 147, 209–213] for other dark matter candidates within the Twin Higgs framework.) In particular, the twin tau annihilates primarily to twin neutrinos or twin bottoms through the twin weak interaction (which is a copy of the SM weak interaction, with $m_{W'} = (f/v) \times m_W$), yielding an acceptable thermal relic density for masses in the range of $m_{\tau'} \sim 50 - 150$ GeV. This "Fraternal Twin WIMP Miracle" plays out almost entirely within the hidden sector: annihilations into the visible sector through the Higgs portal play a subdominant role, except near $m_{\tau'} \sim m_h/2$. However, the Higgs portal does lead to irreducible signatures. Since the entirety of the twin tau mass comes from its Yukawa coupling to the twin Higgs, the twin tau is predicted to have a sizable elastic scattering cross section with nuclei through the Higgs portal. Therefore, constraints from XENON1T and other recent direct detection experiments [1, 3, 192] have by now excluded the entire range of parameter space that yields an acceptable relic abundance in this model.

A very minimal modification of the FTH model is to reintroduce the twin photon, γ'. Recently, a new mechanism was proposed for the Mirror Twin Higgs model to spontaneously break the $\mathbb{Z}_2$ symmetry in the Higgs sector by extending it to include scalars charged under visible and twin hypercharge [150]. One of these new scalars, by definition in the twin sector, acquires a VEV, giving a mass to the twin photon and generating the soft $\mathbb{Z}_2$-breaking Higgs mass term that raises f above v. Depending on the hypercharge of the scalar, various additional twin fermion mass terms can also be generated through this mechanism.

In this paper, we apply the mechanism proposed in Ref. [150], implemented with $Y = 2$ (twin) hypercharge scalars,[21] to a maximally $\mathbb{Z}_2$-symmetric FTH model. We demonstrate that this "$\mathbb{Z}_2$FTH" model with spontaneously broken twin hypercharge provides a viable dark matter candidate in the form of a dominantly right-handed twin tau with a mass on the order of $\sim \mathcal{O}(100\text{ GeV})$ [22]. Unlike dark matter in the conventional FTH model, our scenario is consistent with existing direct detection constraints. This is made possible due to the new τ' Majorana mass terms that are unrelated to the elastic scattering cross section, as well as new annihilation processes mediated by the twin photon. The $\mathbb{Z}_2$FTH scenario leads to a variety of potentially observable signals, including those at future direct detection experiments, exotic Higgs decay searches, CMB measurements, and indirect dark matter searches.

3.2 A New Fraternal Twin WIMP Miracle

In Ref. [150], Batell and Verhaaren augmented the standard Twin Higgs model with new scalars, $\Phi = (\phi, \phi')$, in the visible and twin sectors, respectively. The spontaneous $\mathbb{Z}_2$ breaking can be understood from a simplified Φ-only potential,

$$V_\Phi = -\mu_\Phi^2 |\Phi|^2 + \lambda_\Phi |\Phi|^4 + \delta_\Phi (|\phi|^4 + |\phi'|^4) \,, \tag{3.1}$$

which is $\mathbb{Z}_2$ symmetric and obeys a $U(2)$ symmetry in the $\delta_\Phi \to 0$ limit. If $\delta_\Phi < 0$, one of the scalars has no VEV, while the other scalar (by definition ϕ') acquires a VEV, f_ϕ. The resulting physical degrees of freedom are as follows:

- The twin hypercharge gauge boson, B', acquires a mass of $m_{B'} = \sqrt{2} Y g' f_\phi$, where Y is the hypercharge carried by the new scalars and g' is the twin hypercharge gauge coupling.
- The radial component of ϕ', labeled ρ, is the radial mode of the approximate $U(2)$ breaking with a mass of $m_\rho \sim \sqrt{\lambda_\Phi} f_\phi$. The angular mode is eaten by the B'.

[21] We use the convention $Q = T^3 + Y$ here.

[22] Since the DM candidate needs to be $\mathcal{O}(100\text{ GeV})$ in order to yield the correct relic abundance, we choose to embed this $\mathbb{Z}_2$-breaking mechanism within the FTH framework, where the twin tau can naturally have the right mass and be stable due to the high mirror top mass. One could identify the twin electron in the original model proposed by Batell and Verhaaren [150], but ensuring its stability would require lifting the mass of all other twin fermions above the $\mathcal{O}(100\text{ GeV})$ scale. This results in the same effective theory as the FTH, while possibly reintroducing the hierarchy problem (if the light mirror quarks are lifted by increasing their Yukawa couplings to the mirror Higgs).

- The visible sector charged scalar, ϕ, is a pseudo-Goldstone boson with a mass given by $m_\phi \sim \sqrt{\delta_\Phi} f_\phi$. Note that ϕ can be much lighter than the twin sector radial mode, ρ.

This potential can be integrated into the Twin Higgs scalar sector. The $\mathbb{Z}_2$-symmetric coupling between the hypercharge breaking scalars and the visible and twin electroweak doublet Higgs bosons,

$$\delta_{H\Phi}(|H|^2 - |H'|^2)(|\phi|^2 - |\phi'|^2) \,, \tag{3.2}$$

then generates the $\mathbb{Z}_2$-breaking Higgs mass term once ϕ' acquires its VEV. The mass spectrum of the twin electroweak gauge bosons is straightforward, with the caveat that we always define γ' as the admixture of B' and W'^3 that is predominantly B', while Z' is always predominantly W'^3. Thus $m_{\gamma'} \approx m_{B'}$ when $m_{B'} \gg m_{Z'}$ or $m_{B'} \ll m_{Z'}$, with a discontinuous level crossing in the spectrum around $f_\phi \sim f$, when the twin photon and Z' are similar in mass.

This mechanism accomplishes the required breaking of the $\mathbb{Z}_2$ symmetry in the scalar sector of the Twin Higgs model in a simple and elegant way. Note that the new scalars are protected from quadratic divergences via the same twin mechanism as the SM Higgs. It also makes interesting physical predictions, including the existence of the electrically charged scalar in the visible sector, ϕ. If this scalar were stable, it would be an unacceptable charged relic. To evade this problem, we require that $Y = 1$ or $Y = 2$, allowing for Yukawa couplings that enable ϕ to decay to fermions in each sector. In the $Y = 1$ case, breaking of twin hypercharge would allow twin-electric charge to be violated by units of $\Delta Q' = 1$, making the twin tau unstable. Since we want to identify τ' as a dark matter candidate, we focus on the case of $Y = 2$, where the lightest τ' mass eigenstate can be stable. The visible-sector ϕ must then be heavy enough to evade current bounds on new doubly-charged particles ($m_\phi \gtrsim 500$ GeV [214], assuming that ϕ decays exclusively to taus, or $\gtrsim 600 - 800$ GeV if there are significant decays to electrons or muons). It is convenient to keep in mind that $m_{\gamma'} \approx f_\phi$ in this case (neglecting Z'-mixing).

With these considerations in mind, we define the *maximally $\mathbb{Z}_2$-symmetric Fraternal Twin Higgs scenario* ($\mathbb{Z}_2$FTH) as follows. We begin with the FTH particle spectrum (*i.e.* only 3rd generation twin fermions), requiring all gauge and Yukawa couplings to take on their $\mathbb{Z}_2$ symmetric values (*i.e.* equal to the SM values, up to RGE effects). We then restore the twin photon, and add the $Y = 2$ hypercharge breaking field to the scalar sector in order to generate the spontaneous $\mathbb{Z}_2$ breaking in the Higgs sector and give the twin photon a mass. If some dynamical mechanism were to remove the first two generations of twin fermions from the low-energy spectrum, this theory could be fully $\mathbb{Z}_2$ symmetric in the UV. Alternatively, the discrete symmetry might only apply to the gauge, scalar and third generation fermion sectors, as is the case in some proposed UV completions [111]. In any case, the absence of the 1st and 2nd generation twin fermions in our model has the fortunate side effect of solving the domain wall problem of spontaneous $\mathbb{Z}_2$ breaking that is found in the original implementation of this model [150], since the loop-induced quartic couplings of the ϕ, ϕ' scalars are no longer symmetric

(see Appendix 3.5.1 for details). Therefore, once the asymmetry in the fermion content between the two sectors is established by some other means, this mechanism ensures that the sector containing less matter also has broken hypercharge and a higher Higgs VEV, establishing its identity as the "twin" sector.

The $\mathbb{Z}_2$FTH scenario features new mass terms for the twin tau, generated from interactions with ϕ'. In particular, there is a new Yukawa coupling for the charged right-handed tau field, $\bar{E}'_\tau$, in the twin sector:

$$-\mathcal{L} \supset \lambda_\tau \phi' \bar{E}'_\tau \bar{E}'_\tau + \text{ h.c.}, \tag{3.3}$$

as well as new non-renormalizable interactions involving the charged left-handed lepton field, L'_τ, and Higgs doublet, H':

$$-\mathcal{L} \supset \frac{\xi_\tau}{\Lambda^2}\phi'^*(L'_\tau H'^\dagger)^2 + \frac{\tilde{c}_\tau}{\Lambda^2}|\phi'|^2 L'_\tau H'^\dagger \bar{E}'_\tau \ + \text{h.c.}, \tag{3.4}$$

where Λ is the scale at which the Twin Higgs scenario is UV completed. Note that analogous terms appear in the visible sector, but these do not lead to new mass terms because $\langle\phi\rangle = 0$. Once H, H', and ϕ' acquire their VEVs, these terms give rise to a non-trivial twin tau mass matrix:

$$\mathcal{L} \supset -\frac{1}{2}\bar{\psi}_i (M_{\tau'})_{ij}\psi_j + \text{h.c.}\ , \quad M_{\tau'} = \begin{pmatrix} m_{LL} & m_{LR} \\ m_{LR} & m_{RR} \end{pmatrix}, \tag{3.5}$$

where

$$m_{LR} = \frac{y_\tau}{\sqrt{2}} f + \frac{\tilde{c}_\tau}{\sqrt{2}}\frac{f_\phi^2}{\Lambda^2} f, \tag{3.6}$$

$$m_{LL} = \xi_\tau \frac{f^2}{\Lambda^2} f_\phi, \tag{3.7}$$

$$m_{RR} = 2\lambda_\tau f_\phi, \tag{3.8}$$

and $y_\tau \approx 0.01$ is the $\mathbb{Z}_2$-symmetric twin tau Yukawa coupling. In general, the τ' mass eigenstates will be two Majorana fermions, τ'_1, τ'_2, with masses $m_{\tau'_1} < m_{\tau'_2}$.

Two effects are responsible for the stability of τ'_1 and hence its suitability as a dark matter candidate. First, the high mass of the twin top can forbid hadronic τ'_1 decays into twin sector states, even though τ' lepton number is no longer conserved due to twin hypercharge breaking. Second, the unbroken $U(1)_{\text{EM}}$ in the visible sector ensures the twin tau cannot decay into SM particles.

We can now understand why the twin tau is a viable WIMP in our new $\mathbb{Z}_2$FTH scenario. First, the twin photon enhances the twin tau annihilation cross section to both $\bar{b}'b'$ and $\bar{\nu}'\nu'$ final states, with the latter interaction arising because the $\phi'^2 B'_\mu B'^\mu$ coupling causes the mixing angle between the B'_μ

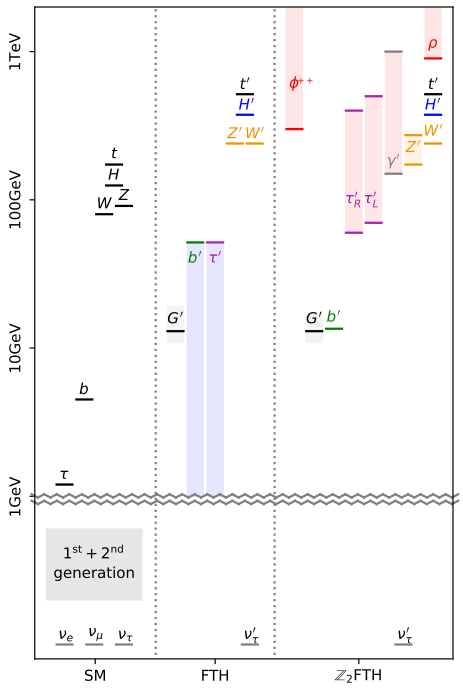

Figure 12. The particle spectrum of the Standard Model (left), compared to that predicted in the original Fraternal Twin Higgs (FTH) model (center), and in the $\mathbb{Z}_2$-symmetric FTH model with τ'_R dark matter as presented in this paper (right). In original FTH model, the masses of twin bottom and tau are controlled by their $\mathbb{Z}_2$-breaking Yukawa couplings, with their allowed range represented in blue. In the $\mathbb{Z}_2$FTH, the masses of twin taus and twin photon are determined by their coupling to $\tilde{\phi}$, with their allowed ranges shown in red. Note that ϕ^{++} is in the visible sector.

and W'^3_μ to differ from the Weinberg angle. We assume that $m_{b'} = (f/v)\, m_b$ to maximally respect the $\mathbb{Z}_2$ symmetry, and that the twin bottoms annihilate or decay to twin glueballs which subsequently decay to the SM through the Higgs portal [23]. Secondly, for $m_{\gamma'} \gtrsim \mathcal{O}(100\ \text{GeV})$, we find that twin taus with $m_{\tau'_1} > m_{b'} \gtrsim 15$ GeV can freeze out with the desired relic density without being excluded by direct detection constraints. In order to raise $m_{\tau'}$ above the twin bottom mass, we make use of the new mass contributions shown in Eqns. (3.6)-(3.8). In contrast to the original FTH scenario, which relied on adjusted twin Yukawa couplings, these new mass terms make it possible to realize τ'_1 as a dark matter candidate while fully respecting the $\mathbb{Z}_2$ symmetry.

In principle, the lightest twin tau in the $\mathbb{Z}_2$FTH model could be mostly τ'_R (if $m_{LL} > m_{RR} \gg m_{LR}$) or mostly τ'_L (if $m_{RR} > m_{LL} \gg m_{LR}$). Alternatively, in the special case in which ξ_τ/Λ^2 and λ_τ are small, the mass splitting between the two twin tau states could be very small, allowing us to treat the two twin tau states as a single pseudo-Dirac fermion. However, the τ'_L or pseudo-Dirac dark matter candidates have an effective Yukawa coupling to the 125 GeV Higgs that scales with their

[23] Even though we assume twin bottom and glueball masses expected from the $\mathbb{Z}_2$ symmetry, their exact masses are not important for the viability of this scenario, as long as they can annihilate or decay into the visible sector.

mass, $y_{\tau_1}^{\text{eff}} \sim (m_{\tau_1}/f)\sin\vartheta$ (where $\sin\vartheta \approx v/f$). This is similar to the original Fraternal Wimp Miracle [116, 118] and is already excluded by direct detection. On the other hand, m_{RR} in Equation (3.8) is entirely generated by the hypercharge breaking VEV. This allows a dominantly τ'_R dark matter candidate to be sufficiently heavy while also avoiding sizeable Higgs portal couplings. We therefore focus on this case for the remainder of our study.

In Figure 12, we show a sketch of the particle spectrum expected in this new $\mathbb{Z}_2$FTH model, for the case in which the lightest twin tau is mostly τ'_R, and compare this to the original FTH scenario. To realize the τ'_R dark matter candidate, the ξ_τ interaction in Equation (3.7) must be sufficiently large to ensure $m_{LL} > m_{RR}$. This will generate a mass correction to H' at loop order, which can spoil the Twin Higgs solution of the little hierarchy problem [150]. An extremely generous upper bound for this coupling can be derived by requiring that this correction be no larger than gauge or top loop corrections, which implies $\xi_\tau \lesssim \Lambda^2/(f f_\phi)$, but any sensible theory should have m_{LL} significantly below this bound. Therefore our model must satisfy

$$m_{\tau'_1} < m_{\tau'_2} < f. \tag{3.9}$$

However, an even stronger constraint is obtained by requiring that the twin-hadronic decay $\tau'_1 \to \nu' b' t'$ is kinematically forbidden,

$$m_{\tau'_1} < m_{t'} + m_{b'}. \tag{3.10}$$

We find that viable scenarios with the correct dark matter relic abundance can easily satisfy these requirements, as long as the scale of the UV completion, Λ, is around a few TeV.

The extended scalar sector plays an important role in the dark matter phenomenology within this model. The radial mode of the twin hypercharge breaking scalar, ρ, mixes slightly with the visible sector Higgs after $\mathbb{Z}_2$ breaking (see Ref. [150] for details). The $h-\rho$ mixing angle is approximately given by

$$\sin\alpha \approx \frac{-f^2 m_h^2}{\sqrt{2} f_\phi v m_\rho^2} \approx -0.01 \left(\frac{f}{v}\right)^2 \left(\frac{\text{TeV}}{m_\rho}\right)^2 \left(\frac{300\text{ GeV}}{f_\phi}\right), \tag{3.11}$$

which is too small to be relevant for LHC phenomenology or to have an impact on the thermal freeze-out of the twin taus. However, this mixing will have important consequences for direct detection, making it necessary to understand the possible size of f_ϕ and m_ρ.

The mixing term and the Higgs mass are parametrically related, since both are generated by the nonzero value of f_ϕ (recall that the visible sector Higgs is a pseudo-Goldstone boson whose mass arises from $\mathbb{Z}_2$-violating effects). Fixing the ratio between the off-diagonal terms and the Higgs mass term bounds the larger mass eigenvalue from below. The mass of the radial mode must therefore satisfy

$$m_\rho - \frac{m_h^2}{m_\rho} \gtrsim \frac{1}{\sqrt{2}} \frac{m_h f^2}{v f_\phi}. \tag{3.12}$$

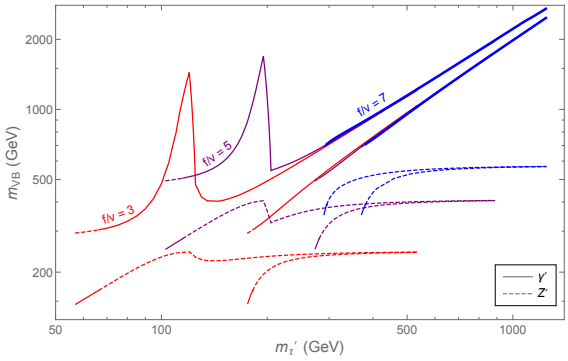

Figure 13. The values of $m_{\gamma'}$ and $m_{Z'}$ (collectively denoted $m_{\rm VB}$, for vector boson) as a function of $m_{\tau'_1}$ that are required to obtain $\Omega_{\tau'_R} h^2 = 0.12$ [11], for the case in which the lightest twin tau is mostly τ'_R. The gauge boson eigenstates are identified such that γ' is always mostly B' and Z' is mostly W'^3. Results are shown for $f/v = 3, 5$ and 7. Note that the dark photon masses coincide for heavy τ'. The maximum τ'_1 mass is given by Equation (3.10).

For $f/v = 3$ and $f_\phi = 300$ GeV, this corresponds to $m_\rho \gtrsim 700$ GeV. In addition, there is a maximum value for the mass of the radial mode,

$$m_\rho \lesssim 2\sqrt{\lambda_\Phi^{\rm max}} f_\phi, \tag{3.13}$$

where $\lambda_\Phi^{\rm max} = (2/3) \times 4\pi$ is the upper bound from unitarity considerations [215]. In addition to bounding the acceptable range for m_ρ, these conditions also require that

$$f_\phi \gtrsim (60 \text{ GeV}) \times \frac{f}{v}\,, \tag{3.14}$$

which further restricts the parameter space of our theory.

The relic abundance of the twin tau is determined in large part by its twin sector annihilation cross section through Z' and γ' exchange to twin bottoms and twin neutrinos (see Appendix 3.5.2). In the special case of $m_{\tau'} \sim m_h/2$, annihilations through the Higgs portal into the visible sector can also play an important role. In Figure 13, we plot the values of the twin photon and twin tau masses that lead to the measured dark matter relic abundance, for the case in which the lightest twin tau is mostly τ'_R and for three representative values of f/v. Since the twin photon plays a crucial role in the determination of the relic abundance, its minimum mass in turn dictates a minimum value of $m_{\tau'_1}$ for each case.

3.3 Experimental Signatures

Although the values of m_ρ, m_{LL} and m_{LR} do not appreciably impact the relic abundance of our τ'_R dark matter candidate, they entirely determine the magnitude of its direct detection signal. The elastic

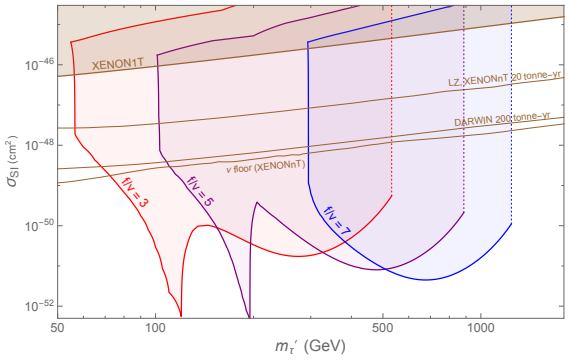

Figure 14. The allowed range in the $\mathbb{Z}_2$FTH model of the twin tau's spin-independent elastic scattering cross section with nuclei. The vertical dashed lines indicate the upper bound on $m_{\tau'_1}$ from requiring stability against twin hadronic decays. Shown in brown are the current constraints from XENON1T [3], and the projected constraints from LUX-Zeplin (LZ) [4] and XENONnT [5] after 20 tonne-years of exposure, as well as from DARWIN [6] with an exposure of 200 tonne-years. The neutrino floor curve was taken from Ref. [5].

scattering cross section with nuclei has two important contributions. First, the coupling of τ'_R with ρ, which in turn mixes with the Higgs, leads to an effective Yukawa coupling $\frac{1}{\sqrt{2}} y_{\tau_1}^{\text{eff,R}} h \bar{\tau}'_1 \tau'_1$ that is given by

$$y_{\tau'_1}^{\text{eff,R}(\rho)} = \sqrt{2} \lambda_\tau \sin\alpha, \tag{3.15}$$

with $\sin\alpha$ defined in Equation (3.11) [24]. This scales as $\sim 1/m_\rho$ across the relevant range of $m_{\gamma'}$. Recall from the discussion in the previous section that the value of m_ρ is bounded from both above and below, allowing us to bound this contribution to the dark matter's coupling to nuclei.

A second contribution to the coupling is generated as a result of the mixing of τ'_R with τ'_L, thereby accessing the usual Higgs portal. The contribution to this coupling is given by

$$y_{\tau'_1}^{\text{eff,R}(\tau'_{\text{L}})} = \frac{\sqrt{2}}{f} \frac{m_{LR}^2}{m_{LL}} \left(\frac{m_{RR}}{m_{LL}}\right)^2 + \mathcal{O}\left(\frac{m_{RR}}{m_{LL}}\right)^3. \tag{3.16}$$

Since $m_{\tau'_2}$ is bounded by Equation (3.9), this contribution to the direct detection signal can also be bounded from both above and below.

The range of the possible direct detection signal is depicted in the shaded regions of Figure 14, for three different values of f/v. The upper boundary represents the largest possible scattering cross section, realized in the pseudo-Dirac limit, where $m_{LL} = m_{RR}$ and $m_{\tau'_2} - m_{\tau'_1} = 2m_{LR}$, with m_{LR} set to the smallest value possible for the minimal assumption of $\tilde{c}_\tau = 0$. Other values would not significantly affect the results. We also maximise $y_{\tau'_1}^{\text{eff,R}(\rho)}$ by minimising the possible value of m_ρ (see Equation (3.12)), but its contribution is negligible compared to $y_{\tau'_1}^{\text{eff,R}(\tau'_{\text{L}})}$.

[24] Note that the Majorana fermion nature of the τ'_1 introduces an extra factor of 2 into the Feynman rule associated with this vertex.

The lower boundary, representing the smallest possible cross section, corresponds to the maximum value of m_ρ (see Equation (3.13)), and to $m_{LL} \approx m_{\tau_2'}$ saturating the upper bound in Equation (3.9). The right boundary of the allowed $m_{\tau_1'}$ range is set by maintaining stability of τ_1' against twin-hadronic decays (see Equation (3.10)). The left boundary is set by the minimum value of $m_{\gamma'}$ (see Equation (3.14) and Figure 13). For τ_1' masses near the minimum allowed value, the lower bound on the scattering cross section is entirely dominated by ρ mixing, while for larger dark matter masses, mixing with τ_L' contributes significantly.

From Figure 14, it is clear that our twin tau dark matter candidate could potentially be discovered at upcoming underground dark matter experiments. In significant portions of the parameter space, however, the elastic scattering cross section is below the so-called "neutrino floor", making it possible that this candidate could escape direct detection. Fortunately, the prospects for indirect detection are also promising in this scenario. The twin tau annihilates in this model mostly into twin bottoms, at a rate given by the thermal annihilation cross section. These twin bottoms then form quirky bound states [35, 216–218] which further annihilate or decay into twin glueballs that in turn decay into SM particles through the Higgs portal (see Appendix 3.5.3). The signals associated with this process could likely be used to place constraints on our scenario, and may be able to explain observed gamma-ray and cosmic-ray excesses [219–223]. A quantitative assessment of this signal is challenging due to the non-perturbative production of twin gluons, but is currently under investigation [224].

The $\mathbb{Z}_2$FTH model could also give rise to a small but tell-tale cosmological signature: a single light twin neutrino that contributes to $\Delta N_{\rm eff}$, assuming ν_τ' does not receive an extra contribution to its mass from an operator similar to the first term in Equation (3.4). The Higgs portal in this model keeps the visible and twin sectors in kinetic equilibrium in the early universe until $T \sim \mathcal{O}(\mathrm{GeV})$, at which point the two sectors decouple [116]. The twin bath at that time consists of twin bottoms and twin neutrinos, with the former keeping the latter in thermal equilibrium with the SM bath until decoupling. Because the twin sector has far fewer active degrees of freedom than the visible sector, and due to subsequent entropy injections in the visible sector below the decoupling temperature, we find that the single twin neutrino only contributes

$$\Delta N_{\rm eff}^{\mathbb{Z}_2\mathrm{FTH}} \approx 0.1 \tag{3.17}$$

to the abundance of dark radiation, in agreement with the results of Ref. [116]. While this is well below current bounds [11], it would be detected by upcoming Stage 4 CMB experiments, which are projected to be sensitive to $\Delta N_{\rm eff} \sim 0.02$ [14].

It has not escaped our attention that charged scalars can contribute to Δa_μ, and thus could possibly resolve the $(g-2)_\mu$ anomaly [225, 226]. In our scenario with m_ϕ above current bounds, however, this would requires a large positive value of ξ_μ and a large negative value of λ_μ, which seems difficult to realize in a reasonable UV completion that respects flavor constraints.

Turning our attention to the collider signature of this model, the charged $Y = 2$ scalar in the visible sector, ϕ, with coupling to taus, also gives rise to important signatures that could allow for colliders to probe this particular scenario. The high-luminosity LHC is projected to be sensitive to m_ϕ up to 1 TeV for decays to taus, and up to 2 TeV for decays to electrons or muons [150, 227]. Since $m_\phi \sim \sqrt{\delta} f_\phi$, where $f_\phi \approx m_\gamma$ (see Figure 13) and δ represents a combination of quartics that should not be very large, this should cover much of this model's parameter space.

The existence of the massive twin photon means that a kinetic mixing with the SM hypercharge gauge boson may be present, $\frac{1}{2}\epsilon B'_{\mu\nu} B^{\mu\nu}$. Depending on the UV completion of the model, this mixing could be generated at one-loop and be large, $\epsilon \sim 0.01 - 0.1$, especially for strongly coupled UV completions. It is also entirely plausible that the kinetic mixing could be many orders of magnitude smaller. The signatures of this kinetic mixing were investigated recently in Ref. [186], and significant parameter space could be covered by the high-luminosity LHC and other future colliders.

Finally, the standard signatures of the FTH scenario are present in the $\mathbb{Z}_2$ scenario as well, including exotic Higgs decays into twin fermions and glueballs which give rise to long-lived particle signatures [35, 96, 99, 100, 112, 155, 228–231], the production of new SM singlet scalar states [87, 96, 97, 99, 232], and possible signals of the UV completion (see e.g. [113]). The long-lived particle signatures are especially spectacular, and are a necessary component of our model since the annihilation of twin taus into twin bottoms relies on the b' decaying or annihilating into SM particles prior to the onset of Big Bang nucleosynthesis, either directly as unstable twin bottomonia, or by annihilating into twin glueballs which decay through the Higgs portal. It is noteworthy that long-lived particle searches at the LHC [233–238] are starting to be sensitive to relevant parts of the FTH parameter space, in particular the production of twin bottomonia which subsequently decay to twin glueballs. While unknown aspects of the non-perturbative dynamics of the hidden sector make precise predictions challenging in some cases, it is clear that there is exciting discovery potential for Twin Higgs signatures at the LHC, with near-complete coverage of Neutral Naturalness expected with planned future experiments. We discuss this in more detail in Appendix 3.5.3.

3.4 Conclusion

In this study, we have presented a $\mathbb{Z}_2$ symmetric version of the Fraternal Twin Higgs model, which contains a viable dark matter candidate in the form of the dominantly right-handed twin tau, $\tau'_1 \approx \tau'_R$. This $\mathbb{Z}_2$FTH model extends the standard Fraternal Twin Higgs scenario by adding twin-hypercharge-breaking scalars with $Y = 2$ in order to supply the necessary $\mathbb{Z}_2$ symmetry breaking [150]. This addition allows us to rescue the Fraternal Twin WIMP Miracle [116, 118] by decoupling the twin tau mass from its Yukawa coupling to the twin Higgs, and by adding annihilation channels which proceed through twin photon exchange. We identify significant regions of parameter space in this model in which an $\mathcal{O}(100\ \mathrm{GeV})$ twin tau can be produced thermally in the early universe with an acceptable relic abundance, while scattering with nuclei at a rate that is consistent with existing direct detection

constraints. Incidentally, the truncated nature of the twin sector in fraternal models also solves the domain wall problem that is ordinarily present in Mirror Twin Higgs realizations of this spontaneous $\mathbb{Z}_2$-breaking mechanism.

This model has a number of observable consequences that will allow for its discovery or exclusion in the coming years. Across much of the currently viable parameter space, the dominantly-τ'_R dark matter candidate could be discovered at upcoming direct detection experiments. In addition, this scenario is predicted to generate a small but detectable contribution to the energy density of dark radiation, $\Delta N_{\text{eff}} \approx 0.1$, from the single generation of light twin neutrino, well within the projected sensitivity of Stage 4 CMB experiments. The prospects for testing this model at colliders are also very promising. In regions of parameter space that are compatible with τ'_R dark matter, the $Y = 2$ visible-sector scalar contained in this model is expected to be within reach of searches at the high-luminosity LHC. Furthermore, the usual signals of Neutral Naturalness, such as Higgs coupling deviations and the production of long-lived particles in exotic Higgs decays, are present in this model as well. As we discuss in Appendix 3.5.3, the LHC is becoming sensitive to these signatures in important regions of parameter space. Finally, indirect detection could provide an early discovery channel for this fraternal twin tau dark matter candidate, once the non-perturbative aspects of the glueball shower produced in the annihilation are understood [224].

In summary, the $\mathbb{Z}_2$FTH model presented here represents a promising and minimal extension of the Fraternal Twin Higgs framework, which addresses several of the shortcomings of the original model while preserving its solution to the little hierarchy problem. This model therefore constitutes an important new benchmark for WIMP dark matter in the Neutral Naturalness paradigm.

3.5 Appendices

3.5.1 A. Domain Walls

The full Lagrangian of the scalar sector of the $\mathbb{Z}_2$FTH model can be split into two parts. First, the $U(2)$ preserving terms are given by

$$\lambda_\Phi(|\phi|^2 + |\phi'|^2)^2 + \mu_\Phi^2(|\phi|^2 + |\phi'|^2), \tag{3.18}$$

while the $U(2)$ breaking terms are written as follows:

$$\delta_\Phi(|\phi|^4 + |\phi'|^4) + m^2(|\phi|^2 - |\phi'|^2) + \delta'(|\phi|^4 - |\phi'|^4). \tag{3.19}$$

While m and δ' also explicitly break the $\mathbb{Z}_2$ symmetry, they are set to zero at tree-level in our model.

The term proportional to δ_Φ ensures that there are only vacua of the form $(f_\phi, 0)$ and $(0, f_\phi)$. It does not, however, split their energy degeneracy; only the m^2 and δ' terms break the degeneracy between the depth of the vacua. As a result, if $m^2 = 0$ and $\delta' = 0$, the model will predict the existence of domain walls which are disfavored by cosmology. As long as the difference between the

energy densities of the two vacua is large compared to the domain wall energy, the domain walls dissipate gravitationally before they dominate the energy density of the universe [240]. This requirement corresponds to

$$\Delta V > \frac{\sigma^2}{m_{\rm Pl}^2}\,, \tag{3.20}$$

where $m_{\rm Pl}$ is the reduced Planck mass, and the domain wall tension σ can be estimated as $\sigma^2 \approx \delta_\Phi f_\phi^6$.

The authors of Ref. [150] included a small $m \neq 0$ term in order to split the vacuum degeneracy. In our case, we get a contribution to ΔV from a nonzero δ', which is generated radiatively because the two sectors have different numbers of fermion flavors. For small δ', the energy density difference between the two vacua is

$$\Delta V = \mu_\Phi^4 \frac{\delta'}{(\delta_\Phi + \lambda_\Phi)^2} \approx \delta' f_\phi^4. \tag{3.21}$$

The radiative correction to δ' is generated by couplings of the first two SM lepton generations to ϕ, analogous to Eq. (3.3), which are absent in the fraternal twin sector:

$$\delta' \sim \sum_{l=e,\mu} \frac{1}{16\pi^2} \lambda_l^4 \log(m_\phi/\Lambda). \tag{3.22}$$

In order to satisfy condition in Eq. (3.20), we require:

$$\lambda_l > \mathcal{O}(1)(f_\phi/m_{\rm Pl})^{1/2} \sim 10^{-8}. \tag{3.23}$$

This a very small coupling, even smaller than the electron Yukawa coupling. Therefore, as long as the ϕ scalar has even a very tiny coupling to the light SM leptons, the vacuum in which ϕ' gets a twin-hypercharge-breaking VEV is preferred and the domain wall problem is resolved.

3.5.2 B. Cross Sections

In this appendix we present analytic expressions for the cross sections required to compute the twin tau's thermal relic abundance. In the following expressions Q_X, W_X, Z_X represent the gauge couplings of the twin photon, W and Z bosons, respectively, to particle X, where all particles are mass eigenstates. For instance $Q_{\tau'}$ represents the coupling of the twin photon mass eigenstate to the lighter τ_1' mass eigenstate (*i.e.* the dark matter candidate). Thus to obtain the correct couplings, both the gauge and τ' mass matrices must first be diagonalized.

The τ' mass eigenstates are

$$\begin{aligned} \tau_1' &= \cos\theta_{\tau'}\tau_L' - \sin\theta_{\tau'}\tau_R', \\ \tau_2' &= \sin\theta_{\tau'}\tau_L' + \cos\theta_{\tau'}\tau_R', \end{aligned} \tag{3.24}$$

where the τ' mixing angle is given by

$$\sin^2\theta_{\tau'} = \frac{1}{2} + \frac{f_\phi(2\lambda_\tau\Lambda^2 - \xi_\tau f^2)}{2\sqrt{2f^2(\tilde{c}_\tau f_\phi^2 + y_\tau\Lambda^2)^2 + f_\phi^2(2\lambda_\tau\Lambda^2 - \xi_\tau f^2)^2}}. \quad (3.25)$$

In analogy to the SM, the twin gauge boson mass eigenstates are given by

$$\begin{aligned} Z'_\mu &= \cos\theta_{W'} W_\mu^{3'} - \sin\theta_{W'} B'_\mu, \\ \gamma'_\mu &= \sin\theta_{W'} W_\mu^{3'} + \cos\theta_{W'} B'_\mu, \end{aligned} \quad (3.26)$$

where the twin Weinberg angle is given by

$$\sin^2\theta_{W'} = \frac{(g^2 - g'^2)f^2 - 32g'^2 f_\phi^2 + \Delta}{2\Delta}, \quad (3.27)$$

with

$$\Delta = \sqrt{1024 g'^4 f_\phi^4 - 64 g'^2(g^2 - g'^2) f_\phi^2 f^2 + (g^2 + g'^2)^2 f^4}. \quad (3.28)$$

Keep in mind that the above definitions for $\theta_{\tau'}$ and $\theta_{W'}$ are subject to relabeling $\sin \leftrightarrow \cos$ in order to maintain τ'_1 as the lightest eigenstate and the Z' as the majority-W' state.

3.5.2.1 $\tau'_1\tau'_1 \to \nu'\nu'$

$$\frac{d\sigma_{\tau'\tau'\to\nu'\nu'}}{d\cos\theta} = \frac{1}{64\pi^2 s}\frac{\sqrt{s}}{\sqrt{s - 4m_{\tau'}^2}}|\mathcal{M}_{\nu'\nu'}|^2, \quad (3.29)$$

with

$$
\begin{aligned}
|\mathcal{M}_{\nu'\nu'}|^2 = &\left(\frac{Q_{\nu'}Q_{\tau'}}{s-m_{\gamma'}^2}+\frac{Z_{\nu'}Z_{\tau'}}{s-m_{Z'}^2}\right)^2(\alpha_+ + \alpha_-) \\
&+ 2|W_{\tau'}|^2\left(\frac{Q_{\nu'}Q_{\tau'}}{s-m_{\gamma'}^2}+\frac{Z_{\nu'}Z_{\tau'}}{s-m_{Z'}^2}\right)\left(\frac{\alpha_+}{t-m_{W'}^2}+\frac{\alpha_-}{u-m_{W'}^2}\right) \\
&+ |W_{\tau'}|^4\left(\frac{\alpha_+}{(t-m_{W'}^2)^2}+\frac{\alpha_-}{(u-m_{W'}^2)^2}\right. \\
&\left.- \frac{8m_{\tau'}^2 s}{(t-m_{W'}^2)(u-m_{W'}^2)}\right) \\
&- \frac{8|W_{\tau'}|^2 m_{\tau'}^2 s\beta}{(s-m_{\gamma'}^2)(s-m_{Z'}^2)}\left(\frac{1}{t-m_{W'}^2}+\frac{1}{u-m_{W'}^2}\right) \\
&- \frac{8m_{\tau'}^2 s\beta^2}{(s-m_{Z'}^2)^2(s-m_{\gamma'}^2)^2}, \qquad (3.30)
\end{aligned}
$$

where

$$
\begin{aligned}
\alpha_\pm &= \left(s \pm \cos\theta\sqrt{s}\sqrt{s-4m_{\tau'}^2}\right)^2 \qquad (3.31)\\
\beta &= Q_{\nu'}Q_{\tau'}(s-m_{Z'}^2) + Z_{\nu'}Z_{\tau'}(s-m_{\gamma'}^2),
\end{aligned}
$$

and

$$
\begin{aligned}
t &= -\frac{s}{4}(1-\cos^2\theta) - \left(\frac{\cos\theta\sqrt{s}}{2} - \sqrt{\frac{s}{4}-m_{\tau'}^2}\right)^2, \\
u &= -\frac{s}{4}(1-\cos^2\theta) - \left(\frac{\cos\theta\sqrt{s}}{2} + \sqrt{\frac{s}{4}-m_{\tau'}^2}\right)^2. \qquad (3.32)
\end{aligned}
$$

3.5.2.2 ${\tau'}_1{\tau'}_1 \to b'\bar{b}'$

$$
\frac{d\sigma_{\tau'\tau'\to b'\bar{b}'}}{d\cos\theta} = \frac{1}{64\pi^2 s}\frac{\sqrt{s-4m_{b'}^2}}{\sqrt{s-4m_{\tau'}^2}}|\mathcal{M}_{b'\bar{b}'}|^2, \qquad (3.33)
$$

with

$$|\mathcal{M}_{b'\bar{b}'}|^2 = \frac{4Q_{\tau'}^2}{(s-m_{\gamma'}^2)^2}\Big((Q_{b'}^2+Q_{\bar{b}'}^2)\kappa + Q_{b'}Q_{\bar{b}'}m_{b'}^2(s-6m_{\tau'}^2)\Big) + \frac{4Z_{\tau'}^2}{(s-m_{Z'}^2)^2}\Big((Z_{b'}^2+Z_{\bar{b}'}^2)\kappa + Z_{b'}Z_{\bar{b}'}m_{b'}^2(s-6m_{\tau'}^2)\Big) + \frac{4Q_{\tau'}Z_{\tau'}}{(s-m_{\gamma'}^2)(s-m_{Z'}^2)}\times \Big(2(Q_{b'}Z_{b'}+Q_{\bar{b}'}Z_{\bar{b}'})\kappa + (Q_{b'}Z_{\bar{b}'}+Q_{\bar{b}'}Z_{b'})m_{b'}^2(s-6m_{\tau'}^2)\Big), \quad (3.34)$$

where

$$\kappa = \frac{1}{8}\Big(s(s-4m_{\tau'}^2)(1+\cos^2\theta) + 4m_{b'}^2(2m_{\tau'}^2(1+2\cos^2\theta)-s\cos^2\theta)\Big) \quad (3.35)$$

and

$$t = -\left(\frac{s}{4}-m_{b'}^2\right)(1-\cos^2\theta) - \left(\cos\theta\sqrt{\frac{s}{4}-m_{b'}^2}-\sqrt{\frac{s}{4}-m_{\tau'}^2}\right)^2, \quad (3.36)$$

$$u = -\left(\frac{s}{4}-m_{b'}^2\right)(1-\cos^2\theta) - \left(\cos\theta\sqrt{\frac{s}{4}-m_{b'}^2}+\sqrt{\frac{s}{4}-m_{\tau'}^2}\right)^2. \quad (3.37)$$

3.5.3 C. Constraints on the Fraternal Twin Higgs from LHC Long-Lived Particle Searches

In the last few years, searches for long-lived particles (LLPs) at the LHC have advanced in great strides, with both ATLAS and CMS obtaining significant sensitivity to LLPs produced in exotic higgs decays in the inner detector [233–235] or outer detectors [236–238], most importantly the muon system. In this appendix, we discuss how these searches are starting to actually access the motivated parameter space of the Fraternal Twin Higgs model.

We make a number of assumptions for simplicity and concreteness in this discussion. First, we let the twin bottom mass obey the $\mathbb{Z}_2$ symmetry as in the $\mathbb{Z}_2$FTH scenario, $m_{b'} = (f/v)\, m_b \approx 14, 23, 32$ GeV for $f/v = 3, 5, 7$. For illustrative purposes, we can assume that the twin bot-

tomonium mass is simply twice the twin bottom mass (this is a reasonable approximation for the most unstable pseudoscalar state, χ_0, but in reality there are different states with different binding energies [35]). Similarly, we focus on just the lightest 0^{++} glueball with the shortest lifetime of all the glueball states [241, 242]. RG arguments favour the glueball mass to be in the range $m_{GB} \sim 10-30$ GeV [155], with a lifetime of $c\tau \sim 1-1000\,\mathrm{m}$ (lighter glueballs being longer-lived), though other masses are certainly possible depending on details of the UV completion.

For this range of parameters, there are two possibilities for the cosmological history of the twin sector: either twin bottoms form bottomonia below the confinement scale, which quickly *decay* to twin glueballs ($m_{GB} \lesssim m_{b'}$), or the twin bottomonia efficiently *annihilate* to twin glueballs ($m_{b'} \lesssim m_{GB} \lesssim 2m_{b'}$). Both of these scenarios are cosmologically viable, since the twin glueballs efficiently annihilate or decay to the SM [118]. Assuming the above mass ranges for twin glueballs, it seems that f/v = 3 (7) slightly favours the twin bottomonium annihilation (twin bottomonium decay) scenario.

Both glueballs and bottomonia are produced in exotic Higgs decays at the LHC, with $\mathrm{Br}(h \to b'b') \sim (0.06) \times (3v/f)$ and $\mathrm{Br}(h \to \text{twin glueballs}) \sim 10^{-5} - 10^{-4}$. In the twin bottomonium decay scenario, the exotic Higgs decays to twin bottomonia would produce further twin glueballs. With all this in mind, we can understand how recent LLP searches at the LHC are starting to constrain the FTH scenario.

The twin bottomonium decay scenario is already probed by searches for LHC decays in the ATLAS or CMS outer detectors [236–238], which can probe LLP lifetimes up to the (1 - 3) $\times 10\,\mathrm{m}$ range for percent-level exotic Higgs decay branching fractions. Assuming the bottomonia promptly decay to twin glueballs, this is sensitive to glueball masses near $m_{b'}$ [25]. By the time of the high-luminosity LHC, these searches will reach into very significant portions of FTH parameter space, though large portions are also unlikely to be excluded for $f/v \gtrsim 4$.

Direct Higgs decays to twin glueballs can occur in both the twin bottomonium decay and annihilation scenarios, but the branching fraction is likely out of reach of main detector searches even at the high-luminosity LHC. However, MATHUSLA [163, 243] would cover this range completely under the above assumptions (for both direct twin glueball production or production in twin bottomonia decays).

In the twin bottomonium annihilation scenario, LLP searches would have to detect the decays of twin bottomonia themselves. The shortest-lived pseudoscalar state, χ_0, has a lifetime in the range of $c\tau \sim (10^{-4} - 10^{-3})\,\mathrm{m}$ [112]. If all exotic Higgs decays produce χ_0's, then there is currently no sensitivity in this lifetime range for the relevant percent-level Higgs branching fractions. This is a very difficult signal to observe [244, 245], even with full high-luminosity LHC data, and direct probes may require future lepton colliders (taking advantage of the clean environment and known initial state) or a 100 TeV proton-proton collider (taking advantage of the high boost of the parent Higgs bosons to

[25] This assumes that a sizeable fraction of produced glueballs are the shortest-lived lightest 0^{++} state, which is backed up by finite-temperature QCD estimates [239]

increase the twin bottomonium decay length). However, in this scenario the presence of other twin bottomonium states could be important, since they can be significantly longer-lived. This could place their lifetime in the $(10^{-2} - 1)$ m window where inner detector searches have sensitivity for exotic Higgs decay production of LLPs with branching ratios of $\sim 10\%$ for for LLP masses below ~ 40 GeV [233, 235], taking advantage of Zh production for triggering, or displaced jet searches with pecent-level branching ratio sensitivity for LLP masses above ~ 40 GeV [234]. For longer lifetimes, the outer detector searches could have relevant sensitivity as well [236–238]. While this discovery prospect is exciting, it is challenging to assess to what extent these searches actually constrain the FTH, since the details of the twin bottomonium spectrum and the lifetime of the higher states are highly uncertain [35, 112].

While LHC LLP searches are already starting to probe important regions of FTH parameter space, there are some regions in which our ability to interpret these bounds is hindered by unknown aspects of the twin sector's non-perturbative dynamics. Future detectors like MATHUSLA would allow for near-complete coverage of the most motivated range of signals with lifetimes above a meter, while future lepton and proton colliders would allow the entire FTH model space to be probed, by a combination of LLP searches [155, 246–248], scalar resonance searches [87, 97, 99, 232], and Higgs coupling measurements [86, 207, 208] that are sensitive to the $\cos\vartheta$ reduction of the Higgs couplings to SM fermions regardless of the detailed twin sector phenomenology.

PART 3:

LEPTOQUARKS, $\mu - e$ CONVERSION, AND THE MINIBOONE ANOMALY

	$SU(3)_C$	$SU(2)_L$	$U(1)_Y$
R_2	**3**	**2**	$7/6$
$\tilde{R}_2$	**3**	**2**	$1/6$
S_1	$\bar{\mathbf{3}}$	**1**	$1/3$
S_3	$\bar{\mathbf{3}}$	**3**	$1/3$

Table 2. Gauge representations of some popular scalar leptoquarks.

4 Leptoquarks, $\mu - e$ Conversion, and the MiniBooNE Anomaly

Leptoquarks models are extremely natural consequences of unification scenarios. Constructions involving leptoquarks have appeared in the literature as early as 1974 with the Pati-Salam model [249] and have brought forth a wealth of interesting physical models with broad experimental consequences. A number of intriguing anomalies in the SM are beginning to solidify at the $2-4\sigma$ level. In Section 1.2.3 we discussed in detail the $R_{D^{(*)}}$ and $R_{K^{(*)}}$ anomalies, which are discrepant in the $2.2-3.3\sigma$ range (depending on the decay products and the energy transfer of the process), and the anomalous magnetic moment of the muon, Δa_μ, which has now been confirmed to disagree with the SM at 4.2σ. In addition, the presence of nonzero neutrino masses continues to be an unsolved puzzle that necessitates new physics beyond the SM.

Leptoquark models, and in particular scalar leptoquark models, are versatile tools that can be used to explain each of these anomalies. The four most commonly used scalar leptoquarks are shown in Table 4, and many different approaches have been taken to use some combination of these and other leptoquarks to explain some combination of the above anomalies [250–265].

Spurred by the success of scalar leptoquark models in explaining recent SM anomalies, in this Chapter we consider the possibility that scalar leptoquarks are also responsible for the recent excess of electron-like events reported by the MiniBooNE collaboration (as briefly mentioned in Section 1.2.3). We begin with a more thorough treatment of the MiniBooNE experimental results.

4.1 The MiniBooNE Anomaly

The MiniBooNE (Mini Booster Neutrino Experiment) experiment was designed as a followup to LSND (Liquid Scintillator Neutrino Detector), which measured decays of stopped μ^+ following the decay chain $\mu^+ \to \bar{\nu}_\mu e^+ \nu_e$. The goal was to measure excess $\bar{\nu}_e$ events, interpret any excess as $\bar{\nu}_\mu \to \bar{\nu}_e$ oscillations, and use that information to constrain the squared mass differences of the three neutrino mass eigenstates.[26] After 6 years of data, the collaboration found an excess of $87.9 \pm 22.4 \pm 6.0$ $\bar{\nu}_e$ events, compared to 33300 ± 3300 events if 100% of produced $\bar{\nu}_\mu$ oscillated to $\bar{\nu}_e$. This was interpreted as a $(0.264 \pm 0.067 \pm 0.045)\%$ oscillation probability [266–268].

The MiniBooNE experiment uses the Booster Neutrino Beam (BNB) at Fermilab, comprised of protons with 8 GeV of kinetic energy each, to strike a beryllium target and produce a variety of

[26] LSND collected data from 1993-1998, when $|\Delta m^2_{12}|$ and $|\Delta m^2_{23}|$ were still poorly constrained.

mesons that decay in flight [269]. The dominant meson produced is the pion, which decays almost exclusively through the process $\pi^+ \to \mu^+\nu_\mu$ ($\pi^- \to \mu^-\bar{\nu}_\mu$), and through the use of an electromagnet the muon can be deflected leading to a relatively pure ν_μ ($\bar{\nu}_\mu$) beam. This beam is sent down a ~ 500m pipeline to a spherical detector 12.2m in diameter filled with 818 tons of mineral oil [270]. An array of photomultiplier tubes look for Chereknov and scintillation light from the outgoing lepton in the charged current quasi-elastic (CCQE) process $\nu_l + n \to l^- + p$. Due to their difference in masses, electrons and muons produce very different Chereknov ring patterns and are easily discernible [271].

After 18.75×10^{20} protons-on-target in neutrino mode and 11.26×10^{20} protons-on-target in antineutrino mode, the MiniBooNE collaboration has detected a 4.8σ excess of ν_e events in their neutrino detector [60–62]. Given the known bounds on neutrino masses [20], these events are inconsistent with regular $\nu_\mu \to \nu_e$ oscillation and must be understood either as misinterpreted SM phenomena or as a sign of new physics.

Several types of new physics explanations have been proposed to explain the anomaly. The most common explanations propose one or more eV-scale sterile neutrinos that induce short baseline oscillations [272–278], but there have also been proposals for heavier sterile neutrinos that decay in the beamline or detector [279–284], as well as a vast array of less minimal explanations that combine aspects of the above models with extra effects such as CPT violation [285–289] and non-standard interactions [290–292].

Our approach in this project was to consider lepton flavour violation in pion decays. Previous work had considered lepton flavour violation in muon decays as a possible source for the anomaly [293, 294], but our work was the first to consider explaining the anomaly through non-standard pion decays.

This approach is viable because the MiniBooNE collaboration uses a GEANT4-based simulation to understand the constituents of their beam (detailed in Ref. [269]). Since the beam is never measured (there is no operational near detector for the beam, although the Short-Baseline Neutrino Detector is expected to come online in 2023 [295]), it is possible that the observed excess of ν_e events could be explained at least in part by non-standard pion decay in the decay pipe. In fact, the current bound on the lepton flavour violating decay $\pi^+ \to \mu^+\nu_e$ is $\text{Br}(\pi^+ \to \mu^+\nu_e) < 8 \times 10^{-3}$ [188], while our initial estimates suggest that the entire excess could be explained by a branching ratio of only $\sim 1 \times 10^{-3}$.

This prospect motivates a search for a suitable model capable of producing this lepton flavour violating decay channel. In this work we explore two simple leptoquark models, but find that a wealth of other constraints make it impossible for these models to produce 100% of the observed MiniBoone excess.

The rest of this chapter is organized as follows. In Section 4.2 we provide the phenomenological details of two leptoquark models that we explored, showing the relevant experimental constraints and discussing the models' viability in explaining the MiniBooNE excess. In Section 4.3 we briefly discuss an alternative outcome of the project, which is to place new constraints on leptoquark couplings

by examining models with loop-level $\mu - e$ conversion in nuclei.

4.2 Scalar Leptoquark Models of Lepton Flavour Violating Pion Decay

Scalar leptoquarks are highly motivated extensions of the SM. They have been used to explain several outstanding anomalies, such as the anomalous ratios $R_{D^{(\star)}}$ and $R_{K^{(\star)}}$, the anomalous magnetic moment of the muon Δa_μ, and neutrino masses [250–256, 258, 260, 263, 265]. Different models use different combinations of scalar leptoquarks (as well as vector leptoquarks in many constructions), and there are many experimental constraints on the possible parameters of these models, particularly for leptoquark couplings to first- and second-generation fermions [296, 297]. Given their aptitude for solving flavour anomalies, scalar leptoquark models were a natural candidate to use in our attempted explanation of the MiniBooNE excess via lepton flavour violating pion decays.

4.2.1 R_2 only

The first model we used involved the addition of a single scalar leptoquark, R_2, which transforms as $(7/6, \mathbf{2}, \mathbf{3})$ under $(U(1), SU(2), SU(3))$. The Lagrangian is [296]

$$\mathcal{L} \supset -y^{RL}_{2ij}\bar{u}^i_R R^a_2 \epsilon^{ab} L^{j,b}_L + y^{LR}_{2ij}\bar{e}^i_R R^{a*}_2 Q^{j,a}_L + \text{h.c.} \tag{4.1}$$

and in terms of particle interactions we find

$$\mathcal{L} \supset -y^{RL}_{2ij}\bar{u}^i_R e^j_L R^{5/3}_2 + y^{RL}_{2,ij}\bar{u}^i_R \nu^j_L R^{2/3}_2 + \left(y^{LR}_2 V^\dagger\right)_{ij} \bar{e}^i_R u^j_L R^{5/3*}_2 + y^{LR}_{2,ij}\bar{e}^i_R d^j_L R^{2/3*}_2 + \text{h.c.} \tag{4.2}$$

where $\bar{\psi} = \psi^\dagger\gamma^0$, the charges of the leptoquarks are indicated by superscripts, and the neutrinos are in their flavour basis.

The above induces π^+ decay to $\mu^+\nu_e$ at tree level, mediated through the $R_2^{2/3}$ leptoquark, with branching ratio proportional to $|y^{RL*}_{2,11}y^{LR}_{2,21}|^2$.

However, this process cannot produce the MiniBoone excess because the required Yukawa couplings are ruled out by muon-electron conversion, which also happens at tree level and is mediated instead by the $R_2^{5/3}$ leptoquark. In principle it would be possible to simply raise the mass of the $R_2^{5/3}$ particle until this process is below the current experimental sensitivities, but precision electroweak measurements of the T parameter (and to a lesser extent the S parameter) demand that the mass splitting within the R_2 electroweak doublet obey $\Delta m < 53$ GeV at 95% C.L. [296]. To obtain a large enough signal, the $R_2^{2/3}$ should be as close as possible to the experimental limit of 1 TeV [296, 298]. Thus the model is not viable.

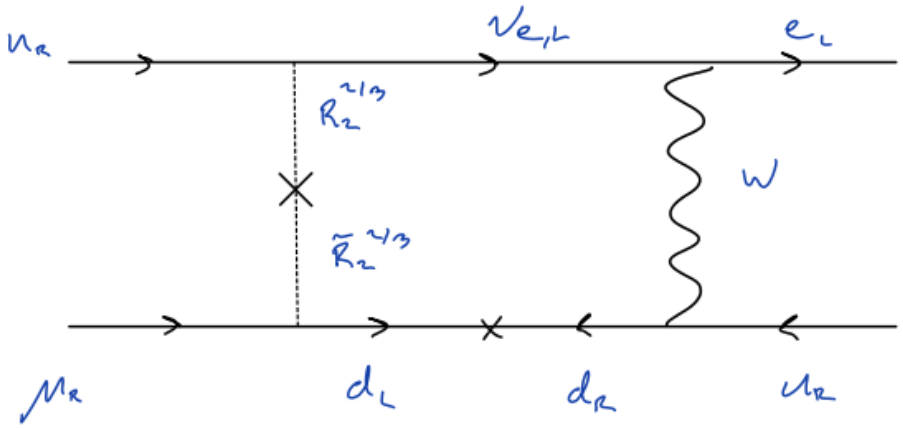

Figure 15. $\mu - e$ conversion diagram in the R_2, $\tilde{R}_2$ model.

4.2.2 R_2, $\tilde{R}_2$

The tree level $\mu - e$ conversion suffered by the R_2-only model above can be removed if we turn off the $y^{LR}_{2,21}$ coupling, and instead include a second leptoquark, $\tilde{R}_2$, which has SM charges $(1/6, \mathbf{2}, \mathbf{3})$ and the following Yukawa interaction:

$$\mathcal{L} \supset -\tilde{y}^{RL}_{2,ij} \bar{d}^i_R \tilde{R}^a_2 \epsilon^{ab} L^{j,b}_L + \text{h.c.} \tag{4.3}$$

leading to

$$\mathcal{L} \supset \tilde{y}^{RL}_{2,ij} \bar{d}^i_R e^j_L \tilde{R}^{2/3}_2 + \tilde{y}^{RL}_{2,ij} \bar{d}^i_R \nu^j_L \tilde{R}^{-1/3}_2 + \text{h.c.} \tag{4.4}$$

where a, b are $SU(2)$ indices and we neglect to include the possibility of right-handed neutrino couplings (see Ref. [296] for the complete Lagrangian). We also include couplings between R_2, $\tilde{R}_2$, and the Higgs, which allows the R_2 and $\tilde{R}_2$ to mass mix. The mixing ensures pion decay can still happen at tree level, but now muon-electron conversion happens only at loop level (see Figure 15). Additionally, the loop requires a chiral flip of the down quark which should suppress the amplitude by a factor of $\sim m_d/m_p$.

However, in this scenario we find that the signal cannot be generated by perturbative Yukawa couplings. For $\mathcal{O}(1)$ mixing between R_2 and $\tilde{R}_2$ and leptoquark mass eigenvalues near their lower bound of 1 TeV [296], which represents the best case scenario, the branching ratio is roughly

$$\text{Br}(\pi^+ \to \mu^+ \nu_e) \sim \left(Y^{RL*}_{2,11} Y^{RL}_{\tilde{2},12} \right)^2 \times 10^{-5} \tag{4.5}$$

and constraints from atomic parity violation demand that $|Y^{RL}_{2,11}| < 0.25$ [296], which for a required

branching ratio of $\sim 10^{-3}$ forces $Y^{RL}_{\tilde{2},12}$ well into the non-perturbative regime. Note that interference effects between the two leptoquark eigenstates complicate the leptoquark mass dependance of the above relation, but the branching ratio always decreases when either leptoquark mass increases. As a result, this model is also not a viable option to explain the MiniBooNE excess.

4.3 A New Direction: Constraining Products of Leptoquark Couplings with Next Generation $\mu - e$ Conversion Experiments

The leading constraints on $\mu - e$ conversion come from the SINDRUM II experiment, which finds the conversion-to-capture rate for gold muonic atoms to be $\Gamma(\mu^- \text{Au} \to e^- \text{Au})/\Gamma_{\text{capture}}(\mu^- \text{Au}) < 7 \times 10^{-13}$ at 90% C.L. [299]. Next generation experiments, Mu2e and COMET, plan to reduce this bound to $\mathcal{O}(10^{-17})$ [300, 301]. Our initial estimates suggest that this level of precision should be able to place meaningful constraints on the product of two leptoquark Yukawa couplings, in models where $\mu - e$ conversion happens only at loop level. We have identified two scalar leptoquark models that see this process only at loop level, namely $R_2 + \tilde{R}_2$ and $\tilde{R}_2$ + S_1, where S_1 transforms as $(\bar{\mathbf{3}}, \mathbf{1}, 1/3)$ under $(SU(3)_C, SU(2)_L, U(1)_Y)$. By estimating the size of the conversion-to-capture rate for these models, new bounds on leptoquark couplings may be found. This work will be continued by my collaborators Jared Barron and F. David Wandler.

PART 4:

CONCLUSION

5 Conclusion

The apparent sensitivity of the Higgs boson mass to large, quadratic corrections up to the Planck scale has been a major driver of model building efforts in the last few decades. The SM in its current form includes the Higgs boson as a fundamental scalar particle with no symmetry mechanism to protect its mass from these dangerous effects, yet the observed mass of the Higgs boson would be an incredibly fine-tuned coincidence if there were truly no underlying reason for its value.

Much of the work presented in this thesis begins from this unsettling philosophical perspective. In lieu of experimental evidence for supersymmetry, Higgs compositeness, or any hints of new physics that might appear at the Large Hadron Collider and begin to guide us toward a deeper understanding of Nature, physicists have constructed theories of Neutral Naturalness, capable of removing the contradiction between the lack of experimental evidence for new physics and the pressing need for a resolution to the hierarchy problem. The Neutral Naturalness model used in Chapters 2 and 3 is the Twin Higgs framework, which introduces an approximately $\mathbb{Z}_2$-symmetric copy of the SM that is, crucially, not charged under the SM gauge groups, but yet is capable of cancelling large quadratic corrections to the Higgs potential at first loop order. Twin Higgs models are both experimentally consistent and philosophically sound.

In addition to solving the hierarchy problem, the Twin Higgs framework as a possible eventual extension of the SM can be seen to yield qualitatively new features that are both useful and interesting with regard to dark matter, another major shortfall of the SM. In Chapter 2 we explored the consequences of the pseudo-Nambu-Goldstone (pNGB) boson nature of the Higgs boson in Twin Higgs theories, which is qualitatively different from the SM realization of the Higgs as merely a complex $SU(2)$ doublet. We found that couplings between a singlet scalar dark matter particle and the Higgs boson could be highly suppressed in direct detection experiments. Combined with the possibility of dark matter dilution through late-time entropy injection, this work shows that a singlet scalar particle minimally coupled to the Higgs – an astonishingly simple dark matter scenario – is still completely possible within the Twin Higgs framework, and may be detectable in the next generation of direct detection experiments.

Another intriguing feature of Twin Higgs models is the broad spectrum of SM-neutral particles that are predicted to exist, even in the most minimal scenarios. Any massive, stable twin sector particle is an a priori dark matter candidate, and in minimal Twin Higgs models the twin tau lepton is a natural choice. By incorporating a recent novel mechanism devised to dynamically break the $\mathbb{Z}_2$ symmetry between the visible and twin sector, we were able to revive the prospect of the twin tau lepton as dark matter candidate (an idea which had been previously thought to be ruled out).

The last portion of this thesis was motivated by the curious fact that the correct number of excess electron neutrino events seen in MiniBooNE could be completely generated by nonstandard pion decays with a $\pi^+ \to \mu\nu_e$ branching fraction of only $\sim 10^{-3}$, currently within the experimental limit.

While building an experimentally consistent leptoquark model to generate the excess proved to be a challenging task, I am reassured knowing that the pursuit of understanding this result will continue in some measure, either by the continued work of my excellent collaborators, or by physicists at large in the years to come.

Acknowledgments

From Chapter 2, Twin Higgs Portal Dark Matter:
DC would like to especially thank Timothy Cohen and Matthew McCullough for important conversations early in this project. We are also grateful to Nathaniel Craig and Seth Koren for useful comments on a draft version of this paper, and to Jack Setford for particularly helpful consultations. We additionally thank Marco Drewes, Zackaria Chacko, and Patrick Fox for useful discussions and correspondence. The research of DC and SG was supported in part by a Discovery Grant from the Natural Sciences and Engineering Research Council of Canada, and by the Canada Research Chair program. The research of SG was supported in part by a Postgraduate Scholarship – Doctoral (PGS D) from the National Sciences and Engineering Research Council of Canada.

From Chapter 3, Resurrecting the Fraternal Twin WIMP Miracle:
The authors would like to thank Jared Evans, Caleb Gemmell and Yuhsin Tsai for helpful discussions. This work was conceived at the Aspen Center for Physics, which is supported by National Science Foundation grant PHY-1607611, for which the authors are very grateful. The research of Setford, Gryba and Curtin is supported in part by a Discovery Grant from the Natural Sciences and Engineering Research Council of Canada, and by the Canada Research Chair program. Setford also acknowledges support from the University of Toronto Faculty of Arts and Science postdoctoral fellowship, and Gryba acknowledges funding from a Postgraduate Doctoral Scholarship (PGS D) provided by the Natural Sciences and Engineering Research Council of Canada. Hooper is supported by the Fermi Research Alliance, LLC under Contract No. DE-AC02-07CH11359 with the U.S. Department of Energy, Office of High Energy Physics. Scholtz is supported by the following grants: DEPARTMENTS OF EXCELLENCE grant awarded by the Italian Ministry of Education, University and Research (MIUR), Research grant *The Dark Universe: A Synergic Multimessenger Approach*, No. 2017X7X85K funded by the Italian Ministry of Education, University and Research (MIUR), and Research grant TASP (Theoretical Astroparticle Physics) funded by Instituto Nazionale di Fisica Nucleare.

References

[1] **LUX** Collaboration, D. S. Akerib et al., *Results from a search for dark matter in the complete LUX exposure*, *Phys. Rev. Lett.* **118** (2017), no. 2 021303, [arXiv:1608.0764].

[2] **PandaX-II** Collaboration, A. Tan et al., *Dark Matter Results from First 98.7 Days of Data from the PandaX-II Experiment*, *Phys. Rev. Lett.* **117** (2016), no. 12 121303, [arXiv:1607.0740].

[3] **XENON** Collaboration, E. Aprile et al., *Dark Matter Search Results from a One Ton-Year Exposure of XENON1T*, *Phys. Rev. Lett.* **121** (2018), no. 11 111302, [arXiv:1805.1256].

[4] **LZ** Collaboration, D. S. Akerib et al., *LUX-ZEPLIN (LZ) Conceptual Design Report*, arXiv:1509.0291.

[5] **XENON** Collaboration, E. Aprile et al., *Physics reach of the XENON1T dark matter experiment*, *JCAP* **04** (2016) 027, [arXiv:1512.0750].

[6] **DARWIN** Collaboration, J. Aalbers et al., *DARWIN: towards the ultimate dark matter detector*, *JCAP* **11** (2016) 017, [arXiv:1606.0700].

[7] **MAGIC, Fermi-LAT** Collaboration, M. L. Ahnen et al., *Limits to Dark Matter Annihilation Cross-Section from a Combined Analysis of MAGIC and Fermi-LAT Observations of Dwarf Satellite Galaxies*, *JCAP* **1602** (2016), no. 02 039, [arXiv:1601.0659].

[8] **Fermi-LAT** Collaboration, M. Ackermann et al., *Updated search for spectral lines from Galactic dark matter interactions with pass 8 data from the Fermi Large Area Telescope*, *Phys. Rev.* **D91** (2015), no. 12 122002, [arXiv:1506.0001].

[9] **CMS** Collaboration, V. Khachatryan et al., *Searches for invisible decays of the Higgs boson in pp collisions at $\sqrt{s}$ = 7, 8, and 13 TeV*, *JHEP* **02** (2017) 135, [arXiv:1610.0921].

[10] J. A. Casas, D. G. Cerdeno, J. M. Moreno, and J. Quilis, *Reopening the Higgs portal for single scalar dark matter*, *JHEP* **05** (2017) 036, [arXiv:1701.0813].

[11] **Planck** Collaboration, N. Aghanim et al., *Planck 2018 results. VI. Cosmological parameters*, arXiv:1807.0620.

[12] N. Craig, S. Koren, and T. Trott, *Cosmological Signals of a Mirror Twin Higgs*, *JHEP* **05** (2017) 038, [arXiv:1611.0797].

[13] L. Husdal, *On Effective Degrees of Freedom in the Early Universe*, *Galaxies* **4** (2016), no. 4 78, [arXiv:1609.0497].

[14] **CMB-S4** Collaboration, K. N. Abazajian et al., *CMB-S4 Science Book, First Edition*, arXiv:1610.0274.

[15] S. Weinberg, *The Quantum Theory of Fields, Vol. 1*. Press Syndicate of the University of Cambridge, 1995.

[16] M. D. Schwartz, *Quantum Field Theory and the Standard Model*. Cambridge University Press, 2014.

[17] M. E. Peskin and D. V. Schroeder, *An Introduction to Quantum Field Theory*. Westview Press, 1995.

[18] J. E. Kim, *Light pseudoscalars, particle physics and cosmology*, *Physics Reports* **150** (1987), no. 1 1–177.

[19] C. Quigg, *Gauge Theories of the Strong, Weak, and Electromagnetic Interactions*. Westview Press, 1983/1997.

[20] **Particle Data Group** Collaboration, P. Zyla et al., *Review of Particle Physics*, *PTEP* **2020** (2020), no. 8 083C01. and 2021 update.

[21] J. Tang, Y. Zhang, and Y.-F. Li, *Probing direct and indirect unitarity violation in future accelerator neutrino facilities*, *Physics Letters B* **774** (2017) 217–224.

[22] F. C. Porter, *Experimental status of the CKM matrix*, *Prog. Part. Nucl. Phys.* **91** (2016) 101–135, [arXiv:1604.0494].

[23] T. Aoyama, T. Kinoshita, and M. Nio, *Revised and Improved Value of the QED Tenth-Order Electron Anomalous Magnetic Moment*, *Phys. Rev. D* **97** (2018), no. 3 036001, [arXiv:1712.0606].

[24] R. Capdevilla, D. Curtin, Y. Kahn, and G. Krnjaic, *No-lose theorem for discovering the new physics of (g-2)μ at muon colliders*, *Phys. Rev. D* **105** (2022), no. 1 015028, [arXiv:2101.1033].

[25] D. Bodeker and W. Buchmuller, *Baryogenesis from the weak scale to the grand unification scale*, *Rev. Mod. Phys.* **93** (2021), no. 3 035004, [arXiv:2009.0729].

[26] A. de Gouvêa, *Neutrino mass models*, *Annual Review of Nuclear and Particle Science* **66** (2016), no. 1 197–217, [https://doi.org/10.1146/annurev-nucl-102115-044600].

[27] F. Feruglio, *Pieces of the Flavour Puzzle*, *Eur. Phys. J. C* **75** (2015), no. 8 373, [arXiv:1503.0407].

[28] C. D. Froggatt and H. B. Nielsen, *Hierarchy of quark masses, cabibbo angles and CP violation*, *Nuclear Physics B* **147** (Jan., 1979) 277–298.

[29] C. Csáki, S. Lombardo, and O. Telem, *TASI Lectures on Non-supersymmetric BSM Models*, pp. 501–570. WSP, 2018. arXiv:1811.0427.

[30] J. H. Schwarz, *The Early History of String Theory and Supersymmetry*, arXiv:1201.0981.

[31] M. C. Rodriguez, *The Minimal Supersymmetric Standard Model (MSSM) and General Singlet Extensions of the MSSM (GSEMSSM), a short review*, arXiv:1911.1304.

[32] **ATLAS** Collaboration, G. Aad et al., *Search for long-lived charginos based on a disappearing-track signature using 136 fb^{-1} of pp collisions at $\sqrt{s}$ = 13 TeV with the ATLAS detector*, arXiv:2201.0247.

[33] B. Batell, M. Low, E. T. Neil, and C. B. Verhaaren, *Review of Neutral Naturalness*, in *2022 Snowmass Summer Study*, 3, 2022. arXiv:2203.0553.

[34] Z. Chacko, H.-S. Goh, and R. Harnik, *The Twin Higgs: Natural electroweak breaking from mirror symmetry*, *Phys. Rev. Lett.* **96** (2006) 231802, [hep-ph/0506256].

[35] N. Craig, A. Katz, M. Strassler, and R. Sundrum, *Naturalness in the Dark at the LHC*, *JHEP* **07** (2015) 105, [arXiv:1501.0531].

[36] N. Craig, S. Knapen, and P. Longhi, *Neutral Naturalness from Orbifold Higgs Models*, *Phys. Rev. Lett.* **114** (2015), no. 6 061803, [arXiv:1410.6808].

[37] R. Barbieri, L. J. Hall, and K. Harigaya, *Minimal Mirror Twin Higgs*, *JHEP* **11** (2016) 172, [arXiv:1609.0558].

[38] Z. Chacko, H.-S. Goh, and R. Harnik, *A Twin Higgs model from left-right symmetry*, *JHEP* **01** (2006) 108, [hep-ph/0512088].

[39] J. Serra and R. Torre, *Neutral naturalness from the brother-higgs model*, *Phys. Rev. D* **97** (Feb, 2018) 035017.

[40] L.-X. Xu, J.-H. Yu, and S.-h. Zhu, *Minimal neutral naturalness model*, *Phys. Rev. D* **101** (May, 2020) 095014.

[41] G. Burdman, Z. Chacko, H.-S. Goh, and R. Harnik, *Folded supersymmetry and the LEP paradox*, *JHEP* **02** (2007) 009, [hep-ph/0609152].

[42] A. Arbey and F. Mahmoudi, *Dark matter and the early Universe: a review*, *Prog. Part. Nucl. Phys.* **119** (2021) 103865, [arXiv:2104.1148].

[43] K. Freese, *Review of Observational Evidence for Dark Matter in the Universe and in upcoming searches for Dark Stars*, *EAS Publ. Ser.* **36** (2009) 113–126, [arXiv:0812.4005].

[44] V. Springel et al., *Simulating the joint evolution of quasars, galaxies and their large-scale distribution*, *Nature* **435** (2005) 629–636, [astro-ph/0504097].

[45] E. W. Kolb and M. S. Turner, *The early universe*. Frontiers in Physics. Westview Press, Boulder, CO, 1990.

[46] N. Bernal, M. Heikinheimo, T. Tenkanen, K. Tuominen, and V. Vaskonen, *The Dawn of FIMP Dark Matter: A Review of Models and Constraints*, *Int. J. Mod. Phys. A* **32** (2017), no. 27 1730023, [arXiv:1706.0744].

[47] N. Fernandez, Y. Kahn, and J. Shelton, *Freeze-in, glaciation, and UV sensitivity from light mediators*, arXiv:2111.1370.

[48] L. Goodenough and D. Hooper, *Possible Evidence For Dark Matter Annihilation In The Inner Milky Way From The Fermi Gamma Ray Space Telescope*, arXiv:0910.2998.

[49] J. Guo, Y. He, J. Liu, and X.-P. Wang, *Heavy long-lived coannihilation partner from inelastic Dark Matter model and its signatures at the LHC*, *JHEP* **04** (2022) 024, [arXiv:2111.0116].

[50] T. Lin, *Dark matter models and direct detection*, *PoS* **333** (2019) 009, [arXiv:1904.0791].

[51] K. Griest and M. Kamionkowski, *Unitarity limits on the mass and radius of dark-matter particles*, *Phys. Rev. Lett.* **64** (Feb, 1990) 615–618.

[52] M. Cirelli, Y. Gouttenoire, K. Petraki, and F. Sala, *Homeopathic Dark Matter, or how diluted heavy substances produce high energy cosmic rays*, *JCAP* **02** (2019) 014, [arXiv:1811.0360].

[53] **LHCb** Collaboration, R. Aaij et al., *Test of lepton universality with $B^0 \to K^{*0}\ell^+\ell^-$ decays*, *JHEP* **08** (2017) 055, [arXiv:1705.0580].

[54] **LHCb** Collaboration, R. Aaij et al., *Test of lepton universality in beauty-quark decays*, *Nature Phys.* **18** (2022), no. 3 277–282, [arXiv:2103.1176].

[55] **LHCb** Collaboration, R. Aaij et al., *Tests of lepton universality using $B^0 \to K^0_S\ell^+\ell^-$ and $B^+ \to K^{*+}\ell^+\ell^-$ decays*, arXiv:2110.0950.

[56] K. Ezzat, G. Faisel, and S. Khalil, *Investigating R_D and R_{D^*} anomalies in a Left-Right model with an Inverse Seesaw*, arXiv:2204.1092.

[57] **Belle** Collaboration, G. Caria et al., *Measurement of $\mathcal{R}(D)$ and $\mathcal{R}(D^*)$ with a semileptonic tagging method*, *Phys. Rev. Lett.* **124** (2020), no. 16 161803, [arXiv:1910.0586].

[58] H. F. A. Group, *Average of R(D) and R(D*) for 2021*, .

[59] B. Abi et al., *Measurement of the positive muon anomalous magnetic moment to 0.46 ppm*, .

[60] **MiniBooNE** Collaboration, A. A. Aguilar-Arevalo et al., *Unexplained Excess of Electron-Like Events From a 1-GeV Neutrino Beam*, *Phys. Rev. Lett.* **102** (2009) 101802, [arXiv:0812.2243].

[61] **MiniBooNE** Collaboration, A. A. Aguilar-Arevalo et al., *Significant Excess of ElectronLike Events in the MiniBooNE Short-Baseline Neutrino Experiment*, *Phys. Rev. Lett.* **121** (2018), no. 22 221801, [arXiv:1805.1202].

[62] **MiniBooNE** Collaboration, A. A. Aguilar-Arevalo et al., *Updated MiniBooNE neutrino oscillation results with increased data and new background studies*, *Phys. Rev. D* **103** (2021), no. 5 052002, [arXiv:2006.1688].

[63] D. Curtin and S. Gryba, *Twin Higgs Portal Dark Matter*, arXiv:2101.1101.

[64] **ATLAS** Collaboration, G. Aad et al., *Observation of a new particle in the search for the Standard Model Higgs boson with the ATLAS detector at the LHC*, *Phys. Lett. B* **716** (2012) 1–29, [arXiv:1207.7214].

[65] **CMS** Collaboration, S. Chatrchyan et al., *Observation of a New Boson at a Mass of 125 GeV with the CMS Experiment at the LHC*, *Phys. Lett. B* **716** (2012) 30–61, [arXiv:1207.7235].

[66] P. Batra, A. Delgado, D. E. Kaplan, and T. M. P. Tait, *The Higgs mass bound in gauge extensions of the minimal supersymmetric standard model*, *JHEP* **02** (2004) 043, [hep-ph/0309149].

[67] U. Ellwanger, C. Hugonie, and A. M. Teixeira, *The Next-to-Minimal Supersymmetric Standard Model*, *Phys. Rept.* **496** (2010) 1–77, [arXiv:0910.1785].

[68] L. J. Hall, D. Pinner, and J. T. Ruderman, *A Natural SUSY Higgs Near 126 GeV*, *JHEP* **04** (2012) 131, [arXiv:1112.2703].

[69] D. Curtin, P. Meade, and P.-J. Tien, *Natural SUSY in Plain Sight*, *Phys. Rev.* **D90** (2014), no. 11 115012, [arXiv:1406.0848].

[70] J. A. Casas, J. M. Moreno, S. Robles, K. Rolbiecki, and B. ZaldÃvar, *What is a Natural SUSY scenario?*, *JHEP* **06** (2015) 070, [arXiv:1407.6966].

[71] D. B. Kaplan, H. Georgi, and S. Dimopoulos, *Composite Higgs Scalars*, *Phys. Lett. B* **136** (1984) 187–190.

[72] N. Arkani-Hamed, A. G. Cohen, and H. Georgi, *Electroweak symmetry breaking from dimensional deconstruction*, *Phys. Lett.* **B513** (2001) 232–240, [hep-ph/0105239].

[73] M. Schmaltz and D. Tucker-Smith, *Little Higgs review*, *Ann. Rev. Nucl. Part. Sci.* **55** (2005) 229–270, [hep-ph/0502182].

[74] **ATLAS** Collaboration, G. Aad et al., *Search for squarks and gluinos in final states with same-sign leptons and jets using 139 fb^{-1} of data collected with the ATLAS detector*, arXiv:1909.0845.

[75] **ATLAS** Collaboration, M. Aaboud et al., *Search for new phenomena using the invariant mass distribution of same-flavour opposite-sign dilepton pairs in events with missing transverse momentum in $\sqrt{s} = 13$ TeV pp collisions with the ATLAS detector*, *Eur. Phys. J.* **C78** (2018), no. 8 625, [arXiv:1805.1138].

[76] **ATLAS** Collaboration, M. Aaboud et al., *Search for top squarks decaying to tau sleptons in pp collisions at $\sqrt{s} = 13$ TeV with the ATLAS detector*, *Phys. Rev.* **D98** (2018), no. 3 032008, [arXiv:1803.1017].

[77] **ATLAS** Collaboration, M. Aaboud et al., *Search for squarks and gluinos in final states with jets and missing transverse momentum using 36 fb^{-1} of $\sqrt{s} = 13$ TeV pp collision data with the ATLAS detector*, *Phys. Rev.* **D97** (2018), no. 11 112001, [arXiv:1712.0233].

[78] **ATLAS** Collaboration, M. Aaboud et al., *Search for top-squark pair production in final states with one lepton, jets, and missing transverse momentum using 36 fb$^{?1}$ of $\sqrt{s} = 13$ TeV pp collision data with the ATLAS detector*, *JHEP* **06** (2018) 108, [arXiv:1711.1152].

[79] **ATLAS** Collaboration, M. Aaboud et al., *Search for supersymmetry in final states with charm jets and missing transverse momentum in 13 TeV pp collisions with the ATLAS detector*, *JHEP* **09** (2018) 050, [arXiv:1805.0164].

[80] **ATLAS** Collaboration, M. Aaboud et al., *Search for dark matter and other new phenomena in events with an energetic jet and large missing transverse momentum using the ATLAS detector*, *JHEP* **01** (2018) 126, [arXiv:1711.0330].

[81] **CMS** Collaboration, A. M. Sirunyan et al., *Search for supersymmetry in proton-proton collisions at 13 TeV in final states with jets and missing transverse momentum*, arXiv:1908.0472.

[82] **CMS** Collaboration, A. M. Sirunyan et al., *Search for the pair production of light top squarks in the $e^{\pm}\mu^{\mp}$ final state in proton-proton collisions at $\sqrt{s}$ = 13 TeV*, *JHEP* **03** (2019) 101, [arXiv:1901.0128].

[83] **CMS** Collaboration, A. M. Sirunyan et al., *Search for supersymmetry in events with a photon, jets,* b *-jets, and missing transverse momentum in proton?proton collisions at 13 TeV*, *Eur. Phys. J.* **C79** (2019), no. 5 444, [arXiv:1901.0672].

[84] **CMS** Collaboration, A. M. Sirunyan et al., *Search for supersymmetry in events with a photon, a lepton, and missing transverse momentum in proton-proton collisions at $\sqrt{s} = 13$ TeV*, *JHEP* **01** (2019) 154, [arXiv:1812.0406].

[85] S. P. Martin, *A Supersymmetry primer*, *Adv. Ser. Direct. High Energy Phys.* **21** (2010) 1–153, [hep-ph/9709356].

[86] G. Burdman, Z. Chacko, R. Harnik, L. de Lima, and C. B. Verhaaren, *Colorless Top Partners, a 125 GeV Higgs, and the Limits on Naturalness*, *Phys. Rev.* **D91** (2015), no. 5 055007, [arXiv:1411.3310].

[87] Z. Chacko, C. Kilic, S. Najjari, and C. B. Verhaaren, *Testing the Scalar Sector of the Twin Higgs Model at Colliders*, *Phys. Rev.* **D97** (2018), no. 5 055031, [arXiv:1711.0530].

[88] **ATLAS** Collaboration, *Search for invisible Higgs boson decays with vector boson fusion signatures with the ATLAS detector using an integrated luminosity of 139 fb^{-1}*, .

[89] **CMS** Collaboration, A. M. Sirunyan et al., *Search for invisible decays of a Higgs boson produced through vector boson fusion in proton-proton collisions at $\sqrt{s} = 13$ TeV*, *Phys. Lett.* **B793** (2019) 520–551, [arXiv:1809.0593].

[90] **CMS** Collaboration, C. Collaboration, *Search for invisible decays of a Higgs boson produced through vector boson fusion at the High-Luminosity LHC*, .

[91] R. Barbieri, D. Greco, R. Rattazzi, and A. Wulzer, *The Composite Twin Higgs scenario*, *JHEP* **08** (2015) 161, [arXiv:1501.0780].

[92] H. Beauchesne, K. Earl, and T. Grégoire, *The spontaneous $\mathbb{Z}_2$ breaking Twin Higgs*, *JHEP* **01** (2016) 130, [arXiv:1510.0606].

[93] R. Harnik, K. Howe, and J. Kearney, *Tadpole-Induced Electroweak Symmetry Breaking and pNGB Higgs Models*, *JHEP* **03** (2017) 111, [arXiv:1603.0377].

[94] H.-S. Goh and C. A. Krenke, *A Little Twin Higgs Model*, *Phys. Rev. D* **76** (2007) 115018, [arXiv:0707.3650].

[95] A. Katz, A. Mariotti, S. Pokorski, D. Redigolo, and R. Ziegler, *SUSY Meets Her Twin*, *JHEP* **01** (2017) 142, [arXiv:1611.0861].

[96] A. Ahmed, *Heavy Higgs of the Twin Higgs Models*, *JHEP* **02** (2018) 048, [arXiv:1711.0310].

[97] D. Buttazzo, F. Sala, and A. Tesi, *Singlet-like Higgs bosons at present and future colliders*, *JHEP* **11** (2015) 158, [arXiv:1505.0548].

[98] **ATLAS** Collaboration, G. Aad et al., *Search for heavy neutral Higgs bosons produced in association with b-quarks and decaying to b-quarks at $\sqrt{s} = 13$ TeV with the ATLAS detector*, arXiv:1907.0274.

[99] C. Kilic, S. Najjari, and C. B. Verhaaren, *Discovering the Twin Higgs Boson with Displaced Decays*, *Phys. Rev. D* **99** (2019), no. 7 075029, [arXiv:1812.0817].

[100] S. Alipour-Fard, N. Craig, S. Gori, S. Koren, and D. Redigolo, *The second Higgs at the lifetime frontier*, *JHEP* **07** (2020) 029, [arXiv:1812.0931].

[101] A. Falkowski, S. Pokorski, and M. Schmaltz, *Twin SUSY*, *Phys. Rev.* **D74** (2006) 035003, [hep-ph/0604066].

[102] S. Chang, L. J. Hall, and N. Weiner, *A Supersymmetric twin Higgs*, *Phys. Rev.* **D75** (2007) 035009, [hep-ph/0604076].

[103] N. Craig and K. Howe, *Doubling down on naturalness with a supersymmetric twin Higgs*, *JHEP* **03** (2014) 140, [arXiv:1312.1341].

[104] M. Badziak and K. Harigaya, *Supersymmetric D-term Twin Higgs*, *JHEP* **06** (2017) 065, [arXiv:1703.0212].

[105] M. Badziak and K. Harigaya, *Minimal Non-Abelian Supersymmetric Twin Higgs*, *JHEP* **10** (2017) 109, [arXiv:1707.0907].

[106] M. Badziak and K. Harigaya, *Asymptotically Free Natural Supersymmetric Twin Higgs Model*, *Phys. Rev. Lett.* **120** (2018), no. 21 211803, [arXiv:1711.1104].

[107] P. Asadi, N. Craig, and Y.-Y. Li, *Twin Turtles*, *JHEP* **02** (2019) 138, [arXiv:1810.0946].

[108] M. Geller and O. Telem, *Holographic Twin Higgs Model*, *Phys. Rev. Lett.* **114** (2015) 191801, [arXiv:1411.2974].

[109] P. Batra and Z. Chacko, *A Composite Twin Higgs Model*, *Phys. Rev.* **D79** (2009) 095012, [arXiv:0811.0394].

[110] M. Low, A. Tesi, and L.-T. Wang, *Twin Higgs mechanism and a composite Higgs boson*, *Phys. Rev.* **D91** (2015) 095012, [arXiv:1501.0789].

[111] N. Craig, S. Knapen, and P. Longhi, *The Orbifold Higgs*, *JHEP* **03** (2015) 106, [arXiv:1411.7393].

[112] H.-C. Cheng, S. Jung, E. Salvioni, and Y. Tsai, *Exotic Quarks in Twin Higgs Models*, *JHEP* **03** (2016) 074, [arXiv:1512.0264].

[113] H.-C. Cheng, E. Salvioni, and Y. Tsai, *Exotic electroweak signals in the twin Higgs model*, *Phys. Rev.* **D95** (2017), no. 11 115035, [arXiv:1612.0317].

[114] L. Li, E. Salvioni, Y. Tsai, and R. Zheng, *Electroweak-Charged Bound States as LHC Probes of Hidden Forces*, *Phys. Rev.* **D97** (2018), no. 1 015010, [arXiv:1710.0643].

[115] V. Prilepina and Y. Tsai, *Reconciling Large And Small-Scale Structure In Twin Higgs Models*, *JHEP* **09** (2017) 033, [arXiv:1611.0587].

[116] N. Craig and A. Katz, *The Fraternal WIMP Miracle*, *JCAP* **10** (2015) 054, [arXiv:1505.0711].

[117] M. Farina, *Asymmetric Twin Dark Matter*, *JCAP* **11** (2015) 017, [arXiv:1506.0352].

[118] I. Garcia Garcia, R. Lasenby, and J. March-Russell, *Twin Higgs WIMP Dark Matter*, *Phys. Rev. D* **92** (2015), no. 5 055034, [arXiv:1505.0710].

[119] I. Garcia Garcia, R. Lasenby, and J. March-Russell, *Twin Higgs Asymmetric Dark Matter*, *Phys. Rev. Lett.* **115** (2015), no. 12 121801, [arXiv:1505.0741].

[120] H.-C. Cheng, L. Li, and R. Zheng, *Coscattering/Coannihilation Dark Matter in a Fraternal Twin Higgs Model*, *JHEP* **09** (2018) 098, [arXiv:1805.1213].

[121] H. Beauchesne, *Mirror neutrons as dark matter in the Mirror Twin Two Higgs Doublet Model*, arXiv:2007.0005.

[122] Y. Hochberg, E. Kuflik, and H. Murayama, *Twin higgs model with strongly interacting massive particle dark matter*, *Phys. Rev. D* **99** (Jan, 2019) 015005.

[123] M. Badziak, G. Grilli Di Cortona, and K. Harigaya, *Natural Twin Neutralino Dark Matter*, *Phys. Rev. Lett.* **124** (2020), no. 12 121803, [arXiv:1911.0348].

[124] V. Silveira and A. Zee, *Scalar phantoms*, *Physics Letters B* **161** (1985), no. 1 136 – 140.

[125] J. McDonald, *Gauge singlet scalars as cold dark matter*, *Phys. Rev.* **D50** (1994) 3637–3649, [hep-ph/0702143].

[126] C. P. Burgess, M. Pospelov, and T. ter Veldhuis, *The Minimal model of nonbaryonic dark matter: A Singlet scalar*, *Nucl. Phys.* **B619** (2001) 709–728, [hep-ph/0011335].

[127] M. Escudero, A. Berlin, D. Hooper, and M.-X. Lin, *Toward (Finally!) Ruling Out Z and Higgs Mediated Dark Matter Models*, *JCAP* **12** (2016) 029, [arXiv:1609.0907].

[128] J. M. Cline, K. Kainulainen, P. Scott, and C. Weniger, *Update on scalar singlet dark matter*, *Phys. Rev.* **D88** (2013) 055025, [arXiv:1306.4710]. [Erratum: Phys. Rev.D92,no.3,039906(2015)].

[129] L. Feng, S. Profumo, and L. Ubaldi, *Closing in on singlet scalar dark matter: LUX, invisible Higgs decays and gamma-ray lines*, *JHEP* **03** (2015) 045, [arXiv:1412.1105].

[130] N. Fonseca, R. Zukanovich Funchal, A. Lessa, and L. Lopez-Honorez, *Dark Matter Constraints on Composite Higgs Models*, *JHEP* **06** (2015) 154, [arXiv:1501.0595].

[131] R. Balkin, M. Ruhdorfer, E. Salvioni, and A. Weiler, *Dark matter shifts away from direct detection*, *JCAP* **11** (2018) 050, [arXiv:1809.0910].

[132] G. Ballesteros, A. Carmona, and M. Chala, *Exceptional Composite Dark Matter*, *Eur. Phys. J. C* **77** (2017), no. 7 468, [arXiv:1704.0738].

[133] R. Balkin, M. Ruhdorfer, E. Salvioni, and A. Weiler, *Charged Composite Scalar Dark Matter*, *JHEP* **11** (2017) 094, [arXiv:1707.0768].

[134] T. Alanne, D. Buarque Franzosi, M. T. Frandsen, and M. Rosenlyst, *Dark matter in (partially) composite Higgs models*, *JHEP* **12** (2018) 088, [arXiv:1808.0751].

[135] A. Ahmed, S. Najjari, and C. B. Verhaaren, *A Minimal Model for Neutral Naturalness and pseudo-Nambu-Goldstone Dark Matter*, *JHEP* **06** (2020) 007, [arXiv:2003.0894].

[136] H. Cai and G. Cacciapaglia, *A Singlet Dark Matter in the SU(6)/SO(6) Composite Higgs Model*, arXiv:2007.0433.

[137] Y. Abe, T. Toma, and K. Tsumura, *Pseudo-Nambu-Goldstone dark matter from gauged $U(1)_{B-L}$ symmetry*, *JHEP* **05** (2020) 057, [arXiv:2001.0395].

[138] T. Alanne, M. Heikinheimo, V. Keus, N. Koivunen, and K. Tuominen, *Direct and indirect probes of Goldstone dark matter*, *Phys. Rev. D* **99** (2019), no. 7 075028, [arXiv:1812.0599].

[139] K. Huitu, N. Koivunen, O. Lebedev, S. Mondal, and T. Toma, *Probing pseudo-Goldstone dark matter at the LHC*, *Phys. Rev. D* **100** (2019), no. 1 015009, [arXiv:1812.0595].

[140] D. Karamitros, *Pseudo Nambu-Goldstone Dark Matter: Examples of Vanishing Direct Detection Cross Section*, *Phys. Rev. D* **99** (2019), no. 9 095036, [arXiv:1901.0975].

[141] X.-M. Jiang, C. Cai, Z.-H. Yu, Y.-P. Zeng, and H.-H. Zhang, *Pseudo-Nambu-Goldstone dark matter and two-Higgs-doublet models*, *Phys. Rev. D* **100** (2019), no. 7 075011, [arXiv:1907.0968].

[142] C. Arina, A. Beniwal, C. Degrande, J. Heisig, and A. Scaffidi, *Global fit of pseudo-Nambu-Goldstone Dark Matter*, *JHEP* **04** (2020) 015, [arXiv:1912.0400].

[143] P. Bandyopadhyay and A. Costantini, *Obscure Higgs boson at Colliders*, *Phys. Rev. D* **103** (2021), no. 1 015025, [arXiv:2010.0259].

[144] D. Berger, S. Ipek, T. M. Tait, and M. Waterbury, *Dark Matter Freeze Out during an Early Cosmological Period of QCD Confinement*, *JHEP* **07** (2020) 192, [arXiv:2004.0672].

[145] Z. Chacko, N. Craig, P. J. Fox, and R. Harnik, *Cosmology in Mirror Twin Higgs and Neutrino Masses*, *JHEP* **07** (2017) 023, [arXiv:1611.0797].

[146] Z. Chacko, D. Curtin, M. Geller, and Y. Tsai, *Cosmological Signatures of a Mirror Twin Higgs*, *JHEP* **09** (2018) 163, [arXiv:1803.0326].

[147] S. Koren and R. McGehee, *Freezing-in twin dark matter*, *Phys. Rev. D* **101** (2020), no. 5 055024, [arXiv:1908.0355].

[148] R. Barbieri, L. J. Hall, and K. Harigaya, *Effective Theory of Flavor for Minimal Mirror Twin Higgs*, *JHEP* **10** (2017) 015, [arXiv:1706.0554].

[149] N. Craig, S. Knapen, P. Longhi, and M. Strassler, *The Vector-like Twin Higgs*, *JHEP* **07** (2016) 002, [arXiv:1601.0718].

[150] B. Batell and C. B. Verhaaren, *Breaking Mirror Twin Hypercharge*, *JHEP* **12** (2019) 010, [arXiv:1904.1046].

[151] J.-H. Yu, *A tale of twin Higgs: natural twin two Higgs doublet models*, *JHEP* **12** (2016) 143, [arXiv:1608.0571].

[152] T. H. Jung, *Spontaneous Twin Symmetry Breaking*, *Phys. Rev.* **D100** (2019), no. 11 115012, [arXiv:1902.1097].

[153] J.-H. Yu, *Radiative-$\mathbb{Z}_2$-breaking twin Higgs model*, *Phys. Rev.* **D94** (2016), no. 11 111704, [arXiv:1608.0131].

[154] R. Barbieri, T. Gregoire, and L. J. Hall, *Mirror world at the large hadron collider*, hep-ph/0509242.

[155] D. Curtin and C. B. Verhaaren, *Discovering Uncolored Naturalness in Exotic Higgs Decays*, *JHEP* **12** (2015) 072, [arXiv:1506.0614].

[156] **ATLAS** Collaboration, G. Aad et al., *Search for long-lived, massive particles in events with a displaced vertex and a muon with large impact parameter in pp collisions at $\sqrt{s} = 13$ TeV with the ATLAS detector*, *Phys. Rev. D* **102** (2020), no. 3 032006, [arXiv:2003.1195].

[157] **ATLAS** Collaboration, G. Aad et al., *Search for long-lived neutral particles produced in pp collisions at $\sqrt{s} = 13$ TeV decaying into displaced hadronic jets in the ATLAS inner detector and muon spectrometer*, *Phys. Rev. D* **101** (2020), no. 5 052013, [arXiv:1911.1257].

[158] **CMS** Collaboration, *Search for long-lived particles decaying into displaced jets*, .

[159] **CMS** Collaboration, A. M. Sirunyan et al., *A deep neural network to search for new long-lived particles decaying to jets*, arXiv:1912.1223.

[160] **LHCb** Collaboration, *Prospects for searches for long-lived particles after the LHCb detector upgrades*, .

[161] J. Beacham et al., *Physics Beyond Colliders at CERN: Beyond the Standard Model Working Group Report*, *J. Phys. G* **47** (2020), no. 1 010501, [arXiv:1901.0996].

[162] **MATHUSLA** Collaboration, H. Lubatti et al., *MATHUSLA: A Detector Proposal to Explore the Lifetime Frontier at the HL-LHC*, *JINST* **15** (2020), no. 06 C06026, [arXiv:1901.0404].

[163] D. Curtin et al., *Long-Lived Particles at the Energy Frontier: The MATHUSLA Physics Case*, *Rept. Prog. Phys.* **82** (2019), no. 11 116201, [arXiv:1806.0739].

[164] V. V. Gligorov, S. Knapen, M. Papucci, and D. J. Robinson, *Searching for Long-lived Particles: A Compact Detector for Exotics at LHCb*, *Phys. Rev. D* **97** (2018), no. 1 015023, [arXiv:1708.0939].

[165] M. Markevitch, A. Gonzalez, D. Clowe, A. Vikhlinin, L. David, W. Forman, C. Jones, S. Murray, and W. Tucker, *Direct constraints on the dark matter self-interaction cross-section from the merging galaxy cluster 1E0657-56*, *Astrophys. J.* **606** (2004) 819–824, [astro-ph/0309303].

[166] F. Kahlhoefer, K. Schmidt-Hoberg, M. T. Frandsen, and S. Sarkar, *Colliding clusters and dark matter self-interactions*, *Mon. Not. Roy. Astron. Soc.* **437** (2014), no. 3 2865–2881, [arXiv:1308.3419].

[167] D. Harvey, R. Massey, T. Kitching, A. Taylor, and E. Tittley, *The non-gravitational interactions of dark matter in colliding galaxy clusters*, *Science* **347** (2015) 1462–1465, [arXiv:1503.0767].

[168] A. Robertson, R. Massey, and V. Eke, *What does the Bullet Cluster tell us about self-interacting dark matter?*, *Mon. Not. Roy. Astron. Soc.* **465** (2017), no. 1 569–587, [arXiv:1605.0430].

[169] D. Wittman, N. Golovich, and W. A. Dawson, *The Mismeasure of Mergers: Revised Limits on Self-interacting Dark Matter in Merging Galaxy Clusters*, *Astrophys. J.* **869** (2018), no. 2 104, [arXiv:1701.0587].

[170] D. Harvey, A. Robertson, R. Massey, and I. G. McCarthy, *Observable tests of self-interacting dark matter in galaxy clusters: BCG wobbles in a constant density core*, *Mon. Not. Roy. Astron. Soc.* **488** (2019), no. 2 1572–1579, [arXiv:1812.0698].

[171] D. Curtin and J. Setford, *Signatures of Mirror Stars*, *JHEP* **03** (2020) 041, [arXiv:1909.0407].

[172] D. Curtin and J. Setford, *How To Discover Mirror Stars*, *Phys. Lett. B* **804** (2020) 135391, [arXiv:1909.0407].

[173] L. Lopez-Honorez, T. Schwetz, and J. Zupan, *Higgs portal, fermionic dark matter, and a Standard Model like Higgs at 125 GeV*, *Phys. Lett. B* **716** (2012) 179–185, [arXiv:1203.2064].

[174] A. De Simone, G. F. Giudice, and A. Strumia, *Benchmarks for Dark Matter Searches at the LHC*, *JHEP* **06** (2014) 081, [arXiv:1402.6287].

[175] M. A. Fedderke, J.-Y. Chen, E. W. Kolb, and L.-T. Wang, *The Fermionic Dark Matter Higgs Portal: an effective field theory approach*, *JHEP* **08** (2014) 122, [arXiv:1404.2283].

[176] P. Gondolo and G. Gelmini, *Cosmic abundances of stable particles: Improved analysis*, *Nucl. Phys. B* **360** (1991) 145–179.

[177] G. Choi, C.-T. Chiang, and M. LoVerde, *Probing Decoupling in Dark Sectors with the Cosmic Microwave Background*, *JCAP* **1806** (2018), no. 06 044, [arXiv:1804.1018].

[178] P. de Salas, M. Lattanzi, G. Mangano, G. Miele, S. Pastor, and O. Pisanti, *Bounds on very low reheating scenarios after Planck*, *Phys. Rev. D* **92** (2015), no. 12 123534, [arXiv:1511.0067].

[179] T. D. Jacques, L. M. Krauss, and C. Lunardini, *Additional Light Sterile Neutrinos and Cosmology*, *Phys. Rev. D* **87** (2013), no. 8 083515, [arXiv:1301.3119]. [Erratum: Phys.Rev.D 88, 109901 (2013)].

[180] S. Hamdan and J. Unwin, *Dark Matter Freeze-out During Matter Domination*, *Mod. Phys. Lett. A* **33** (2018), no. 29 1850181, [arXiv:1710.0375].

[181] J. A. Evans, A. Ghalsasi, S. Gori, M. Tammaro, and J. Zupan, *Light Dark Matter from Entropy Dilution*, *JHEP* **02** (2020) 151, [arXiv:1910.0631].

[182] A. V. Patwardhan, G. M. Fuller, C. T. Kishimoto, and A. Kusenko, *Diluted equilibrium sterile neutrino dark matter*, *Phys. Rev. D* **92** (Nov, 2015) 103509.

[183] P. Arias, N. Bernal, A. Herrera, and C. Maldonado, *Reconstructing Non-standard Cosmologies with Dark Matter*, *JCAP* **10** (2019) 047, [arXiv:1906.0418].

[184] P. Arias, D. Karamitros, and L. Roszkowski, *Frozen-in fermionic singlet dark matter in non-standard cosmology with a decaying fluid*, arXiv:2012.0720.

[185] N. Bernal, C. Cosme, and T. Tenkanen, *Phenomenology of Self-Interacting Dark Matter in a Matter-Dominated Universe*, *Eur. Phys. J. C* **79** (2019), no. 2 99, [arXiv:1803.0806].

[186] Z. Chacko, C. Kilic, S. Najjari, and C. B. Verhaaren, *Collider signals of the Mirror Twin Higgs boson through the hypercharge portal*, *Phys. Rev. D* **100** (2019), no. 3 035037, [arXiv:1904.1199].

[187] M. Drewes, *The Phenomenology of Right Handed Neutrinos*, *Int. J. Mod. Phys. E* **22** (2013) 1330019, [arXiv:1303.6912].

[188] **Particle Data Group** Collaboration, M. Tanabashi et al., *Review of particle physics*, *Phys. Rev. D* **98** (Aug, 2018) 030001.

[189] **LHC Higgs Cross Section Working Group** Collaboration, S. Dittmaier et al., *Handbook of LHC Higgs Cross Sections: 1. Inclusive Observables*, arXiv:1101.0593.

[190] A. Djouadi, *The Anatomy of electro-weak symmetry breaking. I: The Higgs boson in the standard model*, *Phys. Rept.* **457** (2008) 1–216, [hep-ph/0503172].

[191] D. Curtin, S. Gryba, D. Hooper, J. Scholtz, and J. Setford, *Resurrecting the fraternal twin WIMP miracle*, *Phys. Rev. D* **105** (2022), no. 3 035033, [arXiv:2106.1257].

[192] **PandaX-II** Collaboration, X. Cui et al., *Dark Matter Results From 54-Ton-Day Exposure of PandaX-II Experiment*, *Phys. Rev. Lett.* **119** (2017), no. 18 181302, [arXiv:1708.0691].

[193] G. Bertone and D. Hooper, *A History of Dark Matter*, *Submitted to: Rev. Mod. Phys.* (2016) [arXiv:1605.0490].

[194] **ATLAS** Collaboration, M. Aaboud et al., *Search for a scalar partner of the top quark in the jets plus missing transverse momentum final state at $\sqrt{s}$=13 TeV with the ATLAS detector*, *JHEP* **12** (2017) 085, [arXiv:1709.0418].

[195] **CMS** Collaboration, A. M. Sirunyan et al., *Searches for pair production of charginos and top squarks in final states with two oppositely charged leptons in proton-proton collisions at $\sqrt{s} = 13$ TeV*, *JHEP* **11** (2018) 079, [arXiv:1807.0779].

[196] **CMS** Collaboration, A. M. Sirunyan et al., *Search for top squarks and dark matter particles in opposite-charge dilepton final states at $\sqrt{s} = 13$ TeV*, *Phys. Rev.* **D97** (2018), no. 3 032009, [arXiv:1711.0075].

[197] **CMS** Collaboration, A. M. Sirunyan et al., *Search for the pair production of third-generation squarks with two-body decays to a bottom or charm quark and a neutralino in proton–proton collisions at $\sqrt{s}$ = 13 TeV*, *Phys. Lett.* **B778** (2018) 263–291, [arXiv:1707.0727].

[198] Z. Chacko, Y. Nomura, M. Papucci, and G. Perez, *Natural little hierarchy from a partially goldstone twin Higgs*, *JHEP* **01** (2006) 126, [hep-ph/0510273].

[199] H. Cai, H.-C. Cheng, and J. Terning, *A Quirky Little Higgs Model*, *JHEP* **05** (2009) 045, [arXiv:0812.0843].

[200] D. Poland and J. Thaler, *The Dark Top*, *JHEP* **11** (2008) 083, [arXiv:0808.1290].

[201] T. Cohen, N. Craig, G. F. Giudice, and M. Mccullough, *The Hyperbolic Higgs*, *JHEP* **05** (2018) 091, [arXiv:1803.0364].

[202] H.-C. Cheng, L. Li, E. Salvioni, and C. B. Verhaaren, *Singlet Scalar Top Partners from Accidental Supersymmetry*, *JHEP* **05** (2018) 057, [arXiv:1803.0365].

[203] M. Perelstein, *Little Higgs models and their phenomenology*, *Prog. Part. Nucl. Phys.* **58** (2007) 247–291, [hep-ph/0512128].

[204] ATLAS, *A combination of measurements of Higgs boson production and decay using up to 139 fb^{-1} of proton–proton collision data at $\sqrt{s} = 13$ TeV collected with the ATLAS experiment*, ATLAS-CONF-2020-027.

[205] **CMS** Collaboration, A. M. Sirunyan et al., *Combined measurements of Higgs boson couplings in proton–proton collisions at $\sqrt{s} = 13$ TeV*, *Eur. Phys. J. C* **79** (2019), no. 5 421, [arXiv:1809.1073].

[206] C. Csáki, C.-S. Guan, T. Ma, and J. Shu, *Twin Higgs with exact Z_2*, *JHEP* **12** (2020) 005, [arXiv:1910.1408].

[207] S. Dawson et al., *Working Group Report: Higgs Boson*, in *Community Summer Study 2013: Snowmass on the Mississippi*, 10, 2013. arXiv:1310.8361.

[208] N. Craig, C. Englert, and M. McCullough, *New Probe of Naturalness*, *Phys. Rev. Lett.* **111** (2013), no. 12 121803, [arXiv:1305.5251].

[209] M. Farina, A. Monteux, and C. S. Shin, *Twin mechanism for baryon and dark matter asymmetries*, *Phys. Rev.* **D94** (2016), no. 3 035017, [arXiv:1604.0821].

[210] M. Freytsis, S. Knapen, D. J. Robinson, and Y. Tsai, *Gamma-rays from Dark Showers with Twin Higgs Models*, *JHEP* **05** (2016) 018, [arXiv:1601.0755].

[211] Y. Hochberg, E. Kuflik, and H. Murayama, *Twin Higgs model with strongly interacting massive particle dark matter*, *Phys. Rev.* **D99** (2019), no. 1 015005, [arXiv:1805.0934].

[212] J. Terning, C. B. Verhaaren, and K. Zora, *Composite Twin Dark Matter*, *Phys. Rev. D* **99** (2019), no. 9 095020, [arXiv:1902.0821].

[213] A. C. Ritter and R. R. Volkas, *Implementing Asymmetric Dark Matter and Dark Electroweak Baryogenesis in a Mirror Two-Higgs-Doublet Model*, arXiv:2101.0742.

[214] **CMS** Collaboration, *A search for doubly-charged Higgs boson production in three and four lepton final states at* $\sqrt{s} = 13$ TeV, .

[215] M. D. Goodsell and F. Staub, *Unitarity constraints on general scalar couplings with SARAH*, *Eur. Phys. J. C* **78** (2018), no. 8 649, [arXiv:1805.0730].

[216] L. B. Okun, *THETONS*, *Pisma Zh. Eksp. Teor. Fiz.* **31** (1979) 156–159.

[217] L. B. Okun, *THETA PARTICLES*, *Nucl. Phys. B* **173** (1980) 1–12.

[218] J. Kang and M. A. Luty, *Macroscopic Strings and 'Quirks' at Colliders*, *JHEP* **11** (2009) 065, [arXiv:0805.4642].

[219] T. Daylan, D. P. Finkbeiner, D. Hooper, T. Linden, S. K. N. Portillo, N. L. Rodd, and T. R. Slatyer, *The characterization of the gamma-ray signal from the central Milky Way: A case for annihilating dark matter*, *Phys. Dark Univ.* **12** (2016) 1–23, [arXiv:1402.6703].

[220] D. Hooper and L. Goodenough, *Dark Matter Annihilation in The Galactic Center As Seen by the Fermi Gamma Ray Space Telescope*, *Phys. Lett. B* **697** (2011) 412–428, [arXiv:1010.2752].

[221] A. Cuoco, M. Krämer, and M. Korsmeier, *Novel Dark Matter Constraints from Antiprotons in Light of AMS-02*, *Phys. Rev. Lett.* **118** (2017), no. 19 191102, [arXiv:1610.0307].

[222] M.-Y. Cui, Q. Yuan, Y.-L. S. Tsai, and Y.-Z. Fan, *Possible dark matter annihilation signal in the AMS-02 antiproton data*, *Phys. Rev. Lett.* **118** (2017), no. 19 191101, [arXiv:1610.0384].

[223] I. Cholis, T. Linden, and D. Hooper, *A Robust Excess in the Cosmic-Ray Antiproton Spectrum: Implications for Annihilating Dark Matter*, *Phys. Rev. D* **99** (2019), no. 10 103026, [arXiv:1903.0254].

[224] D. Curtin and C. Gemmell, *Indirect Detection Signatures of Dark Showers*, *In preparation.* (2021).

[225] **Muon g-2** Collaboration, G. W. Bennett et al., *Final Report of the Muon E821 Anomalous Magnetic Moment Measurement at BNL*, *Phys. Rev. D* **73** (2006) 072003, [hep-ex/0602035].

[226] **Muon g-2** Collaboration, B. Abi et al., *Measurement of the Positive Muon Anomalous Magnetic Moment to 0.46 ppm*, *Phys. Rev. Lett.* **126** (2021), no. 14 141801, [arXiv:2104.0328].

[227] B. Fuks, M. Klasen, D. R. Lamprea, and M. Rothering, *Revisiting slepton pair production at the Large Hadron Collider*, *JHEP* **01** (2014) 168, [arXiv:1310.2621].

[228] C. Csaki, E. Kuflik, S. Lombardo, and O. Slone, *Searching for displaced Higgs boson decays*, *Phys. Rev. D* **92** (2015), no. 7 073008, [arXiv:1508.0152].

[229] A. Pierce, B. Shakya, Y. Tsai, and Y. Zhao, *Searching for confining hidden valleys at LHCb, ATLAS, and CMS*, *Phys. Rev. D* **97** (2018), no. 9 095033, [arXiv:1708.0538].

[230] G. Burdman and G. Lichtenstein, *Displaced Vertices from Hidden Glue*, *JHEP* **08** (2018) 146, [arXiv:1807.0380].

[231] L. Li and Y. Tsai, *Detector-size Upper Bounds on Dark Hadron Lifetime from Cosmology*, *JHEP* **05** (2019) 072, [arXiv:1901.0993].

[232] F. Bishara and C. B. Verhaaren, *Singleton Portals to the Twin Sector*, *JHEP* **05** (2019) 016, [arXiv:1811.0597].

[233] ATLAS, *Search for exotic decays of the Higgs boson to long-lived particles in pp collisions at* $\sqrt{s} = 13$ *TeV using displaced vertices in the ATLAS inner detector*, ATLAS-CONF-2021-005.

[234] **CMS** Collaboration, A. M. Sirunyan et al., *Search for long-lived particles using displaced jets in proton-proton collisions at* $\sqrt{s} = 13$ *TeV*, arXiv:2012.0158.

[235] CMS, *Search for Higgs boson decays into long-lived particles in associated* Z *boson production*, CMS-PAS-EXO-20-003.

[236] **ATLAS** Collaboration, M. Aaboud et al., *Search for long-lived particles produced in pp collisions at* $\sqrt{s} = 13$ *TeV that decay into displaced hadronic jets in the ATLAS muon spectrometer*, *Phys. Rev. D* **99** (2019), no. 5 052005, [arXiv:1811.0737].

[237] **ATLAS** Collaboration, M. Aaboud et al., *Search for long-lived neutral particles in pp collisions at* $\sqrt{s}$ *= 13 TeV that decay into displaced hadronic jets in the ATLAS calorimeter*, *Eur. Phys. J. C* **79** (2019), no. 6 481, [arXiv:1902.0309].

[238] CMS, *Search for Long-lived Particles Decaying in the CMS Endcap Muon System in Proton-Proton Collisions at* $\sqrt{s} = 13$ TeV, CMS-PAS-EXO-20-015.

[239] J. E. Juknevich, *Phenomenology of pure-gauge hidden valleys at Hadron colliders*. PhD thesis, Rutgers U., Piscataway, 2010.

[240] A. Vilenkin, *Gravitational Field of Vacuum Domain Walls and Strings*, *Phys. Rev. D* **23** (1981) 852–857.

[241] J. E. Juknevich, D. Melnikov, and M. J. Strassler, *A Pure-Glue Hidden Valley I. States and Decays*, *JHEP* **07** (2009) 055, [arXiv:0903.0883].

[242] J. E. Juknevich, *Pure-glue hidden valleys through the Higgs portal*, *JHEP* **08** (2010) 121, [arXiv:0911.5616].

[243] **MATHUSLA** Collaboration, C. Alpigiani et al., *An Update to the Letter of Intent for MATHUSLA: Search for Long-Lived Particles at the HL-LHC*, arXiv:2009.0169.

[244] H. Ito, O. Jinnouchi, T. Moroi, N. Nagata, and H. Otono, *Extending the LHC Reach for New Physics with Sub-Millimeter Displaced Vertices*, *Phys. Lett. B* **771** (2017) 568–575, [arXiv:1702.0861].

[245] H. Ito, O. Jinnouchi, T. Moroi, N. Nagata, and H. Otono, *Searching for Metastable Particles with Sub-Millimeter Displaced Vertices at Hadron Colliders*, *JHEP* **06** (2018) 112, [arXiv:1803.0023].

[246] Z. Liu, L.-T. Wang, and H. Zhang, *Exotic decays of the 125 GeV Higgs boson at future e^+e^- lepton colliders*, *Chin. Phys. C* **41** (2017), no. 6 063102, [arXiv:1612.0928].

[247] S. Alipour-Fard, N. Craig, M. Jiang, and S. Koren, *Long Live the Higgs Factory: Higgs Decays to Long-Lived Particles at Future Lepton Colliders*, *Chin. Phys. C* **43** (2019), no. 5 053101, [arXiv:1812.0558].

[248] K. Cheung and Z. S. Wang, *Probing Long-lived Particles at Higgs Factories*, *Phys. Rev. D* **101** (2020), no. 3 035003, [arXiv:1911.0872].

[249] J. C. Pati and A. Salam, *Lepton number as the fourth "color"*, *Phys. Rev. D* **10** (Jul, 1974) 275–289.

[250] O. Popov, M. A. Schmidt, and G. White, *R_2 as a single leptoquark solution to $R_{D^{(*)}}$ and $R_{K^{(*)}}$*, *Phys. Rev. D* **100** (2019), no. 3 035028, [arXiv:1905.0633].

[251] S. Saad, *Combined explanations of $(g-2)_\mu$, $R_{D^{(*)}}$, $R_{K^{(*)}}$ anomalies in a two-loop radiative neutrino mass model*, *Phys. Rev. D* **102** (2020), no. 1 015019, [arXiv:2005.0435].

[252] I. Bigaran, J. Gargalionis, and R. R. Volkas, *A near-minimal leptoquark model for reconciling flavour anomalies and generating radiative neutrino masses*, *JHEP* **10** (2019) 106, [arXiv:1906.0187].

[253] C.-H. Chen, T. Nomura, and H. Okada, *Excesses of muon $g-2$, $R_{D^{(*)}}$, and R_K in a leptoquark model*, *Phys. Lett. B* **774** (2017) 456–464, [arXiv:1703.0325].

[254] I. Doršner, S. Fajfer, D. A. Faroughy, and N. Košnik, *The role of the S_3 GUT leptoquark in flavor universality and collider searches*, *JHEP* **10** (2017) 188, [arXiv:1706.0777].

[255] S. Saad and A. Thapa, *Common origin of neutrino masses and $R_{D^{(*)}}$, $R_{K^{(*)}}$ anomalies*, *Phys. Rev. D* **102** (2020), no. 1 015014, [arXiv:2004.0788].

[256] Y. Cai, J. Gargalionis, M. A. Schmidt, and R. R. Volkas, *Reconsidering the One Leptoquark solution: flavor anomalies and neutrino mass*, *JHEP* **10** (2017) 047, [arXiv:1704.0584].

[257] A. Greljo, P. Stangl, and A. E. Thomsen, *A model of muon anomalies*, *Phys. Lett. B* **820** (2021) 136554, [arXiv:2103.1399].

[258] J. Julio, S. Saad, and A. Thapa, *Marriage between neutrino mass and flavor anomalies*, arXiv:2203.1549.

[259] A. Crivellin, B. Fuks, and L. Schnell, *Explaining the hints for lepton flavour universality violation with three S_2 leptoquark generations*, arXiv:2203.1011.

[260] J. Julio, S. Saad, and A. Thapa, *A Tale of Flavor Anomalies and the Origin of Neutrino Mass*, arXiv:2202.1047.

[261] D. Zhang, *Radiative neutrino masses, lepton flavor mixing and muon $g-2$ in a leptoquark model*, *JHEP* **07** (2021) 069, [arXiv:2105.0867].

[262] P. F. Perez, C. Murgui, and A. D. Plascencia, *Leptoquarks and matter unification: Flavor anomalies and the muon g-2*, *Phys. Rev. D* **104** (2021), no. 3 035041, [arXiv:2104.1122].

[263] T. Nomura and H. Okada, *Explanations for anomalies of muon anomalous magnetic dipole moment, $b \to s\mu\bar{\mu}$ and radiative neutrino masses in a leptoquark model*, *Phys. Rev. D* **104** (2021), no. 3 035042, [arXiv:2104.0324].

[264] A. Angelescu, D. Bečirević, D. A. Faroughy, F. Jaffredo, and O. Sumensari, *Single leptoquark solutions to the B-physics anomalies*, *Phys. Rev. D* **104** (2021), no. 5 055017, [arXiv:2103.1250].

[265] M. Bauer and M. Neubert, *Minimal Leptoquark Explanation for the $R_{D^{(*)}}$, R_K, and $(g-2)_\mu$ Anomalies*, *Physical Review Letters* **116** (04, 2016).

[266] **LSND** Collaboration, C. Athanassopoulos et al., *Candidate events in a search for anti-muon-neutrino —> anti-electron-neutrino oscillations*, *Phys. Rev. Lett.* **75** (1995) 2650–2653, [nucl-ex/9504002].

[267] **LSND** Collaboration, C. Athanassopoulos et al., *Evidence for neutrino oscillations from muon decay at rest*, *Phys. Rev. C* **54** (1996) 2685–2708, [nucl-ex/9605001].

[268] **LSND** Collaboration, A. Aguilar-Arevalo et al., *Evidence for neutrino oscillations from the observation of $\bar{\nu}_e$ appearance in a $\bar{\nu}_\mu$ beam*, *Phys. Rev. D* **64** (2001) 112007, [hep-ex/0104049].

[269] **MiniBooNE** Collaboration, A. A. Aguilar-Arevalo et al., *The Neutrino Flux prediction at MiniBooNE*, *Phys. Rev. D* **79** (2009) 072002, [arXiv:0806.1449].

[270] **MiniBooNE** Collaboration, A. A. Aguilar-Arevalo et al., *The MiniBooNE Detector*, *Nucl. Instrum. Meth. A* **599** (2009) 28–46, [arXiv:0806.4201].

[271] R. B. Patterson, E. M. Laird, Y. Liu, P. D. Meyers, I. Stancu, and H. A. Tanaka, *The Extended-track reconstruction for MiniBooNE*, *Nucl. Instrum. Meth. A* **608** (2009) 206–224, [arXiv:0902.2222].

[272] A. Diaz, C. A. Argüelles, G. H. Collin, J. M. Conrad, and M. H. Shaevitz, *Where Are We With Light Sterile Neutrinos?*, *Phys. Rept.* **884** (2020) 1–59, [arXiv:1906.0004].

[273] M. Carena, Y.-Y. Li, C. S. Machado, P. A. N. Machado, and C. E. M. Wagner, *Neutrinos in Large Extra Dimensions and Short-Baseline ν_e Appearance*, *Phys. Rev. D* **96** (2017), no. 9 095014, [arXiv:1708.0954].

[274] M. Sorel, J. M. Conrad, and M. Shaevitz, *A Combined analysis of short baseline neutrino experiments in the (3+1) and (3+2) sterile neutrino oscillation hypotheses*, *Phys. Rev. D* **70** (2004) 073004, [hep-ph/0305255].

[275] C. Giunti and E. M. Zavanin, *Appearance–disappearance relation in $3+N_s$ short-baseline neutrino oscillations*, *Mod. Phys. Lett. A* **31** (2015), no. 01 1650003, [arXiv:1508.0317].

[276] J. Kopp, P. A. N. Machado, M. Maltoni, and T. Schwetz, *Sterile Neutrino Oscillations: The Global Picture*, *JHEP* **05** (2013) 050, [arXiv:1303.3011].

[277] J. Kopp, M. Maltoni, and T. Schwetz, *Are There Sterile Neutrinos at the eV Scale?*, *Phys. Rev. Lett.* **107** (2011) 091801, [arXiv:1103.4570].

[278] J. Fan and P. Langacker, *Light Sterile Neutrinos and Short Baseline Neutrino Oscillation Anomalies*, *JHEP* **04** (2012) 083, [arXiv:1201.6662].

[279] E. Kuflik, S. D. McDermott, and K. M. Zurek, *Neutrino Phenomenology in a 3+1+1 Framework*, *Phys. Rev. D* **86** (2012) 033015, [arXiv:1205.1791].

[280] S. N. Gninenko, *Miniboone anomaly and heavy neutrino decay*, *Phys. Rev. Lett.* **103** (Dec, 2009) 241802.

[281] O. Fischer, A. Hernández-Cabezudo, and T. Schwetz, *Explaining the MiniBooNE excess by a decaying sterile neutrino with mass in the 250 MeV range*, *Phys. Rev. D* **101** (2020), no. 7 075045, [arXiv:1909.0956].

[282] S. N. Gninenko, *Resolution of puzzles from the lsnd, karmen, and miniboone experiments*, *Phys. Rev. D* **83** (Jan, 2011) 015015.

[283] M. Masip, P. Masjuan, and D. Meloni, *Heavy neutrino decays at MiniBooNE*, *JHEP* **01** (2013) 106, [arXiv:1210.1519].

[284] G. Magill, R. Plestid, M. Pospelov, and Y.-D. Tsai, *Dipole portal to heavy neutral leptons*, *Phys. Rev. D* **98** (Dec, 2018) 115015.

[285] G. Barenboim, L. Borissov, and J. D. Lykken, *CPT Violating Neutrinos in the Light of KamLAND*, hep-ph/0212116.

[286] J. S. Diaz and V. A. Kostelecky, *Three-parameter Lorentz-violating texture for neutrino mixing*, *Phys. Lett. B* **700** (2011) 25–28, [arXiv:1012.5985].

[287] M. C. Gonzalez-Garcia, M. Maltoni, and T. Schwetz, *Status of the* CPT *violating interpretations of the lsnd signal*, *Phys. Rev. D* **68** (Sep, 2003) 053007.

[288] V. Barger, D. Marfatia, and K. Whisnant, *Lsnd anomaly from cpt violation in four-neutrino models*, *Physics Letters B* **576** (2003), no. 3 303–308.

[289] G. Barenboim and N. E. Mavromatos, *CPT violating decoherence and LSND: a possible window to planck scale physics*, *Journal of High Energy Physics* **2005** (jan, 2005) 034–034.

[290] E. Akhmedov and T. Schwetz, *MiniBooNE and LSND data: Non-standard neutrino interactions in a (3+1) scheme versus (3+2) oscillations*, *JHEP* **10** (2010) 115, [arXiv:1007.4171].

[291] D. Döring, H. Päs, P. Sicking, and T. J. Weiler, *Sterile neutrinos with altered dispersion relations as an explanation for neutrino anomalies*, *Eur. Phys. J. C* **80** (2020), no. 12 1202, [arXiv:1808.0746].

[292] K. M. Zurek, *New matter effects in neutrino oscillation experiments*, *Journal of High Energy Physics* **2004** (oct, 2004) 058–058.

[293] K. S. Babu and S. Pakvasa, *Lepton number violating muon decay and the LSND neutrino anomaly*, hep-ph/0204236.

[294] B. Armbruster et al., *Improved limits on anti-nu(e) emission from mu+ decay*, *Phys. Rev. Lett.* **90** (2003) 181804, [hep-ex/0302017].

[295] *Short-baseline near detector (sbnd)*, *Fermilab — Short-Baseline Near Detector — Home*.

[296] I. Doršner, S. Fajfer, A. Greljo, J. F. Kamenik, and N. Košnik, *Physics of leptoquarks in precision experiments and at particle colliders*, *Phys. Rept.* **641** (2016) 1–68, [arXiv:1603.0499].

[297] K. S. Babu, P. S. B. Dev, S. Jana, and A. Thapa, *Unified framework for B-anomalies, muon g - 2 and neutrino masses*, *JHEP* **03** (2021) 179, [arXiv:2009.0177].

[298] **CMS** Collaboration, A. M. Sirunyan et al., *Search for third-generation scalar leptoquarks decaying to a top quark and a τ lepton at $\sqrt{s} = 13$ TeV*, *Eur. Phys. J. C* **78** (2018) 707, [arXiv:1803.0286].

[299] Bertl, W., Engfer, R., Hermes, E.A., Kurz, G., Kozlowski, T., Kuth, J., Otter, G., Rosenbaum, F., Ryskulov, N.M., van der Schaaf, A., Wintz, P., Zychor, I., and The SINDRUM II Collaboration, *A search for onversion in muonic gold*, *Eur. Phys. J. C* **47** (2006), no. 2 337–346.

[300] **COMET** Collaboration, M. Moritsu, *Search for muon-to-electron conversion with the COMET experiment*, *Universe* **8** (2022) 196, [arXiv:2203.0636].

[301] **Mu2e-II** Collaboration, K. Byrum et al., *Mu2e-II: Muon to electron conversion with PIP-II*, in *2022 Snowmass Summer Study*, 3, 2022. arXiv:2203.0756.